

# STUDY OF ARTIFICIAL NEURAL NETWORK AND OBSERVER BASED HIGH PERFORMANCE INDUCTION MOTOR DRIVES

A Thesis submitted to  
Bangladesh Institute of Technology, Khulna  
for the partial fulfillment of the degree  
Of



**Master of Science in Engineering**

**By**

**MD. ABDUR RAFIQ**

**Roll No: -943002**

DEPARTMENT OF ELECTRICAL & ELECTRONIC ENGINEERING  
BANGLADESH INSTITUTE OF TECHNOLOGY, KHULNA



BANGLADESH INSTITUTE OF TECHNOLOGY, KHULNA  
DEPARTMENT OF ELECTRICAL & ELECTRONIC ENGINEERING

We hereby recommended that the thesis report prepared by  
Md. Abdur Rafiq

Entitled "Study Of Artificial Neural Network And Observer-Based High Performance Induction Motor Drives" be accepted as fulfilling this part of the requirements for the degree of Master of science in Engineering (Electrical and Electronic Engineering).

 07.03.2001

Dr. A. K. Azad  
Associate professor & Head  
Department of Electrical & Electronic Engineering  
Bangladesh Institute of Technology, Khulna.

Chairman

  
01.03.2001


Prof. Dr. B. C. Ghosh  
Department of Electrical & Electronic Engineering  
Bangladesh Institute of Technology, Khulna.

Member (Supervisor)



Prof. Dr. M. A. Samad 1.3.2001.  
Department of Electrical & Electronic Engineering  
Bangladesh Institute of Technology, Khulna.

Member

  
01/03/2001

Dr. M. M. A. Hashem  
Associate professor  
Department of Electrical & Electronic Engineering  
Bangladesh Institute of Technology, Khulna.

Member



Prof. Dr. Shahidul Islam Khan  
Department of Electrical & Electronic Engineering  
Bangladesh University of Engineering and Technology, Dhaka.

Member (External)

March, 2001

**Dedicated to my Parents**

## CERTIFICATE

This is to certify that the thesis entitled “Study of Artificial Neural Network and Observer Based High Performance Induction Motor Drives” submitted by Md. Abdur Rafiq to the Department of Electrical & Electronic Engineering, Bangladesh Institute of Technology Khulna, for the partial fulfillment of the degree of Master of Science in Engineering, is a record of bonafide research work carried out by him under my supervision.



20/2/2001

(Prof. Dr. Bashudeb Chandra Ghosh)

BIT, Khulna

March, 2001

Department of Electrical & Electronics Engineering

Bangladesh Institute of Technology (BIT), Khulna

Khulna-9203.

## CONTENTS

<b>Certificate from Supervisor</b>	iii
<b>Acknowledgement</b>	viii
<b>Abstract</b>	ix
<b>List of symbols</b>	xi
<b>List of figures</b>	xvi
<b>Chapter I</b> Introduction	
1.1            Introduction	1
1.2            Literature Review	2
1.3            Scope of the Thesis	5
1.4            Contents of the Study in Brief	6
<b>Chapter II</b> Mathematical Model of Induction Motor	
2.1            Introduction	8
2.2            Stationary Two-Axis Model	8
2.2.1          Induction Motor Model	9
2.2.2          Phase Relationship	11
2.2.3          Voltage Source Inverter Feeding an Induction Motor	12
2.3            Rotating Two-Axis Model	13
2.3.1          Current Source Inverter Fed System	15

### **Chapter III** Flux Observers

3.1	Introduction	18
3.2	Mathematical Background	18
3.3	Full-Order Observer	21
3.3.1	The Separation Principle	22
3.4	Reduced-Order Observers	24
3.4.1	Reduced Order (Gopinath) Observer	27
3.4.2	Reduced Order (Generalised) Observer	28
3.5	Deadbeat Control	30
3.6	Deadbeat (Pole at origin) Observers	31

### **Chapter IV** Artificial Neural Networks

4.1	Introduction	33
4.2	Feedforward Neural Networks	33
4.3	Feedforward-Backpropagation Network	36
4.4	Mapping	37
4.5	Structure of Neural-Networks	38
4.6	Training	39
4.7	Backpropagation Algorithm	39

### **Chapter V** Field Orientation Control of Induction Motor

5.1	Introduction	42
5.2	Principle of Vector (Field-Orientation) Control	43
5.3	Direct method of vector Control	47

5.4	Voltage Regulated Induction Motor Drive	50
5.5	Current Regulated Induction Motor Drive	52
5.6	Indirect Method of Voltage Control	53
5.7	Current Source Inverter Fed Induction Motor Under Field Orientation Control	56
5.8	Flux Observer Based Field Orientation Controller	60

**Chapter VI** Simulation Study of Observer-Based Field-Oriented Induction  
Motor Drive

6.1	Introduction	65
6.2	Full order Observer based System	65
6.2.1	Voltage Source Inverter Fed Induction Motor Drive	65
6.2.2	Current Source Inverter Fed Induction motor Drive	68
6.3	Reduced order Observer-based System (Gopinath Type)	70
6.4	Reduced Order Observer-based System (Generalized Type)	72
6.4.1	Rotor Resistance Adaptation for Indirect Vector Control	77
6.5	Dead Beat Observer-based System Study	81

**Chapter VII** Flux Estimation Using ANN

7.1	Introduction	82
7.2	Neural-Network Rotor-Flux Estimator	82
7.3	Simulation Results	83
7.4	Neural-Network Rotor-Flux Estimator and Direct Field Orientation	85

## **Chapter VIII Conclusion**

8.1	Conclusion	88
8.2	Suggestions For Further Study	89

## **Appendices**

Appendix I	Tables of Induction Motor Drives	90
Appendix II	Simulation Model Discrete	91

<b>References</b>		<b>92</b>
-------------------	--	-----------



## ACKNOWLEDGEMENT

I would like to express my sincerest gratitude to my supervisor Prof. Dr. B. C. Ghosh for suggesting the subject of this dissertation and for his spontaneous guidance and cooperation in every respect of my research work until its completion.


I also express my deep appreciation and indebtedness to Prof. Dr. M. A. Samad, Director of this Institute and Assoc. Prof. Dr. A. K. Azad, Head of the Department of Electrical & Electronic Engineering for providing me with all possible facilities without which I could not think of the completion of research work.

I also acknowledge with gratitude the help of other faculty members who have always been willing to discuss and exchange ideas.

I am thankful to the staff members of laboratory/computer centre of the department.

B. I. T Khulna

March, 2001.

  
(Md. Abdur Rafiq)

## ABSTRACT

The main subject matter of this dissertation is to study the performance of artificial neural network and observer based high performance induction motor drive. Four suitable flux observers compatible with drive control law are discussed and flux estimation with these observers along with effectiveness is studied.

Study of the artificial neural networks for flux estimation with backpropagation training algorithm for simulation is presented in this dissertation. It also presents the general idea about feedforward neural networks, mapping and training of an artificial neural network.

The direct and indirect field orientation control methods of induction motor for variable operating conditions are evaluated in this study. In the direct method, flux estimation is applied for vector rotators which controls drive current or voltage magnitude as well as position so that the rotor flux can be kept constant. In the indirect method flux estimation is used for parameter compensation.

Digital simulation procedures are presented to study the performance of these observer-based field oriented induction motor drives. Speed of an induction machine is also estimated with full order observer and parameter adaptation is also presented for sensorless field orientation control.

The main drawback of indirect method of field orientation is due to variation of rotor resistance that degrades performance and requires tuning. Observers are used for detecting the parameter mismatch condition and correcting the controller resistance. By flux feedback the rotor resistance is adapted and the effectiveness of observers is also examined. Reduced order observer in generalized form is used for parameter adaptation of current source inverter fed system.

Flux estimation with artificial neural network has been carried out and extended to direct field orientation of voltage source inverter fed induction motor system. Finally, comparison with the results obtained by artificial neural network is given.

## LIST OF SYMBOLS

$C_j^m$	inverse temperature co-efficient of ANN.
$d - q$	arbitrary synchronous reference frame
$E$	performance index of ANN.
$e$	error containing column vector of ANN.
$e_j$	$j$ th component of output error at output layer of ANN.
$G$	gain matrix
$H$	Hessian matrix of ANN.
$I$	identity matrix
$I_a$	armature or torque component of current
$I_f$	field or flux component of current
$I_s$	per phase rms stator current
$i_{ds}, i_{qs}$	$d$ - and $q$ -axis instantaneous stator current components
$i_{dr}, i_{qr}$	$d$ - and $q$ -axis instantaneous rotor current components
$i_{ds}^*, i_{qs}^*$	command $d$ - and $q$ -axis instantaneous stator current components to the controller
$i_R$	dc link current for CSI
$i_r$	per phase instantaneous rotor current
$i_s$	per phase instantaneous stator current
$\hat{i}_s$	estimated per phase instantaneous stator current
$J$	Jacobian matrix
$K$	feedback matrix for state feedback control system

$L_f$	dc link filter inductance for CSI
$L_s$	stator self inductance per phase
$L_m$	mutual inductance per phase referred to stator
$L_r$	rotor self inductance per phase referred to stator
$M_1[i][j]$	weight on the connection from the $i$ th input neuron to the $j$ th neuron in the hidden layer of ANN.
$M_2[i][j]$	weight on the connection from the $i$ th hidden neuron to the $j$ th neuron in the output layer of ANN.
$m_j^n$	weight of layer $n$ connected preceding layer neuron $i$ to neuron $j$ of ANN.
$p$	$\equiv \frac{d}{dt}$ , differential operator
$P_l$	inverter input power for CSI
$P_p$	pole pairs
$P_R$	rectifier output power for CSI
$R_l$	resistance of dc link filter for CSI
$R_r$	rotor resistance per phase referred to stator
$R_s$	stator resistance per phase
$R_s^*$	command stator resistance per phase
$r(t)$	reference input vector of ANN.
$T_{em}$	developed electromagnetic torque
$T_j^n$	temperature co-efficient of ANN.

$t_j$	$j$ th component of output error at hidden layer of ANN.
$th_j^n$	threshold of layer $n$ connected to neuron $j$ of ANN.
$V_s$	stator rms voltage per phase
$V_g$	air gap voltage
$v_{ds}, v_{qs}$	$d$ - and $q$ -axis instantaneous stator voltage components
$v_l$	instantaneous inverter input voltage
$v_l'$	$= \frac{\Pi}{3\sqrt{3}} v_l$
$v_R$	instantaneous converter output voltage
$v_s$	stator phase voltage
$v_{\alpha s}, v_{\beta s}$	$\alpha$ - and $\beta$ -axis stator voltage components
$x(t)$	state vector
$x_i^{n-1}$	output of preceding layer $n-1$ of neuron $i$ acts input for layer $n$ of ANN.
$x_j$	output of $j$ th input layer of ANN.
$x_j^n$	output of layer $n$ of neuron $j$
$\hat{x}(t)$	estimated input vector
$\tilde{x}(t)$	error vector between estimated and actual value
$y(t)$	state output vector
$y_j^n$	internal sum of layer $n$ of neuron $j$ of ANN.
$y_j$	output of $j$ th hidden layer of ANN.
$z_j$	output of $j$ th output layer of ANN.

$\alpha$	momentum parameter of ANN.
$\alpha - \beta$	orthogonal stationary reference frame
$\beta_0$	learning rate parameter of output layer neuron of ANN.
$\beta_h$	learning rate parameter of hidden layer neuron of ANN.
$\lambda$	eigen value of characteristic equation
$\lambda_{dr}, \lambda_{qr}$	$d$ - and $q$ -axis rotor flux linkage components in stator terms
$\lambda_r$	rotor flux linkage
$\hat{\lambda}_r$	estimated rotor flux
$\lambda_r^*$	command rotor flux
$\sigma = L_{\sigma}$	leakage inductance
$\omega_r$	rotor angular velocity rad/sec
$\omega_e$	speed of the reference frame relative to stator, electrical rad/sec
$\omega_{sl}$	slip speed in electrical rad/sec relative to the rotor flux
$\tau_r$	rotor time constant in sec.
$\hat{\omega}_r$	estimated rotor speed rad/sec.
$\omega_r^*$	command rotor speed rad/sec.
$\theta_e$	angular position between $q$ -and $\beta$ -axis
$\theta_r$	rotor angular position
$\theta_{sl}$	slip angle of the rotor
$\zeta$	observed state
$\hat{\zeta}$	estimated state vector
$\nabla E$	gradient vector of ANN.

- $\Delta M_1[i][j]$  adjustment of weight on the connection from the  $i$ th input neuron to the  $j$ th neuron in the hidden layer of ANN.
- $\Delta M_2[i][j]$  weight on the connection from the  $i$ th hidden neuron to the  $j$ th neuron in the output layer of ANN.
- $\Delta \theta_j$  adjustment of threshold value for  $j$ th hidden layer neuron of ANN.
- $\Delta \tau_j$  adjustment of threshold value for  $j$ th output layer neuron of ANN.
- $\Lambda$  symmetric positive definite matrix of ANN.



## LIST OF FIGURES

Fig. 2.1	Physical coil system of the stator and the rotor of a 3-phase induction motor	10
Fig. 2.2	Mutually perpendicular fictitious/coils of the 3-phase equivalent induction motor	10
Fig. 2.3	Physical and fictitious two-axis phasors	11
Fig. 2.4	Relation between various co-ordinate systems and principle of field orientation	14
Fig. 2.5	CSI-IM drive system	15
Fig. 3.1	Structure of a state feedback system	19
Fig. 3.2	Reconstruction of the state	20
Fig. 3.3	Rotor flux estimation with full order observer	22
Fig. 3.4	Use of the observer to implement state feedback control law	24
Fig. 3.5	Configuration of reduced order (Gopinath) flux observer	27
Fig. 3.6	Rotor flux estimation with the reduced order Gopinath type observer	28
Fig. 3.7	Rotor flux estimation with the reduced order generalized type observer	30
Fig. 3.8	Rotor flux estimation with deadbeat type observer	32
Fig. 4.1	The infrastructure of a neuron	34
Fig. 4.2	Structure of a feed forward ANN showing backpropagation training	37
Fig. 4.3	Layout of a feedforward backpropagation networks	38
Fig. 5.1	Analogy of induction motor and the dc machine in vector control	44

Fig. 5.2	Phasor diagrams in the direct vector control (in terms of peak value)	45
Fig. 5.3	Vector control implementation with the machine model	46
Fig. 5.4	Synthesis of unit vector	47
Fig. 5.5	Synthesis of rotor fluxes	48
Fig. 5.6	Block diagram of the flux observer based field orientation (FOFO) control with voltage fed inverter	51
Fig. 5.7	Block diagram of the flux observer based field orientation (FOFO) control with current fed inverter	52
Fig. 5.8	Phasor diagram for indirect field control	53
Fig. 5.9	Block diagram of the machine model with decoupling control	55
Fig. 5.10	Flux observer based field orientation (FOFO) control for voltage fed inverter	62
Fig. 6.1	Speed under starting condition for voltage source inverter	66
Fig. 6.2	Speed adaptation with full order observer	66
Fig. 6.3	(a) Speed and (b) flux when the reference speed is decreased in step from 150 rad/sec to 100 rad /sec.	68
Fig. 6.4	(a) Speed and (b) flux for current controlled inverter	69
Fig. 6.5	(a) Speed (b) flux estimation and (c) rotor resistance for 50% increment in rotor resistance in step for voltage source inverter	71
Fig. 6.6	(a) Motor speed (b) slip speed and (c) rotor resistance for 25% increment in rotor resistance for voltage source inverter	74
Fig. 6.7	Variation of the poles of the system due to the variation of slip speed and motor speed	75

Fig. 6.8	Motor speed and flux estimation under starting condition for current source inverter	76
Fig. 6.9	Estimation of rotor flux for 25% increment in rotor resistance for current source inverter	76
Fig. 6.10	Block diagram of rotor resistance adaptation process	77
Fig. 6.11	(a) Motor speed (b) slip speed (c) actual flux (d) adapted rotor resistance using estimated rotor flux for voltage source inverter	79
Fig. 6.12	Actual rotor flux, estimated rotor flux and, adapted rotor resistance using estimated rotor flux for current source inverter	80
Fig. 6.13	Starting performance for voltage source inverter	81
Fig. 7.1	Principle for training the ANN-flux estimator	83
Fig. 7.2	Three-layer ANN rotor-flux estimator	84
Fig. 7.3	ANN estimated rotor flux (a) d-axis (b) q-axis	85
Fig. 7.4	ANN rotor flux estimator based direct field orientation controller for voltage fed inverter	86
Fig. 7.5	ANN estimated rotor flux (a) d-axis (b) q-axis of direct field orientation based voltage fed inverter	87
Fig. B.1	First order filter in speed feedback loop	91

# CHAPTER I

## INTRODUCTION

### 1.1 INTRODUCTION

Polyphase induction motors are widely used power converting machines and are called 'the Workhorse' of industries. They are simple and low cost in construction and mechanically robust to have a long life. The squirrel cage rotor offers advantages such as simplicity, robustness and low weight to torque ratio. Like other rotating machines, the rotor of a polyphase induction motor is separated from the stator by a small air gap. The stator is polyphase wound and kept stationary by fixing it with the yoke.

The polyphase induction motor receives power from a balanced supply system through its stator. The balanced currents produce an mmf and flux system, which rotates at synchronous speed. The rotor receives power from the stator by induction. Torque developed in a motor may be viewed as an interaction of rotor flux and stator mmf. The polyphase induction motor does not provide separate channels for flux and torque which makes the controlling of the motor a difficult one.

After the introduction of vector control theory by F. Blaschke and subsequent advancement in digital electronics, it is possible to control the induction motor like a separately excited dc motor. Such a drive is often referred to as high performance induction motor drive. The control law is normally termed as field orientation control and considers the generic nature of torque generation in any electrical machine. This concept considers that in any rotating electrical machine there is a flux system and a mmf perpendicular to this flux is responsible for torque production. In an induction motor there are three systems of flux: viz., the stator flux, the mutual flux and the rotor flux. The rotor flux and its perpendicular stator mmf are generally considered as vectors to be controlled in a polyphase induction motor. Since the time constant of flux path in a polyphase induction motor is large, any change in the value of flux causes slow dynamics. This is why the value of flux is normally kept constant. In vector control schemes, the function of a field orientation (vector) controller is to decouple the flux and torque channels and to establish independent control over each of them.

Basically, there are two vector control methods (a) the direct method and (b) the indirect method. In the direct method the position and magnitude of flux vector is sensed or observed and the stator mmf magnitude and position are adjusted to have requisite torque

generation. On the other hand, the indirect method is simple software dependent and easy to implement. However, this method suffers from a serious drawback due to the mismatch of parameters of the motor and controller during operation. This further requires adaptive and tuning methods so that the slip calculator of the vector controller sees the exact rotor time constant of the induction motor. Sensing of flux inside the motor requires additional circuitry to be imparted inside the machine and is difficult and costly.

The flux inside the induction motor may be observed and estimated with suitable observer and estimators. The observer is normally developed from the mathematical model of the system with some rule so that the error dynamics is reduced to zero. The most commonly used observers are (a) full order (b) reduced order and (c) deadbeat types. Each of these has some merits and demerits. For full order and reduced order observers selection of poles is vital and improper selection of poles create unwanted dynamics. The designer has to compromise with stability and fast response to get a negotiable design. Another important aspect is the insensitivity of the observer with parameter perturbation i.e., the observer should estimate the flux position and magnitude accurately in case of parameter variation of the induction motor. Due to advancement in digital computer technology, observers have wide applicability in induction motor control.

Besides the flux observers, the Artificial Neural Network (ANN) offers some promising aspects in respect of estimation of flux in the induction motor. The ANN method requires modification of structure and adjustment of weights to converge the error within a tolerable limit. It requires training in which both time and computer memories are involved. At present ANN is being used to estimate states and flux of electrical machines. This technology has a bright prospect in respect of induction motor control.

## **1.2 LITERATURE REVIEW**

After the introduction of power electronics in industrial control, research was going on to use induction motors for high performance applications such as machine tools, robotics etc. It was F.Blaschke [1] and K.Hasse [2] who first proposed the vector control methodologies for induction motors. Blaschke [1] proposed the direct method of field orientation and Hasse [2] introduced the indirect method of field orientation. The technology has been developed over the last three decades and at present is in the matured stage. This can be visualized from a large number of literatures available in this field,

some of which are included in the literature [1- 18]. A detailed explanation of this theory is given in [3].

Availability of microprocessors and consequent reduction of cost of the processor and peripherals has made possible implementation of the vector control on-line. Considerations regarding microprocessor or multi microprocessor-based implementation of the control strategy is given in [4,5]. Current source inverter fed induction motor drive system offers sluggish performance due to high inertia of the filter inductor. However, the drive performance may be improved and fast response is possible if field orientation control is used with proper feedback. This aspect is indicated in [6]. Field orientation control may be applied considering any one of stators, rotor or mutual flux. A comparison of the control aspects is given in [7], which concludes that the rotor flux system offers the simplest structure for the system.

The direct method of field orientation may be implemented with sensing devices to the motor or using extra hardware for signal processing. Such systems are given in [8,9], which [8] shows tapping of stator windings for flux sensor. To implement the scheme, prior modification of the motor windings should be carried out.

Simulations are normally carried out to study the effectiveness of the proposed methodology. Since field orientation control is complex in nature, theoretical analysis is a must prior to implementation of the control law in a practical environment. Advancement of digital computer technology offers the facility to judge the viability of the control law in digital environment. Simulation studies of a field oriented induction motor with nominal parameters is given in [10]. The effect of parameter deviation from their nominal values results in saturation and such studies are given in [11]. Modeling and simulation of CSI fed induction motor under vector control is shown in [12]. This paper gives a relationship between motor and inverter parameters. To enhance the dynamics of the drive system injection of a component of dc link voltage is given in [13]. They have claimed faster dynamics compared to voltage-fed system as offered by a CSI-fed system. D.I. Kim, et, al, [14] have proposed feedback linearization which offers input output decoupling and the action resembles to field orientation control. They have provided only the theoretical development. Indirect field orientation control requires identification of rotor time constant for proper functioning of the controller. In [15] a microprocessor-based scheme with rotor resistance identification aspect is given. L.J.Garces [16] shows

the effect of parameter deviation on the performance of indirect field orientation control schemes. He has suggested a methodology based on var measurement to adapt the rotor resistance in a vector controller. Adaptation of rotor parameters by air-gap power measurement is given in [17]. Rotor time constant detection using voltage injection is shown in [18]. This scheme requires complex signal processing task. A method of rotor resistance adaptation of a CSI-fed IM drive under indirect field orientation is given in [19], which considers magnetic saturation effect due to detuning of the controller.

Very fast computation and data acquisition facilities have encouraged the researchers to work with observer design and its implementation in the induction motor control. The field orientation is applied in direct method in most of the cases. A good number of literature [22-29] is available in this subject. In [22] and [23] emphasis is given on the selection of poles to have a robust structure for the observer. Full order observers for flux estimation with speed adaptation capability have been described in [32,33]. The feedback gain is deduced from the system matrix and estimated value of speed is incorporated in its elements so that in convergence, the estimated speed equals the actual speed of the motor. Reduced order rotor flux observer is used for direct field orientation control. Their proposed observer is less sensitive to rotor parameter variation. Digital signal processor is proposed and used [22] for implementation of the observer [24] for CSI-fed induction motor drive operating under indirect field orientation control. The flux observer is used as the slip calculator and flux control loop. The flux observers proposed in [25] and [26] uses stator flux estimation technique. These schemes calculate stator flux by integration and uses the d-q axes components of flux for angle calculation in the vector rotator. DSP-based implementation is proposed in [26]. An improvement over the stator flux oriented drive is proposed in [27]. They consider the problem associated with the time lag in the converter transistor switching. After simulation, they have shown that if the time lag is kept constant for all power switches, the distortion may be eliminated drastically. An improved flux observer reported in [28] over that reported in [22] doesn't require speed transducer. Two flux models, one based on voltage independent of speed and the other based on current independent of speed are used to calculate the speed. The adaptive observer proposed in [29] uses adaptive poles dependent on motor speed for stable and fast computation of flux.

Artificial Neural Networks (ANN) technique has been applied to induction motor recently for flux estimation. An earlier publication [30] proposes speed estimation using ANN for induction motor control. In it estimated flux from voltage and current based flux models are used to estimate speed using ANN concept. A three-layer ANN using four inputs and four outputs is proposed in [31]. An LPF integrator is used in the scheme for integration purpose. A DSP based scheme is compared with the ANN performance for the vector controlled induction motor drive. Learning techniques to train ANN as a state selector for induction machines for direct torque control application is proposed in [32]. They have analyzed performance of backpropagation, adaptive neuron model, extended Kalman filter and recursive prediction algorithms for training the ANN system. Prediction error methods have been proposed as a promising method. Field orientations control utilizing ANN based flux estimators is proposed in [33]. The ANN technique estimates the stator flux components from which the rotor flux components are estimated. The other control blocks such as vector rotator and torque and torque flux control loops are used in conventional form.

### **1.3 SCOPE OF THE THESIS**

Field orientation controls of induction motors are widely used in industries now a days. However, they require complex and costly hardware for their implementation. Alternatives to this may be the flux observers and estimators. Due to huge development in digital computer technology, rapid computation is possible. Besides this, the recently introduced Artificial Neural Network based flux estimation and field orientation control have been claimed to work fruitfully. The present study intends to see the effectiveness of different types of observers for field orientation control and the application of ANN based systems for the purpose of direct and indirect field orientation control.

It is well known that an induction motor may be modeled in mutually perpendicular axes which results two rotor flux and two stator current variables. From the mechanical sides speed appears as another state variables; therefore five state variables are required to describe the induction motor completely. The rotor flux components are not directly accessible and require an observer to estimate them. In this thesis a full order observer is proposed that estimates rotor flux components and also estimates the speed of the



induction motor. The gain of the observer is adjusted in such a way that the system does not oscillate and gives stable estimation of rotor fluxes. This observer is used for direct field orientation and to study whether the method works satisfactorily under rotor resistance changes.

The reduced order observers require less calculation and is very popular in control of induction motor. In our study we have considered generalized type, Gopinath type with pole variation and deadbeat type. Reduced order observers have been used for direct and indirect field orientation. In the indirect method it is assumed that the rotor resistance is adapted properly. The effectiveness of the observer are also examined. Then (Gopinath type) minimum orders high performance flux Observer based field orientation controller for induction machines has been studied and examined for its robustness. An observer-based on deadbeat control law (hence forth termed as deadbeat observer) is introduced in the study.

Recently Artificial Neural Networks are being used as controllers in many industrial applications and the systems have drawn much attention. ANN systems for flux estimator with backpropagation and the adaptive algorithm are also studied.

#### 1.4 CONTENTS OF THE STUDY IN BRIEF

Chapter-I begins with a general discussion on drive systems, inverters, field oriented control pertaining to induction motor, controller's etc. This is followed by an overview of a few selected contributions to indicate, in brief, the various studies that have been made over the past two decades in the area of vector controlled induction motor. The chapter also discusses in brief the literature survey, scope of the present study. The chapter concludes with the contents of the study of others chapter in brief.

Chapter-II commences with the two-axis model of the induction machine in both stationary and rotating reference frame and proceeds, under justifiable assumptions, to obtain a general model involving the voltage source inverter fed and current source inverter fed system of induction motor.

Chapter-III discusses about flux observers for induction motors. It proposes three schemes for estimate rotor flux. In one scheme full order observer can estimate rotor flux and other two schemes are reduced order observer and deadbeat observer.

Chapter-IV discusses in general artificial neural network, feedforward neural network, and feedforward backpropagation network. It also discusses about how mapping is achieved, neural network structure, how a network can be trained and the backpropagation algorithm.

Chapter-V discusses field orientation control of induction motor. It also discusses principle of field orientation, direct and indirect vector control method. It also discusses voltage fed, current fed, field orientation based controller.

Chapter-VI presents the observer performance. It also presents transient and steady states performance of observer with parameter mismatch between the controller and the machine and rotor resistance adaptation conditions.

Chapter-VII presents flux estimation using artificial neural network. It also discusses how the simulation is achieved.

Finally, conclusions are drawn in chapter-VIII with a few proposals for further research work related to the present work.

## CHAPTER II

### MATHEMATICAL MODEL OF INDUCTION MOTOR

#### 2.1 INTRODUCTION

A polyphase induction motor has a complex structure comprising of mutually coupled magnetic and electric circuits. When the stator and rotor coils are excited by balanced source, fluxes are produced in the stator and rotor core. The mutual flux system is common to coils both in stator and rotor and is responsible for the effective operation of the motor. The leakage flux is responsible for causing voltage drop in the coils. Due to mutual coupling between stator and rotor coils, rotor receives power by induction. There are three system of fluxes in an induction motor, viz, the stator flux, the air gap flux and the rotor flux. In a dc motor, torque is viewed as the product of field flux and armature mmf, which are mutually perpendicular to each other. Similarly, in an induction motor it can assumed that the flux of rotor and perpendicular mmf in the stator or vice versa generates the electromagnetic torque. Other viewpoint assumes power in the rotor resistance as a measure of torque expressed in synchronous watts.

To study the performances of different control systems and drives, the motor requires to be represented by a set of differential equations in time domain. Complexity arises due to variable coupling between the physical coils of the stator and the rotor. The complexity is further enhanced due to the effect of back emf in the rotor circuit. So it is not wise to model an induction motor using the physical coils.

Based on operating conditions, there are a number of mathematical models for induction motors. To study the transient/dynamic conditions generally mutually perpendicular stationary/synchronously rotating fictitious coil are considered.

#### 2.2 STATIONARY TWO-AXIS MODEL

In an induction motor the stampings, which are slotted to receive the three phase windings and the stator carries a three phase winding and is fed from a three phase supply. The rotor also consists of core for carrying three phase windings bars. Mathematically a winding can be modeled as self-inductance  $L$  some internal resistance  $R$ . Suffices  $s$  and  $r$  indicates stator and rotor. The transfer of energy from stator to the

rotor of an induction motor takes place entirely inductively with the help of a flux mutually linking the two. So the term mutual inductance  $L_m$  comes between the two.

It is well documented in the literature [35] that an induction motor can adequately be modeled using a two-axis representation. Under the usual assumptions of sinusoidal distribution of MMFs, ignoring the effect of iron loss and saturation, etc, the dynamic equations which describes a symmetrical induction motor in orthogonal stationary reference frame  $\alpha - \beta$  fixed on the stator may be expressed as:

### 2.2.1 INDUCTION MOTOR MODEL

A 3-phase induction motor has three coils in the rotor and three coils in the stator. The rotor coils are rotating with an angular velocity  $\omega_r$ . The three-phase winding and their orientation are shown in Fig. 2.1. It appears that the coupling between the stator and rotor coils is a function of position of the rotor and is continuously variable. So it is not wise to model an induction motor using its physical windings. The variables of an induction motor are phases and it can be modeled by equivalent two windings in lieu of three. In this consideration three stationary stator windings may easily be represented by two equivalent stationary windings. To avoid the complexity of variable coupling, two equivalent stationary windings are considered for rotor circuit. In this connection voltages due to rotor speed are duly considered. In the mutually perpendicular frame there is no coupling between the axes quantities, which results in a simple system. Considering the voltage drops in the stator due to resistance, self and mutual inductance the stator circuit equations are written. In addition to these the speed voltage terms are considered for rotor circuit. The stator and rotor circuit voltage equations of an induction motor are given in eqn. (2.1). Well judged assumptions of no saturation, sinusoidal distribution of flux and mmf and ignoring the effect of iron loss results this set of equations. The stationary axes are identified as  $\alpha - \beta$  [19]

$$\begin{bmatrix} v_{\alpha S} \\ v_{\beta S} \\ 0 \\ 0 \end{bmatrix} = \begin{bmatrix} R_s + L_s p & 0 & L_m p & 0 \\ 0 & R_s + L_s p & 0 & L_m p \\ L_m p & L_m \omega_r & R_r + L_r p & L_r \omega_r \\ -L_m \omega_r & L_m p & -L_r \omega_r & R_r + L_r p \end{bmatrix} \begin{bmatrix} i_{\alpha s} \\ i_{\beta s} \\ i_{\alpha r} \\ i_{\beta r} \end{bmatrix} \quad (2.1)$$



The developed electro-magnetic torque for an induction motor of  $P_p$  -pole pairs is

$$T_{em} = P_p (i_{ar} [L_m i_{\beta s} + L_r i_{\beta r}] - i_{\beta r} [L_m i_{\alpha s} + L_r i_{\alpha r}]) \quad (2.2a)$$

And the torque balance equation is

$$T_{em} = J \frac{d\omega_m}{dt} + B\omega_m + T_L \quad (2.2b)$$

In the above equations

$v_{\alpha s}, v_{\beta s}$        $\alpha$  -and  $\beta$  -axis stator voltage components

$i_{\alpha s}, i_{\beta s}$        $\alpha$  -and  $\beta$  -axis stator current components

$i_{\alpha r}, i_{\beta r}$        $\alpha$  -and  $\beta$  -axis rotor current components

$J$                       moment of inertia

$B$                       rotational damping coefficient

$\omega_m$                    speed of the motor

$T_L$                     load torque

### 2.2.2 PHASE RELATIONSHIP

The physical phasors and the fictitious two-axis phasors are shown in Fig. 2.3. Considering the voltages in the axes systems, the relationship among them is established as:

$$\begin{aligned} v_{\alpha} &= v_a - \frac{1}{2}v_b - \frac{1}{2}v_c \\ v_{\beta} &= -\frac{\sqrt{3}}{2}v_b + \frac{\sqrt{3}}{2}v_c \end{aligned} \quad (2.3)$$

Similar relationship exists between the currents.

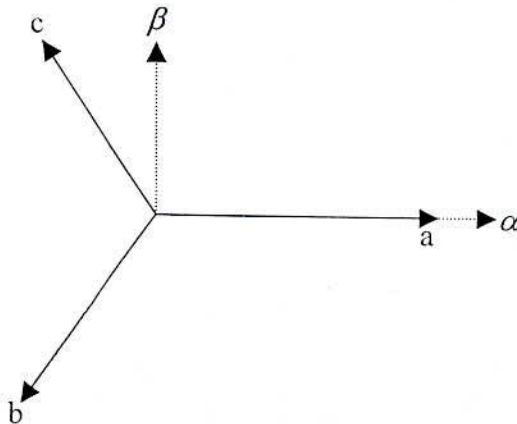


Fig. 2.3 Physical and fictitious two-axis phasors.

### 2.2.3 VOLTAGE SOURCE INVERTER FEEDING AN INDUCTION MOTOR

In speed controlled induction motor drive the motor is fed from a three-phase inverter. The inverter output voltage and current are controlled in a number of ways. The PWM method uses a number of positive and negative pulses per half cycle to control the magnitude and frequency of fundamental component of ac voltage. The simplest inverter generates square voltage waves at the output. From equation (2.1), the basic circuit equations in the stationary reference frame of induction machine can be written

$$\text{as } \begin{bmatrix} v_s \\ 0 \end{bmatrix} = \begin{bmatrix} (R_s + pL_s)I & pL_m I \\ pL_m I - \omega_r L_m J & (R_r + pL_r)I - L_r \omega_r J \end{bmatrix} \begin{bmatrix} i_s \\ i_r \end{bmatrix} \quad (2.4)$$

$$\lambda_r = L_m i_s + L_r i_r \quad (2.5)$$

Where  $p = \frac{d}{dt}$  is the time derivative.

The state and output equations are easily derived from equation (2.4) and (2.5) as:

$$\frac{d}{dt} \begin{bmatrix} i_s \\ \lambda_r \end{bmatrix} = \begin{bmatrix} A_{11} & A_{12} \\ A_{21} & A_{22} \end{bmatrix} \begin{bmatrix} i_s \\ \lambda_r \end{bmatrix} + \begin{bmatrix} B_1 \\ 0 \end{bmatrix} v_s \quad (2.6)$$

$$i_s = [I \quad 0] \begin{bmatrix} i_s \\ \lambda_r \end{bmatrix} \quad (2.7)$$

Where,

$$A_{11} = - \left\{ \frac{R_s}{\sigma L_s} + R_r \frac{(1 - \sigma^2)}{\sigma L_r} \right\} I$$

$$A_{12} = \frac{L_m}{\sigma L_s} L_r \left\{ \frac{R_r}{L_r} \right\} I - \omega_r J$$

$$A_{21} = \frac{L_m R_r}{L_r} I$$

$$A_{22} = -\frac{R_r}{L_r} I + \omega_r J$$

$$B_1 = \frac{1}{\sigma L_s} I$$

$$I = \begin{bmatrix} 1 & 0 \\ 0 & 1 \end{bmatrix}, J = \begin{bmatrix} 0 & -1 \\ 1 & 0 \end{bmatrix} \quad (2.8)$$

$$\sigma = 1 - \left( \frac{L_m^2}{L_s L_r} \right); \text{ leakage coefficient} \quad (2.9)$$

The state variables are the primary current  $i_s = [i_{\alpha s}, i_{\beta s}]^T$  and the rotor flux  $\lambda_r = [\lambda_{\alpha r}, \lambda_{\beta r}]^T$ .

The input is the primary voltage  $v_s = [v_{\alpha s}, v_{\beta s}]^T$ .

### 2.3 ROTATING TWO-AXIS MODEL

It is well known that the flux and mmf of an induction motor are synchronously rotating. To visualize the phenomenon of torque production and performance of the induction motor the synchronously rotating mutually perpendicular axes system is considered. This model is also suitable for current fed inverted-coupled system. According to two-axis machine theory, when a symmetrical induction motor is described in a reference frame that rotates in synchronism with the stator mmf, all the ac phase-variable sets get transformed into equivalent dc variables. Under the usual assumptions of no hysteresis, eddy currents, space harmonics, etc., the basic system equation of an induction motor in terms of a 2-phase model (d-q variables) in an arbitrary synchronous reference frame is [19]

$$\begin{bmatrix} v_{ds} \\ v_{qs} \\ 0 \\ 0 \end{bmatrix} = \begin{bmatrix} R_s + pL_s & -\omega_e L_s & pL_m & -L_m \omega_e \\ \omega_e L_s & R_s + pL_s & L_m \omega_e & pL_m \\ pL_m & -L_m \omega_{sl} & R_r + pL_r & -L_r \omega_{sl} \\ L_m \omega_{sl} & pL_m & L_r \omega_{sl} & R_r + pL_r \end{bmatrix} \begin{bmatrix} i_{ds} \\ i_{qs} \\ i_{dr} \\ i_{qr} \end{bmatrix} \quad (2.10)$$

Fig. 2.4 shows the spatial relationship between the axes of different frames of reference viz. stator-fixed, rotor-fixed, and synchronously rotating d-q reference frames.

$$\text{The electromagnetic torque is } T_{em} = \frac{3}{2} P_p (\lambda_{qr} i_{dr} - \lambda_{dr} i_{qr}) \quad (2.11)$$



and the torque balance equation remain unchanged as in equn. 2.2(b).

Where

$$\lambda_{dr} = L_r i_{dr} + L_m i_{ds} \quad (2.12a)$$

$$\lambda_{qr} = L_r i_{qr} + L_m i_{qs} \quad (2.12b)$$

The variables  $\lambda_{dr}$  and  $\lambda_{qr}$  imply flux linkages with the rotor circuits along the synchronously rotating d- and q-axis respectively.

Substitution of (2.12a) and (2.12b) in (2.11) yields

$$T_{em} = \frac{3}{2} P_p L_m (i_{qs} i_{dr} - i_{ds} i_{qr}) \quad (2.13)$$

With reference to Fig. 2.4 if  $i_{dq}$  is the magnitude of the vector current  $\bar{I}_{dq}$ , the corresponding d- and q-axis currents in the synchronous reference frame are

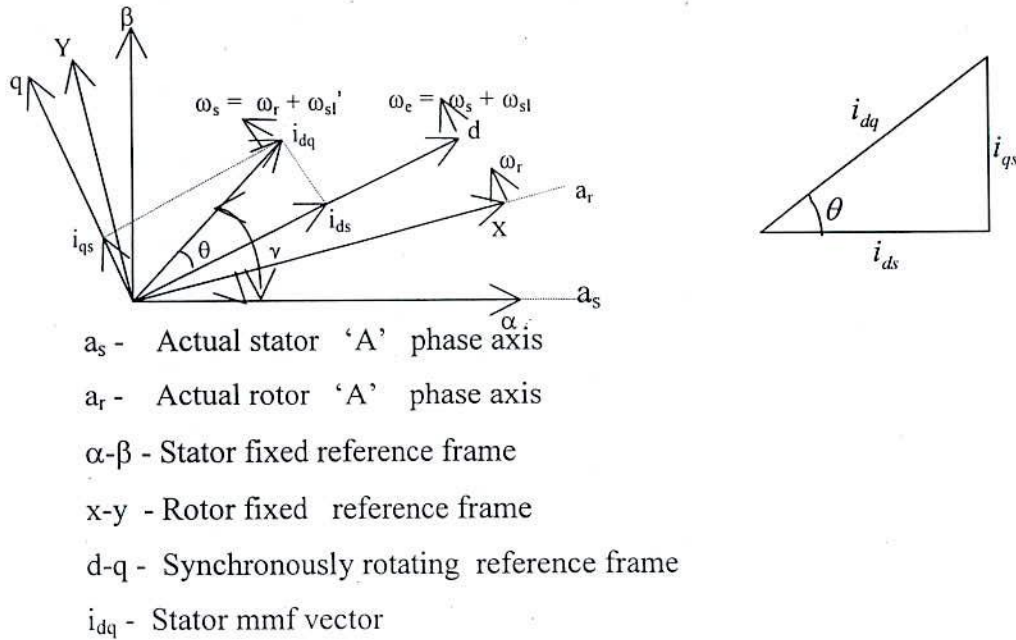


Fig.2.4: Relation between various co-ordinate systems and principle of field orientation.

$$\begin{aligned} i_{ds} &= i_{dq} g_{ds} \\ i_{qs} &= i_{dq} g_{qs} \end{aligned} \quad (2.14)$$

Where

$$g_{ds} = \cos \theta$$

$$g_{qs} = \sin \theta$$

$$\tan \theta = \frac{i_{qs}}{i_{ds}} \quad (2.15)$$

### 2.3.1 CURRENT SOURCE INVERTER FED SYSTEM

For the current-fed induction motor drive system in Fig.2.2, the power balance equation, with no loss in the inverter, is

$$v_I i_R = \frac{3}{2} (v_{ds} i_{ds} + v_{qs} i_{qs}) \quad (2.16)$$

Use of (2.14) in (2.16) yields

$$v_I i_R = \frac{3}{2} i_{dq} (v_{ds} g_{ds} + v_{qs} g_{qs}) \quad (2.17)$$

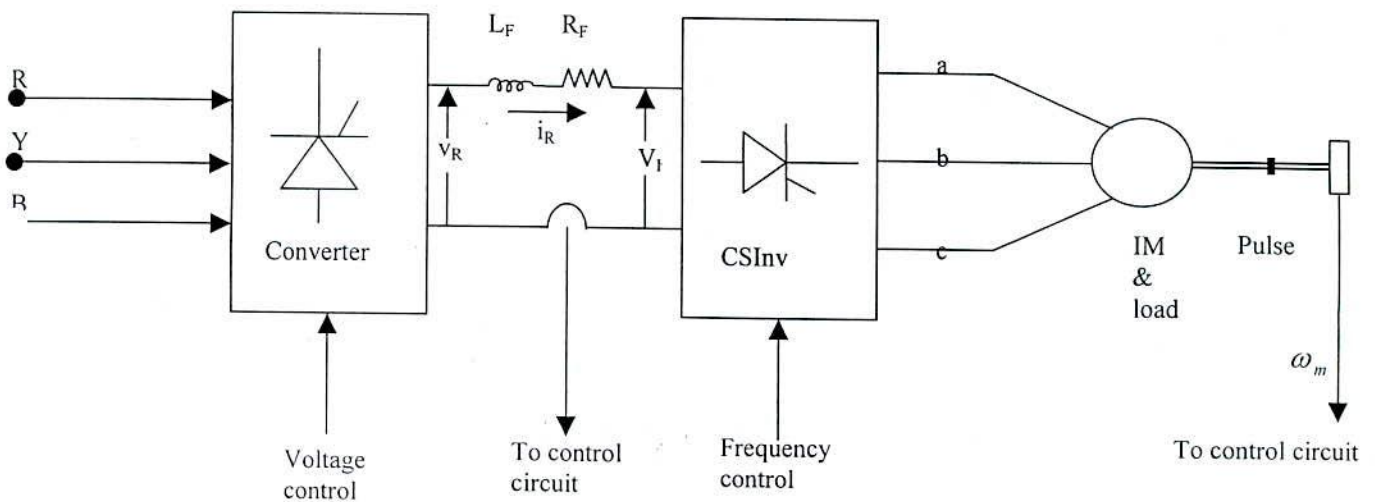


Fig.2.5 CSI-IM drive system.

If the commutation effect is ignored, the stator current of the induction motor, supplied by a current source inverter, is a  $120^\circ$  wide square wave of magnitude  $I_R$  in each half cycle. Other than causing ohmic losses, the harmonic currents have no significant contribution to the generation of net torque [36]. Neglecting the harmonics, the fundamental component of vector current magnitude  $I_{dq}$  in (2.17) is related to the dc link current  $i_R$  by

$$i_{dq} = \frac{2\sqrt{3}}{\pi} i_R \quad (\text{Fundamental component}) \quad (2.18)$$

$$= i'_R$$

Substitution of (2.18) in (2.17) gives

$$v_I = \frac{3\sqrt{3}}{\pi} (v_{ds} g_{ds} + v_{qs} g_{qs})$$

Or,  $v'_I = v_{ds} g_{ds} + v_{qs} g_{qs}$  (2.19)

Where,  $v'_I = \frac{\pi}{3\sqrt{3}} v_I$  (2.19a)

Although the steady state operation of controlled current induction motor drives do neither involve the stator input voltage nor the rectifier output voltage responsible for maintaining the dc link current at the required level, the transient behavior of the dc link current significantly affects the dynamic behavior of the CSIM drives.

For the dc link circuit (Fig.2.5) the voltage equation is

$$v_R = v_I + (R_f + pL_f) i_R \quad (2.20)$$

Combining (2.19a) and (2.20), and using the relation in (2.18), yields

$$v'_R = v'_I + (R'_f + pL'_f) i'_R \quad (2.21)$$

Where

$$v'_R = \frac{\pi v_R}{3\sqrt{3}}$$

$$R'_f = \frac{\pi^2}{18} R_f$$

$$L'_f = \frac{\pi^2}{18} L_f$$

Rectifier output power and inverter input are given by (2.22) and (2.23) respectively

$$P_R = v_R i_R = \frac{3}{2} v'_R i'_R \quad (2.22)$$

$$P_I = v_I i_R = \frac{3}{2} v'_I i'_R \quad (2.23)$$

From the relations in (2.14) and (2.18) it is noted that

$$i'_R = i_{ds} g_{ds} + i_{qs} g_{qs} \quad (2.24)$$

Substituting the expression for  $v_{ds}$  and  $v_{qs}$  from (2.10) in (2.19) and using (2.14) and (2.18), one obtains

$$v'_l = (R_s + pL_s)i'_R + L_m(g_{ds}pi_{dr} + g_{qs}pi_{qr}) + L_m\omega_e(g_{qs}i_{dr} - g_{ds}i_{qr}) \quad (2.25)$$

Using (2.25) in (2.21) gives

$$v'_R = [(R_s + R'_f) + (L_s + L'_f)p]i'_R + L_m(g_{ds}pi_{dr} + g_{qs}pi_{qr}) + L_m\omega_e(g_{qs}i_{dr} - g_{ds}i_{qr}) \quad (2.26)$$

## CHAPTER III

### FLUX OBSERVERS

#### 3.1 INTRODUCTION

The very first step in the analytical study of systems is to set up mathematical equations to describe the systems. Because of different analytical methods used, it may be often set up different mathematical models to describe the same system. When, for any reason, the analysis in the time-domain is to be preferred, the use of so-called state-space approach will offer a great deal of convenience conceptually, notationally, and sometimes analytically. The conceptual convenience is derived from the elegant representation of the instantaneous condition of the system by the notation of the system state. The notational and analytical conveniences come through the use of vector-matrix representation, which allows the system equations and the form of solutions to be written compactly. The adaptation of state-space representation to the numerical solution is an added advantage, particularly when the system to be investigated contains time-varying and nonlinear elements.

Unfortunately, in practice, not all the state variables are accessible to measurements. It can assume that only the outputs and inputs are measurable. So, the need of a subsystem that performs the observation of the state variables based on the information received from the measurement of the input and output is needed. This subsystem is called an observer and whose design is based on the observability.

#### 3.2 MATHEMATICAL BACKGROUND

Consider the linear time-invariant system

$$\dot{x}(t) = Ax(t) + Bu(t) \tag{3.1}$$

$$y(t) = Cx(t) + Du(t) \tag{3.2}$$

Where  $x$  is the  $n \times 1$  state vector,  $u$  is the  $p \times 1$  input vector,  $y$  is the  $q \times 1$  output vector and  $A, B, C$  and  $D$  are, respectively,  $n \times n, n \times p, q \times n$  and  $q \times p$  real constant matrices respectively. The time interval of interest is  $[0, \infty]$ .

For this system, the control law depends linearly on  $r(t)$  and  $x(t)$  and is of the form

$$u(t) = r(t) + Kx(t) \dots(3.2)$$

Where  $r(t)$  stands for reference input and  $K$  is some real constant matrix called the feedback matrix. Finding the best  $K$  is the scope of optimal control theory. Here the effect of introducing linear feedback of the form (3.2) will be discussed and what can be achieved by introducing this state feedback will be studied.

The state model of the closed-loop system obtained from eqns. (3.1) and (3.2) is

$$\dot{x}(t) = (A + BK)x(t) + Br(t) \quad (3.3)$$

$$y(t) = (C + DK)x(t) + Dr(t) \quad (3.4)$$

This closed-loop system is represented schematically in Fig. 3.1, with the block of dotted lines enclosing

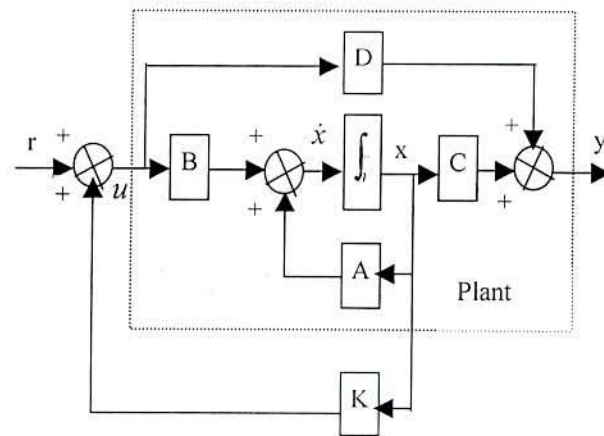


Fig. 3.1 Structure of a state feedback control system.

Another related problem taken up in this chapter is that of the implementation of the linear state feedback control law (3.2), which requires the ability to directly measure the entire state vector  $x(t)$ . In general, however, only the input vector  $u(t)$  and the output vector  $y(t)$  are directly measurable and so the state feedback control law cannot be implemented. Thus, either a new approach that directly accounts for the nonavailability of entire state vector is to be devised or a suitable approximation (reconstruction) of the state vector must be determined. The latter approach is much simpler in many situations.

There are two simple solutions to the problem of the reconstruction of a state vector. One is to construct a model of the system, which has all of its state variables directly measurable. Any input signal is applied to the system as well as to the model. Thus, even if the state vector of the original system cannot be measured, the model's state variables, which are equivalent to those of the system, are available (Fig. 3.2). It is also necessary to set the current initial conditions on the model.

There are two disadvantages in using this method of reconstruction. First, the initial state must be identified and set each time we use the estimator. The second and more serious is that, if the matrix  $A$  has an eigenvalue with positive real part, then even for a very small difference between  $x(t_0)$  and  $\hat{x}(t_0)$  at some  $t = t_0$ , which may be caused by a disturbance entering the system but is not in the model or by incorrect estimation of the initial state, the difference between the real state  $x(t)$ , and the reconstructed state  $\hat{x}(t)$  will increase with time.

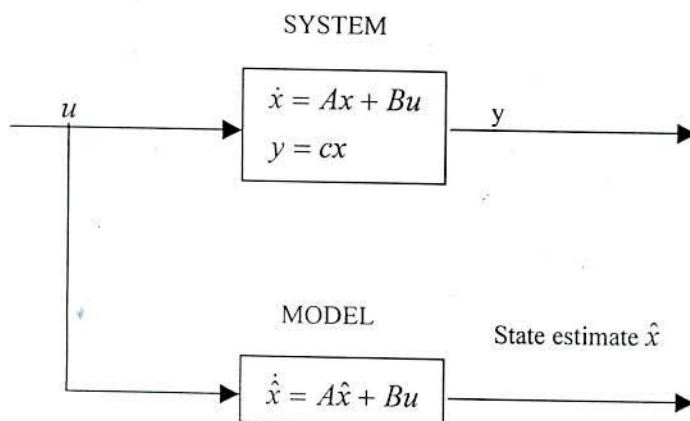


Fig.3.2 Reconstruction of the state.

Another method consists of differentiating the output (and input) variables a certain number of times and combining these terms to form the unmeasured state variables. The poor noise characteristics and the difficulty of building good differentiators generally make this method impractical.

### 3.3 FULL-ORDER OBSERVER

A full order observer is the observer, which would attempt to estimate all of the variables of a system (or equivalent combinations of them) that together make up the state variables in the model of that system.

Based on (2.6), a full-order observer for estimating  $\{i_s, \lambda_r\}$  can be implemented by following:

$$P \begin{bmatrix} \hat{i}_s \\ \hat{\lambda}_r \end{bmatrix} = \begin{bmatrix} A_{11} & A_{12} \\ A_{21} & A_{22} \end{bmatrix} \begin{bmatrix} \hat{i}_s \\ \hat{\lambda}_r \end{bmatrix} + \begin{bmatrix} B_1 \\ 0 \end{bmatrix} v_s + G(\hat{i}_s - i_s) \quad (3.5)$$

where  $\{\hat{i}_s, \hat{\lambda}_r\}$  are estimated stator current and rotor flux vectors, respectively.  $A_{ij}$  is the matrix in which  $\omega_r$  and  $R_s$  are replaced by estimated rotor speed  $\hat{\omega}_r$  and stator resistance  $R_s^*$  set in the observer.  $G$  is the feedback gain of the observer. Other parameter values of  $A_{ij}$  are assumed to be set as normal values. If the pole position of the observer is assigned as  $k$  times ( $k \leq 1$ ) as that of the motor,  $G$  will be a function of the rotor speed, and the observer will be stable at any rotor speed.  $G$  is defined in (3.6). As a result, the estimated states will converge to actual values in any rotor speed range.

$$G = \begin{bmatrix} g_1 I + g_2 J \\ g_3 I + g_4 J \end{bmatrix} = \begin{bmatrix} g_1 & g_2 & g_3 & g_4 \\ -g_2 & g_1 & -g_4 & g_3 \end{bmatrix}^T \quad (3.6)$$

where,

$$\begin{aligned} g_1 &= (k-1)(\hat{a}_{r11} + \hat{a}_{r22}), \\ g_2 &= (k-1)\hat{a}_{r22}, \\ g_3 &= (k^2-1)(\hat{a}_{r21} - \rho\hat{a}_{r11}) + \rho g_1, \\ g_4 &= \rho g_2. \end{aligned}$$

According to a model reference adaptive system (MRAS). The error between the states  $\{i_s, \lambda_r\}$  and the states  $\{\hat{i}_s - \hat{\lambda}_r\}$  can be used to drive an adaptive mechanism to adjust estimated speed  $\hat{\omega}_r$ . The adaptive mechanism should guarantee that, when  $\hat{\omega}_r$  is adjusted to  $\omega_r$ , estimated vector  $\begin{bmatrix} \hat{i}_s \\ \hat{\lambda}_r \end{bmatrix}^T$  will converge to vector  $\begin{bmatrix} i_s \\ \lambda_r \end{bmatrix}^T$ . Fig. 3.3 and Fig 3.4



shows the Rotor Flux estimation and motor speed estimation with full order observer respectively.

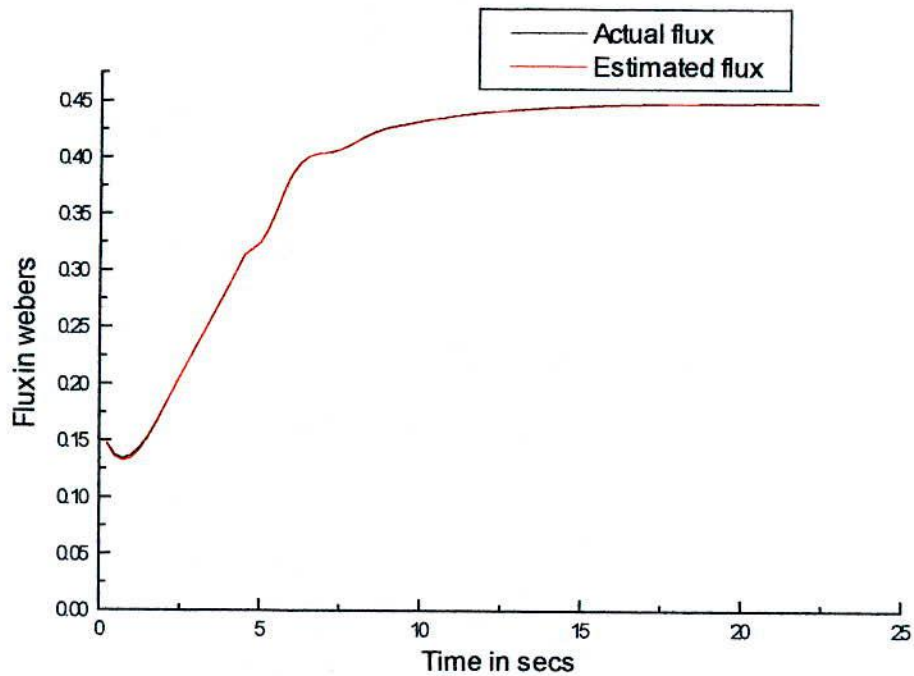


Fig. 3.3 Rotor Flux estimation with full order observer.

### 3.3.1 THE SEPARATION PRINCIPLE

To obtain a fast convergence of the estimation error  $\tilde{x}$  to zero, it will be tempted to choose  $M$  so that the observer poles are quite deep in the left half plane. For pole placement by state feedback, it will be observed that state feedback control law can be used on a linear system to place its closed loop poles in any desired configuration. If the entire state is not available for feedback, it looks reasonable to estimate the state employing an observer and using the estimate in the control law. In this subsection, we consider control systems requiring both the feedback control and the state estimation.

Consider a controllable and observable time-invariant  $n$ -dimensional system

$$\begin{aligned}\dot{x} &= Ax + Bu \\ y &= Cx\end{aligned}\tag{3.7}$$

It is assumed that a control law of the form

$$u = kx + r\tag{3.8}$$

has been found to place the poles of the closed-loop system in any desired configuration. If the state is not directly available for measurement, it can be proposed to construct an observer of the form

$$\dot{\hat{x}} = (A + MC)\hat{x} + Bu - My\tag{3.9}$$

and interconnect the control law with the reconstructed state  $\hat{x}$ :

$$u = K\hat{x} + r\tag{3.10}$$

Fig. 3.4 depicts the interconnection of the plant, the observer and the control law. For the purpose of analysis, it may look upon the plant (3.7) and observer (3.9) as a composite system of dimension  $2n$ ,

$$\begin{bmatrix} \dot{x} \\ \dot{\hat{x}} \end{bmatrix} = \begin{bmatrix} A & BK \\ -MC & A + MC + BK \end{bmatrix} \begin{bmatrix} x \\ \hat{x} \end{bmatrix} + \begin{bmatrix} B \\ B \end{bmatrix} r\tag{3.11}$$

By the equivalence transformation

$$\begin{bmatrix} x \\ \tilde{x} \end{bmatrix} = \begin{bmatrix} I & 0 \\ I & -I \end{bmatrix} \begin{bmatrix} x \\ \hat{x} \end{bmatrix} = \begin{bmatrix} x \\ x - \hat{x} \end{bmatrix}$$

Eqn. 3.11 becomes

$$\begin{bmatrix} \dot{x} \\ \dot{\tilde{x}} \end{bmatrix} = \begin{bmatrix} A + BK & -BK \\ 0 & A + MC \end{bmatrix} \begin{bmatrix} x \\ \tilde{x} \end{bmatrix} + \begin{bmatrix} B \\ 0 \end{bmatrix} r\tag{3.12}$$

The eigenvalues of (3.12), which are the eigenvalues of (3.11), are the zeros of

$$\begin{aligned}\det \begin{bmatrix} sI - (A + BK) & BK \\ 0 & sI - (A + MC) \end{bmatrix} \\ = \det(sI - (A + BK)) \det(sI - (A + MC))\end{aligned}$$

Consequently, the set of closed-loop eigenvalues comprises the eigenvalues of  $A+BK$  and the eigenvalues of  $A+MC$ . Thus, it may consider the problem of determining a stable

observer and the state feedback control law separately, since their interconnection results in a stable control system. This property is often called the separation principal.

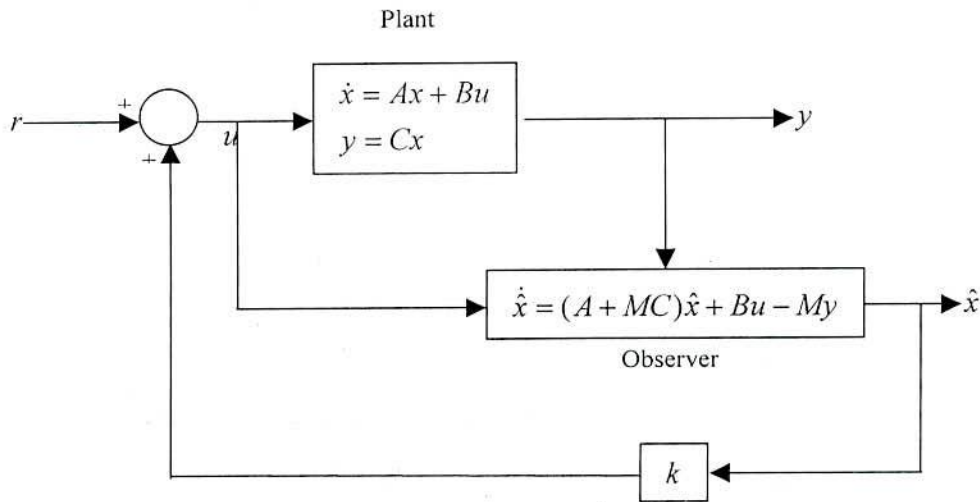


Fig. 3.4 Use of the observer to implement state feedback control law.

### 3.4 REDUCED-ORDER OBSERVERS

The state observer discussed in the earlier section, was derived by setting up a model of the plant and feeding back a “correction term” proportional to the difference between the actual and estimated outputs. Such an observer contains redundancy because  $q$  state variables can be directly obtained from  $q$  outputs which are available for measurement and need not be estimated. The remaining  $(n - q)$  state variables can be estimated using an observer of order  $(n - q)$ , as will be seen below.

Let the given observable plant be

$$\begin{aligned} \dot{x} &= Ax + Bu \\ y &= Cx \end{aligned} \tag{3.13}$$

Where  $A$  and  $C$  are in the multivariable observable companion form. Assuming  $C$  to be of full rank, there will be  $q$  observability indices,  $\mu_1, \mu_2, \dots, \mu_q$ . Thus  $A$  and  $C$  each

has  $q$  significant columns  $\sigma^k = \sum_{i=1}^k \mu_i$  for  $k = 1, 2, \dots, q$ .

$$\text{Let } x_2 = \begin{bmatrix} x_{\sigma_1} \\ x_{\sigma_2} \\ \vdots \\ x_{\sigma_q} \end{bmatrix} \text{ and } x_1 = \begin{bmatrix} x_1 \\ \vdots \\ x_{\sigma_1-1} \\ x_{\sigma_1+1} \\ \vdots \\ x_{\sigma_q-1} \end{bmatrix} \quad (3.14)$$

I.e., the state vector is partitioned into two groups.

The system (3.13), in the observable companion form, may be rearranged as follows:

$$\begin{bmatrix} \dot{x}_1 \\ \dot{x}_2 \end{bmatrix} = \begin{bmatrix} A_{11} & A_{12} \\ A_{21} & A_{22} \end{bmatrix} \begin{bmatrix} x_1 \\ x_2 \end{bmatrix} + \begin{bmatrix} B_1 \\ B_2 \end{bmatrix} u \quad (3.15a)$$

$$y = \begin{bmatrix} 0 & C_q \end{bmatrix} \begin{bmatrix} x_1 \\ x_2 \end{bmatrix} \quad (3.15b)$$

The  $q$  state variables  $x_2$  can be directly obtained from (3.15b) as

$$x_2 = [C_q]^{-1} y \quad (3.16)$$

The remaining  $(n-q)$  state variables require an observer for estimation.

By manipulating the equations in (3.15),  $x_1$  may be viewed as the state of a  $(n-q)$  dimensional sub-system.

$$\begin{aligned} \dot{x}_1 &= A_{11}x_1 + A_{12}x_2 + B_1u \\ &= A_{11}x_1 + v \end{aligned}$$

$$z = A_{21}x_1$$

$$\text{where,} \quad (3.17)$$

$$\begin{aligned} v &= A_{12}x_2 + B_1u \\ &= A_{12}[C_q]^{-1}y + B_1u \end{aligned}$$

$v$  can be treated as a known input since  $u$  is known and  $y$  is directly measurable.

The "output vector"  $z$  may be expressed as

$$\begin{aligned} z &= A_{21}x_1 \\ &= \dot{x}_2 - A_{22}x_2 - B_2u \\ &= [C_q]^{-1}\dot{y} - A_{22}[C_q]^{-1}y - B_2u \end{aligned} \quad (3.18)$$

$x_1$  can estimate with an observer

$$\dot{\hat{x}}_1 = (A_{11} + M_1 A_{21})\hat{x}_1 + v - M_1 z \quad (3.19)$$

where, the  $(n-q) \times q$  matrix  $M_1$  may be chosen so as to place the poles of (3.19) in any desired configuration. Substituting for  $v$  and  $z$  from (3.17) and (3.18) respectively, it has been obtain

$$\begin{aligned} \dot{\hat{x}}_1 &= (A_{11} + M_1 A_{21})\hat{x}_1 + A_{12}[C_q]^{-1}y + B_1 u \\ &- M_1[C_q]^{-1}\dot{y} + M_1 A_{22}[C_q]^{-1}y + M_1 B_2 u \end{aligned} \quad (3.20)$$

Which is an  $(n \times q)$  dimensional observer for the system (3.13).

The only apparent difficulty in implementing the observer (3.20) is that differentiation of the output  $y$  is required. This can be avoided by redefining the state of the observer to be

$$\bar{x}(t) = \hat{x}_1(t) + M_1[C_q]^{-1}y(t) \quad (3.21)$$

Substituting (3.21) in (3.20), we get

$$\begin{aligned} \dot{\bar{x}} &= (A_{11} + M_1 A_{21})\bar{x} + (B_1 + M_1 B_2)u \\ &+ [A_{12} + M_1 A_{22} - (A_{11} + M_1 A_{21})M_1][C_q]^{-1}y \end{aligned} \quad (3.22)$$

The estimate of the full state  $x$  is given by

$$\begin{aligned} \hat{x} &= \begin{bmatrix} \hat{x}_1 \\ [C_q]^{-1}y \end{bmatrix} = \begin{bmatrix} \bar{x} - M_1[C_q]^{-1}y \\ [C_q]^{-1}y \end{bmatrix} \\ &= \begin{bmatrix} I \\ 0 \end{bmatrix} \bar{x} + \begin{bmatrix} -M_1 \\ I \end{bmatrix} [C_q]^{-1}y \end{aligned} \quad (3.23)$$

Since the reduced order observer has a direct link from the observed variable  $y(t)$  to the estimated state  $\hat{x}(t)$ , the estimate  $\hat{x}(t)$  will be more sensitive to measurement errors in  $y(t)$  than the estimate generated by a full-order observer. This is because the noise bypasses the natural filtering action of the observer dynamics. It may be verified that the separation principle holds for observer of any dimension.

### 3.4.1 REDUCED ORDER (GOPINATH) OBSERVER

It is a combination of the flux simulator and the predictive error correction feedback.

$$\begin{aligned}\dot{\hat{\lambda}}_r &= A_{21}i_s + A_{22}\hat{\lambda}_r + G[(d/dt)i_s - (A_{11}i_s + A_{12}\hat{\lambda}_r + B_1v_s)] \\ &= (A_{22} - GA_{12})\hat{\lambda}_r + (A_{21} - GA_{11})i_s - GB_1v_s + G(d/dt)i_s\end{aligned}\quad (3.24)$$

$\hat{\phantom{x}}$  means the estimated value. The block diagram is shown in Fig. 3.6. In the case of no parameter variations, the dynamics of the estimation error:  $e = \hat{\lambda}_r - \lambda_r$  takes the form of

$$(d/dt)e = (A_{22} - GA_{12})e = -He \quad (3.25)$$

We can assign the observer poles any conjugate complex numbers by choosing the observer gain  $G$  approximately, because this system satisfies the observability condition.

Fig. 3.6 shows the estimation of rotor flux using this type of observer.

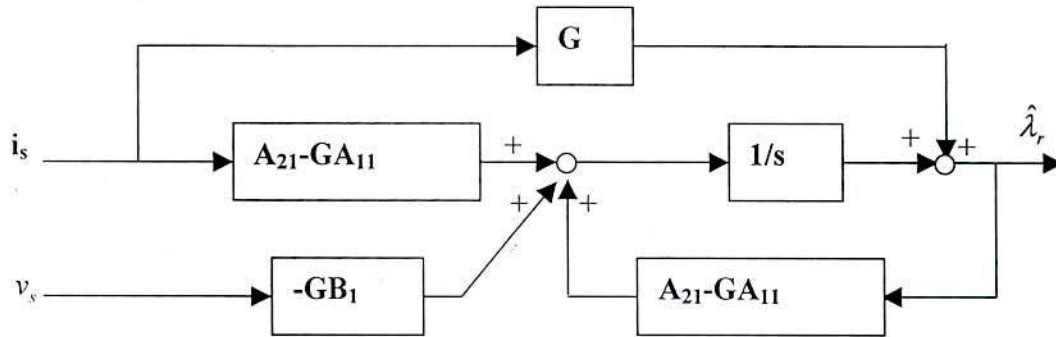


Fig. 3.5 Configuration of the Reduced Order (Gopinath) Flux Observer.

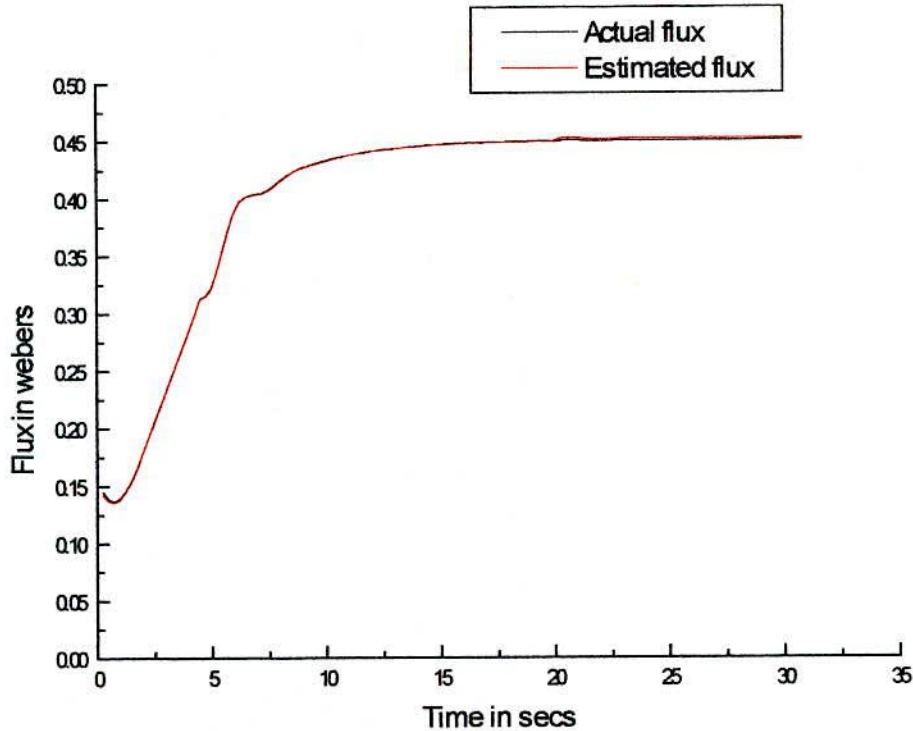


Fig. 3.6 Rotor flux estimation with the reducer order Gopinath type observer.

### 3.4.2 REDUCED ORDER (GENERALIZED) OBSERVER

For observer design, it is necessary to write the system equations in state space form with the rotor flux linkages as state variables. The standard state space representation of the system is written as:

$$\begin{aligned} \dot{x} &= Ax + Bu \\ y &= Cx \end{aligned} \tag{3.26}$$

The system described in (3.26) consists of the state variables  $\lambda_{dr}$  and  $\lambda_{qr}$  which are not measurable but the dc link current is easily measurable. For this system two out of the three state variables are needed to be observed. This requires reduced order observer proposed in [34]. The relationship between the observed and state variables are written as:

$$\xi = Tx. \tag{3.27}$$

Combining the output equation

$$\begin{pmatrix} y \\ \xi \end{pmatrix} = \begin{pmatrix} C \\ T \end{pmatrix} x \tag{3.28}$$

With reference to [34] the observer state space equation is written as:

$$\dot{\hat{\xi}} = D\hat{\xi} + Eu + Fy \quad (3.29)$$

Where,  $\hat{\xi}$  is the estimated state vector. D is the observer system matrix written in decoupled form with the eigen value as,

$$D = \begin{bmatrix} \lambda_1 & 0 \\ 0 & \lambda_2 \end{bmatrix} \quad (3.30)$$

E and F correlate the input and output with the observed variables. The error equation may be extracted from (3.29), (3.27) and (3.26) as

$$\dot{\hat{\xi}} - \dot{\xi} = D\hat{\xi} + Eu - Fcx - Tax - TBu \quad (3.31)$$

To have the error ( $\hat{\xi} - \xi$ ) driven to zero at suitable time elapse, the terms containing u should vanish, i.e

$$E = TB \quad (3.32)$$

With this criterion equation (3.31) may be written in the modified form as,

$$\overline{\dot{\hat{\xi}} - \dot{\xi}} = D(\hat{\xi} - \xi) + (DT - TA + FC)x \quad (3.33)$$

For the estimation error to decay with time as shown in (3.33) the versatile condition for reduced order observer is extracted below:

$$DT - TA + FC = 0 \quad (3.34)$$

Fig. 3.7 shows the estimation of rotor flux using this type of observer.



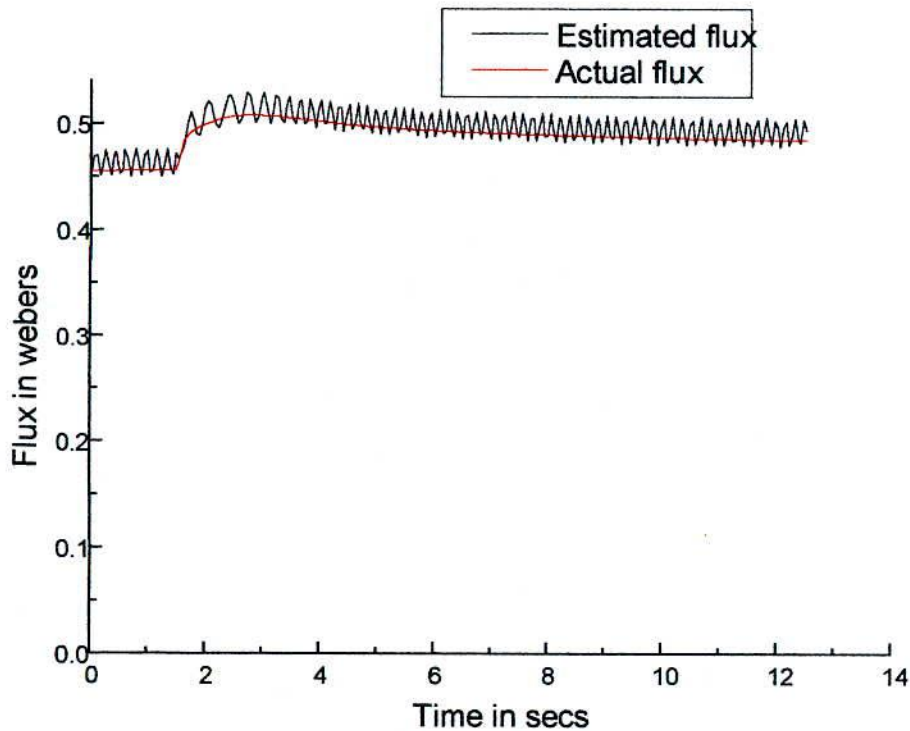


Fig. 3.7 Rotor flux estimation with the reducer order generalized type observer.

### 3.5 DEADBEAT CONTROL

In this and the next section, control and estimation problems of linear time-invariant discrete-time systems can be considered.

$$\begin{aligned} x(k+1) &= Fx(k) + Gu(k); \quad x(0) = x^o \\ y(k) &= Cx(k) \end{aligned} \tag{3.35}$$

where,  $F, G$  and  $C$  are  $n \times n, n \times p$  and  $q \times n$  real constant matrices respectively.

Feedback control laws may be derived for discrete-time systems using the techniques that have been developed for the continuous-time case. Linear feedback from state to input has the form

$$u(k) = Kx(k) + r(k) \tag{3.36}$$

Where,  $K$  is a constant,  $p \times n$  feedback gain matrix and  $r(k)$  is an external input.

Substituting (3.36) into (3.35), we get the following closed-loop system.

$$\begin{aligned}x(k+1) &= (F + GK)x(k) + Gr(k) \\y(k) &= Cx(k)\end{aligned}\tag{3.37}$$

The closed-loop poles, i.e., the eigenvalues of  $(F + GK)$  can be arbitrarily located in the complex plane (subject to conjugate pairing) by choosing  $K$  suitably if and only if (3.35) is completely controllable. It is possible to choose  $K$  such that the closed-loop system (3.37) is stable if and only if (3.35) is stable.

The computational methods of assigning closed-loop poles are identical to those developed for continuous-time case.

A case of special interest occurs when a state feedback control law is chosen which places all the closed-loop poles at the origin, i.e.,

$$\det(\lambda I - (F + GK)) = \lambda^n = 0$$

According to the Cayley-Hamilton theorem, any matrix satisfies its own characteristic equation. Therefore,

$$(F + GK)^n = 0$$

i.e.,  $(F + GK)$  is a nilpotent matrix of index  $n$ . This result implies that the force-free response of closed-loop system (3.37),

$$x(k) = (F + GK)^k x^0 = 0 \text{ for } k \geq n$$

In other words, any initial state  $x^0$  is driven to zero in (at most)  $n$  steps. The feedback control law that assigns all the closed-loop poles to origin, is therefore, a deadbeat control law.

### 3.6 DEADBEAT (POLE AT ORIGIN) OBSERVERS

In this section, discrete-time observers that are able to reconstruct the state of the system (3.35) has been considered. The results are identical to those of the continuous-time case. The system

$$\bar{x}(k+1) = (F + MC)\bar{x}(k) + Gu(k) - My(k); \quad \bar{x}(0) = \bar{x}^0\tag{3.38}$$

is a full-order observer for the observable system (3.35). The observer poles, i.e., eigenvalues of  $(F + MC)$  can arbitrarily be located in the complex plane (subject to conjugate pairing) by suitably choosing the gain matrix  $M$ .

As obtained from (3.35) and (3.38), the estimation error is governed by the equation

$$\tilde{x}(k+1) = x(k+1) - \hat{x}(k+1) = (F + MC)\tilde{x}(k) \quad (3.39)$$

The techniques of obtaining the M matrix are identical to the continuous time case. The block diagram realization is also identical except that the integrators are replaced by a delay of one-period.

A case of special interest occurs when all the observer poles are located at the origin, i.e., all the eigenvalues of  $(F + MC)$  are zero. Then

$$\det(\lambda I - (F + MC)) = \lambda^n = 0 \quad (3.40)$$

This implies as per Cayley-Hamilton theorem that,

$$(F + MC)^n = 0$$

Therefore, from (3.39) we have

$$\tilde{x}(n) = (F + MC)^n \tilde{x}^o = 0 \quad (3.41)$$

Thus, every initial value of the estimation error is reduced to zero in (at most) n steps. In analogy with the deadbeat control law, we refer to observers with this property as deadbeat observers.

The reduced-order discrete-time observers can be obtained analogously to the continuous-time case. The separation principle also carries over to the discrete-time systems. Fig. 3.8 shows the rotor flux estimation with deadbeat type observer.

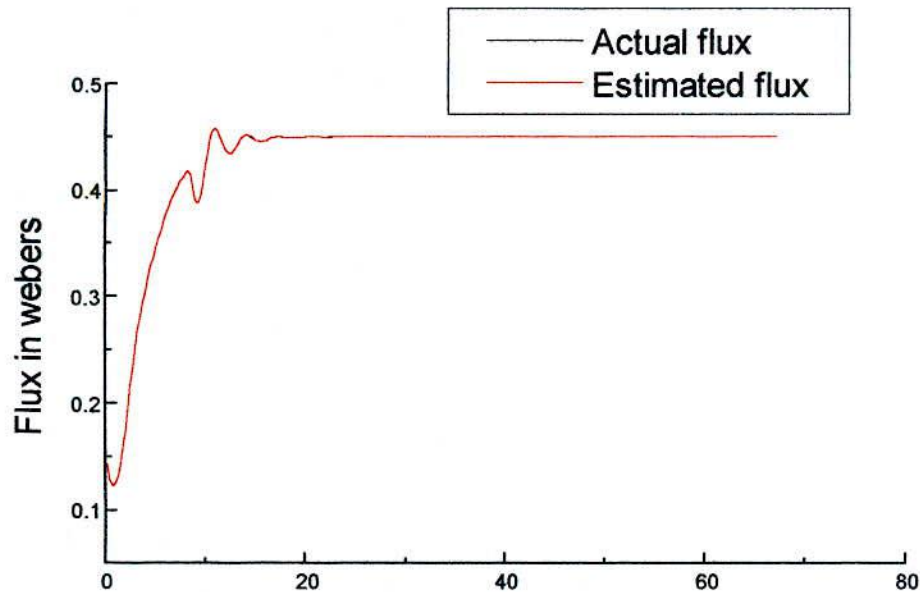


Fig. 3.8 Rotor flux estimation with the deadbeat type observer.

## CHAPTER IV

### ARTIFICIAL NEURAL NETWORK

#### 4.1 INTRODUCTION

An Artificial Neural Network (ANN) is a machine like the human brain with the properties of learning capability and generalization. It is used to represent functions as weighted sums of nonlinear terms. It has the property of learning capability, which makes it able to approximate very complicated nonlinear functions, and therefore, can be considered as a universal approximator. It has been shown [fig. 4.1] that a three-layer neural network with an input layer, an output layer and a hidden layer can represent almost any function with a determined number of neurons. The number of neurons in the hidden layer determines the accuracy of a specific application. Neural networks also have the property of being adaptive, which makes them very powerful in applications, where, the dynamics of a plant change with time or where the model of the system is partially known. Neural networks are gaining potential as controllers for many industrial applications due to the fact that they present better properties than the conventional controllers. However, they require a lot of training to understand the model of a plant or a process. The training algorithm used has an effect on issues such as learning speed, stability, and weight convergence. These issues remain as area of research and comparison of many training algorithms.

#### 4.2 FEEDFORWARD NEURAL NETWORKS

Feedforward neural networks are basically layers of neurons connected in cascade. The internal structure of a neuron consists of a summer and a nonlinearity as shown in Fig. 4.1. For the  $j$ th neuron of layer  $n$  of a neural network, there are  $n_{n-1}$  neurons in the preceding layer  $n-1$ , each having an output signal  $x_i^{n-1}$  and a threshold connected to neuron  $j$  by weights  $m_{ij}^n$  and  $th_j^n$ , respectively. The sum of these signals gives the internal sum  $y_j^n$ , which passes through a nonlinear function to give the output of the  $j$  neuron,  $x_j^n$ . This nonlinear function is also called the sigmoid function. There are many sigmoid functions in use, from which the mostly used function is

$$x_j^n = 1 - \frac{2}{1 + \exp(-c_j^n y_j^n)} \quad (4.1)$$

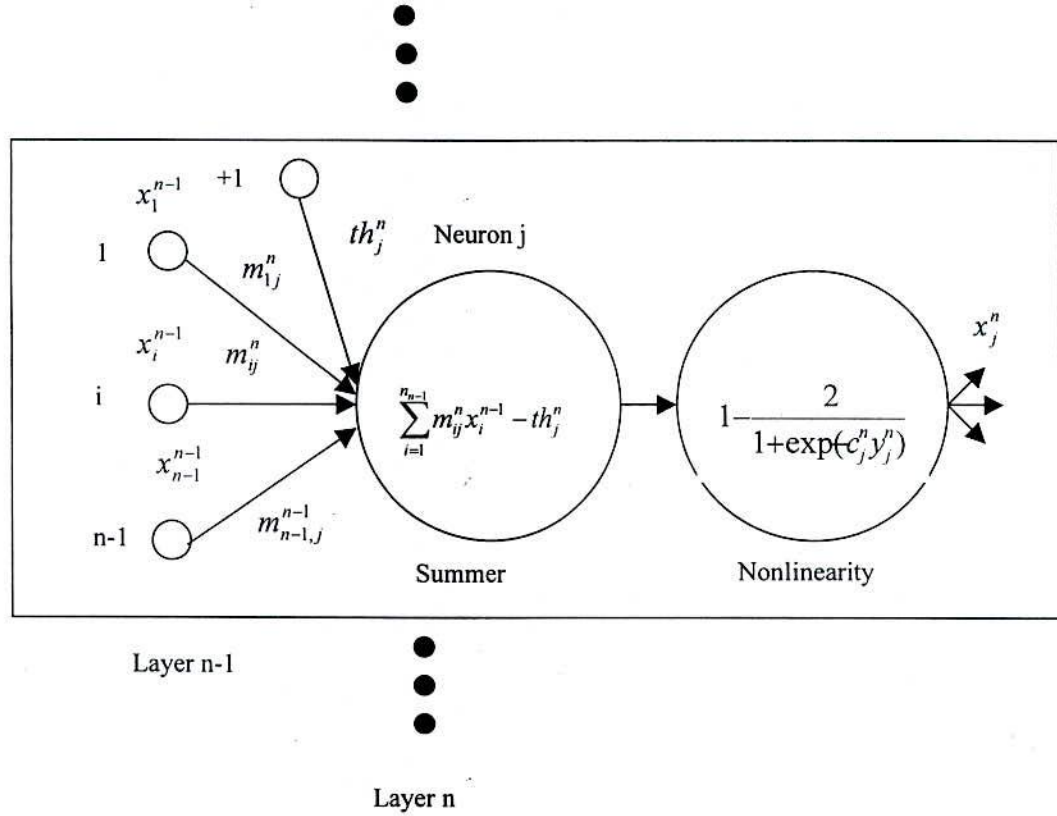


Fig. 4.1 The infrastructure of a neuron.

Where,

$$y_j^n = \sum_{i=1}^{n-1} m_{ij}^n x_i^{n-1} - th_j^n \quad (4.2)$$

$m_{ij}^n$  is the weight connecting neuron  $i$  and  $j$  of adjacent layers  $n-1$  and  $n$ , respectively, and  $x_i^{n-1}$  is the output of the neuron  $i$  in layer  $n-1$ .  $th_j^n$ ,  $y_j^n$ ,  $x_j^n$ , and  $c_j^n$  are the threshold, internal sum, output signal, and the inverse temperature coefficient of neuron  $j$  in layer  $n$ , denoted by  $T_j^n$ , is defined as  $\frac{1}{c_j^n}$ .

The thresholds and weights have to be tuned using any training algorithm that minimizes a functional that depends on the difference between the desired outputs and the neural network outputs. The desired outputs are the outputs of the plant, controllers or system model from which the neural network is learning. Now suppose that the  $i$ th output of the plant and the neural network are given by  $u_i$  and  $t_i$  respectively, the  $i$ th error  $e_i$  is given by

$$e_i = u_i - t_i \quad (4.3)$$

In order to match the outputs, we have to find an algorithm that updates the weights. This is basically an optimization problem for which a performance index  $E$  has to be minimized. The most used performance index  $E$  has the following shape:

$$E = \frac{1}{2} e^T \Lambda^{-1} e \quad (4.4)$$

Where,  $e$  is a column vector containing errors of the form (4.3) and  $\Lambda$  is a  $n \times n$  symmetric positive definite matrix. Let  $m$  be a vector containing all thresholds and weights of a neural network and  $m^*$  be the optimum vector that minimizes (4.4). Then, a Taylor series expansion of (4.4) around  $m$ , neglecting high-order terms gives

$$E(x) = E(m) + \nabla E^T (x - m) + \frac{1}{2} (x - m)^T H (x - m) \quad (4.5)$$

Where  $x$  represent a set of weights near to  $m$ ,  $\nabla E$  and  $H$  are the gradient vectors and the Hessian matrix of  $E(m)$  given by

$$\nabla E = \left. \frac{\delta E}{\delta m} \right|_m \quad H = \left. \frac{\delta^2 E}{\delta m^2} \right|_m \quad (4.6)$$

Now, the performance  $E$  reaches its minimum at the point  $x = m^*$ .

$$E(m^*) = E(m) + \nabla E^T (m^* - m) + \frac{1}{2} (m^* - m)^T H (m^* - m) \quad (4.7)$$

Therefore, the optimum set of weights  $m^*$  can be found if we set  $\frac{\delta E}{\delta m^*} = 0$ , which lead to

$$\nabla E + H(m^* - m) = 0 \quad (4.8)$$

We can get the optimal change in  $m$  as

$$\Delta m = m^* - m = -H^{-1} \nabla E \quad (4.9)$$

Equation (4.9) will be used in the determination of the updating formulas for each algorithm. There are many training algorithms that approximate the inverse of the

Hessian matrix as the identity matrix  $I$  multiplied by a constant to be defined by the algorithm. The algorithms that use this methodology are called the gradient descent algorithms. Algorithms that consider the complete Hessian matrix in the derivation of the updating formulas are called Newton algorithms since they use the second derivative of the functional  $E(m)$ . The Newton algorithms deal with a great amount of calculations because they have to evaluate the Hessian matrix and get its inverse. Some algorithms try to avoid this inversion by approximating the inverse of the Hessian matrix as a matrix, which is easier to evaluate than the original  $H^{-1}$ . These algorithms are called the quasi-Newton training algorithms.

#### **4.3 FEEDFORWARD-BACKPROPAGATION NETWORK**

The feedforward backpropagation network is a very popular model in neural networks, which is shown in Fig. 4.2. It does not have the feedback connections, but errors are back-propagated during training. Least mean squared error is used. Many applications can be formulated for using a feedforward backpropagation network, and the methodology has been a model for most multilayer neural networks. Errors in the output determine measures of hidden layer output errors, which are used as a basis for adjustment of connection weights between the input and hidden layers. Adjusting the two sets of weights between the pairs of layers and recalculating the outputs in an iterative process that is carried on until the errors fall below a tolerance level. Learning rate parameters scale the adjustments to weights. A momentum parameter can also be used in scaling the adjustments from a previous iteration and adding to the adjustments in the current iteration.

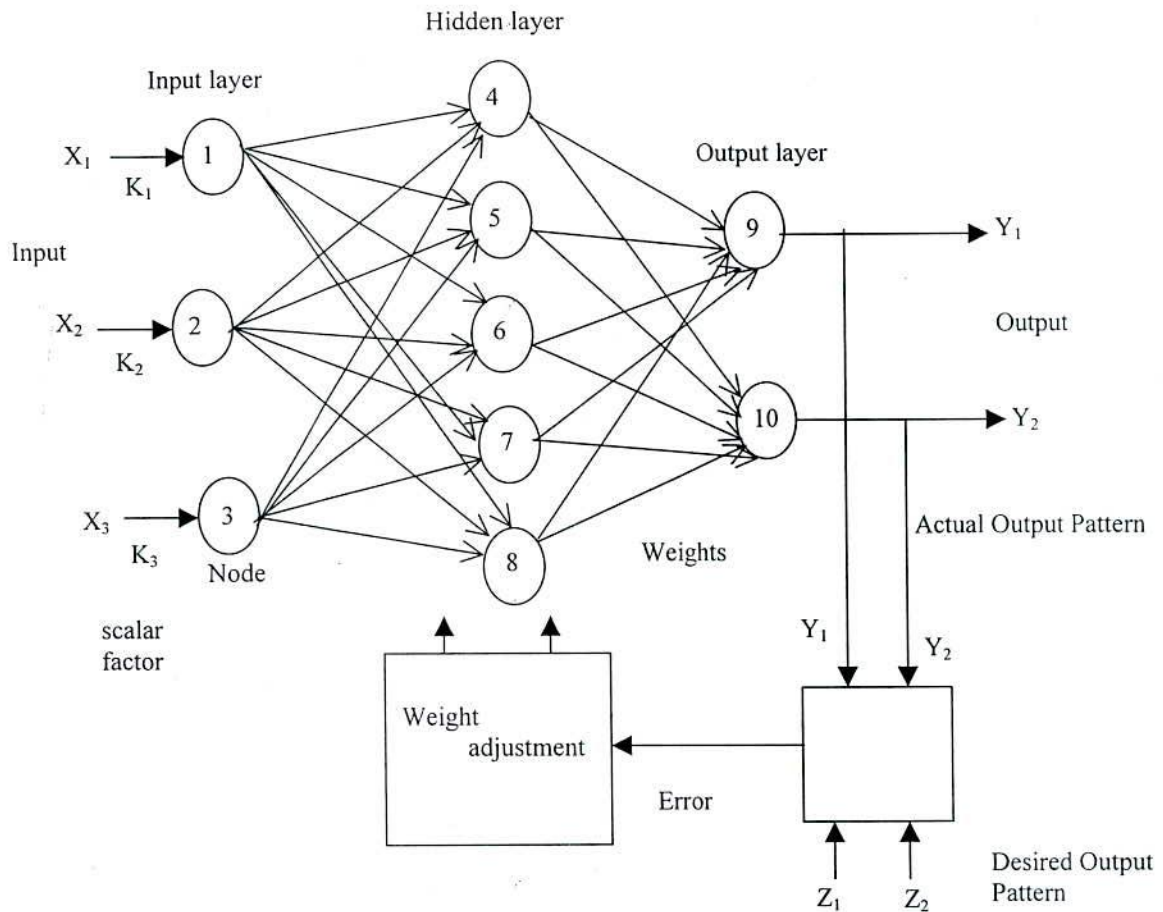


Fig:-4.2 Structure of a feedforward ANN showing back propagation training

#### 4.4 MAPPING

The feedforward backpropagation network maps the input vectors to output vectors. Pairs of input and output vectors are chosen to train the network first. Once training is completed, the weights are set and the network can be used to find outputs for new inputs. The dimension of the input vector determines the number of neurons in the input layer, and the dimension of the output vector determines the number of neurons in the output layer. If there are  $k$  neurons in the input layer and  $m$  neurons in the output layer, then this network can make a mapping from  $k$ -dimensional space to an  $m$ -dimensional space. Once trained, the network gives the image of a new input vector under this mapping. Knowing what mapping is wanted the feedforward backpropagation network to be trained



for implies the dimensions of the input space and the output space, so that one can determine the numbers of neurons to have the input and output layers.

#### 4.5 STRUCTURE OF NEURAL-NETWORK

The architecture of a feedforward backpropagation network is shown in Figure 4.3. While there can be many hidden layers, it will be illustrated that this network with only one hidden layer. Also, the number of neurons in the input layer and that in the output layer are determined by the dimensions of the input and output patterns, respectively. It is not easy to determine how many neurons are needed for the hidden layer. In order to avoid cluttering the figure, it will be shown that the layout in figure 4.3 with five input neurons, three neurons in the hidden layer, and four output neurons, with a few representative connections.

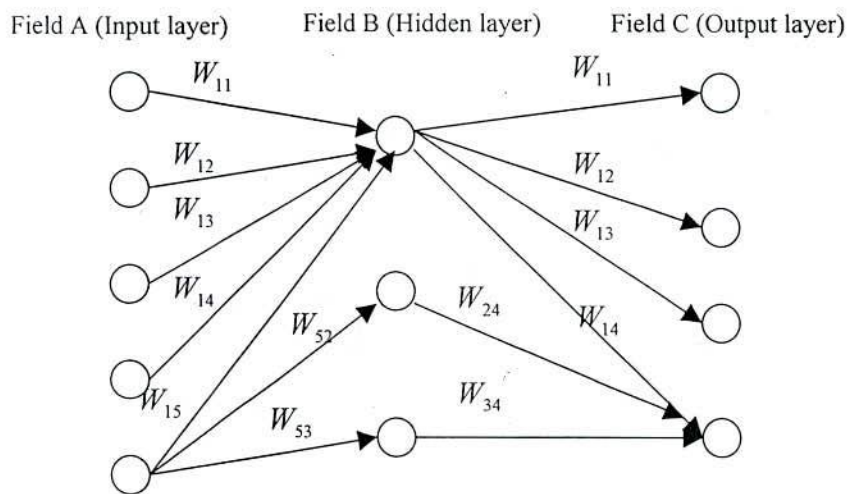


Fig. 4.3 Layout of a feedforward backpropagation networks.

The network has three fields of neurons: one for input neurons, one for hidden processing elements, and one for the output neurons. As already stated, connections are for feed forward activity. There are connections from every neuron in field A to every one in field B, and in turn, from every neuron in field B to every neuron in field C. Thus, there are two sets of weights, those figuring in the activation of hidden layer neurons and those to determine the output neuron activation. In training, all of these weights are adjusted by

considering what can be called a cost function in terms of the error in the computed output pattern and the desired output pattern.

#### **4.6 TRAINING**

The feedforward backpropagation network undergoes supervised training, with a finite number of pattern pairs consisting of an input pattern and a desired or targets output pattern. An input pattern is presented at the input layer. The neurons here pass the pattern activation to the next layer neurons, which are in a hidden layer. The outputs of the hidden layer neurons are obtained by using perhaps a bias, and also a threshold function with the activation determined by the weights and the inputs. These hidden layer outputs become inputs to the output neurons, which process the inputs using an optional bias and a threshold function. The final output of the network is determined by the activation from the output layer.

The computed pattern and the input pattern are compared, a function of this error for each component of the pattern is determined, and adjustment to weights of connections between the hidden layer and the output layer is computed. A similar computation, still based on the error in the output, is made for the connection weights between the input and hidden layers. The procedure is repeated with each pattern pair assigned for training the network. Each pass through all the training patterns is called a cycle or an epoch. The process is then repeated as many cycles as needed until the error is within a prescribed tolerance.

#### **4.7 BACKPROPAGATION ALGORITHM**

Let us consider two matrices whose elements are the weights on connections. One matrix refers to the interface between the input and hidden layers, and the second refers to that between the hidden layer and the output layer. Since connections exist from each neuron in one layer to every neuron in the next layer, there is a vector of weights on the connections going out from any one neuron. Putting this vector into a row of the matrix, we get as many rows as there are neurons from which connections are established.

Let  $M_1$  and  $M_2$  be these matrices of weights.  $M_1[i][j]$  denotes the weight on the connection from the  $i$ th input neuron to the  $j$ th neuron in the hidden layer. Similarly,

$M_2[i][j]$  denotes the weight on the connection from the  $i$ th neuron in the hidden layer and the  $j$ th output neuron.

Next,  $x, y, z$  will be used for the outputs of neurons in the input layer, hidden layer and output layer, respectively, with a subscript attached to denote which neuron in a given layer we are referring to. Let  $p$  denote the desired output pattern, with  $p_i$  as the components. Let  $m$  be the number of input neurons, so that according to notation  $(x_1, x_2, \dots, x_m)$  will denote the input pattern. If  $p$  have, say,  $r$  components, the output layer needs  $r$  neurons. Let the number of hidden layer neurons be  $n$ . Let  $\theta$  with the appropriate subscript represent the threshold value or bias for a hidden layer neuron, and  $\tau$  with an appropriate subscript refer to the threshold value of an output neuron.

Let the errors at the output layer be denoted by  $e_j$ 's and those at the hidden layer by  $t_j$ 's.

If we use a  $\Delta$  prefix of any parameter, then we are looking at the change in or adjustment to that parameter. Also the thresholding function we would use is the sigmoid function,

$$f(x) = 1 - \frac{2}{1 + \exp(-x)} \quad (4.10)$$

Output of  $j$ th hidden layer neuron:

$$y_j = f\left(\left(\sum_i x_i M_1[i][j]\right) + \theta_j\right) \quad (4.11)$$

Output of  $j$ th output layer neuron :

$$z_j = f\left(\left(\sum_i y_i M_2[i][j]\right) + \tau_j\right) \quad (4.12)$$

$i$ th component of vector of output differences:

$$e_i = \text{desired value} - \text{computed value} = p_i - z_i$$

$j$ th component of output error at the output layer :

$$e_j = (1 - z_j^2) \times e_i \quad (4.13)$$

$i$ th component of output error at the hidden layer:

$$t_j = (1 - y_j^2) \left( \sum_i y_i M_2[i][j] e_j \right) \quad (4.14)$$

Adjustment for weight between  $i$ th neuron in hidden layer and  $j$ th output neuron:

$$\Delta M_2[i][j] = \beta_o y_i e_j \quad (4.15)$$

Where,  $\beta_o$  is the learning rate parameter for the output layer.

Adjustment for weight between  $i$  th input neuron and  $j$ th neuron in hidden layer:

$$\Delta M_1[i][j] = \beta_h x_i t_j \quad (4.16)$$

Adjustment to the threshold value or bias for the  $j$  th output neuron :

$$\Delta \tau_j = \beta_o e_j \quad (4.17)$$

Adjustment to the threshold value or bias for the  $j$  th hidden layer neuron :

$$\Delta \theta_j = \beta_h e_j \quad (4.18)$$

Where,  $\beta_h$  is the learning rate parameter for the hidden layer.

For use of momentum parameter  $\alpha$ , equations (4.15) and (4.16) becomes:

$$\Delta M_2[i][j](t) = \beta_o y_i e_j + \alpha \Delta M_2[i][j](t-1) \quad (4.19)$$

And

$$\Delta M_1[i][j](t) = \beta_h x_i t_j + \alpha \Delta M_1[i][j](t-1) \quad (4.20)$$

## CHAPTER V

### FIELD ORIENTATION CONTROL OF INDUCTION MOTOR

#### 5.1 INTRODUCTION

The polyphase induction motor has a very simple and robust mechanical structure. But the stator windings of the motor carry both the flux and torque producing currents. High performance drives require decoupling of the channels and independent control over flux and torque producing currents. Scalar control methods are not capable of producing desired input variables. After F. Blashke, the concept of vector control was introduced for high performance control of induction motors.

It is well known that the mmf and flux vectors of an induction motor rotate at synchronous speed. The direct method of field orientation senses the magnitude and position of the flux and then determines the magnitude and position of mmf so that the flux (rotor flux) is kept constant and the stator mmf is adjusted to meet the torque demand. This avoids the sluggish performance of the induction motor as the flux and torque channels are decoupled and slow dynamics of flux path does not affect the performance of the induction motor. The position and magnitude of flux in an induction motor may be sensed by imparting coils that require extra hardware and involves costs. On the other hand use of flux observers with suitable design may be used to obtain the magnitude and position of flux accurately. This gives direct field orientation control.

The indirect method of field orientation control does not require sensing the magnitude and position of flux. Rather it generates slip frequency, which is added to rotor speed to calculate the inputs motor frequency. To meet the torque demand, the angular position as well as the magnitude of the stator mmf is adjusted. It is simple in implementation but suffers from a serious drawback due to variation of rotor parameters (especially the rotor resistance) from their nominal values incorporated in the controller. There are methods for correcting the rotor parameters. Observers may be used for detecting the parameter mismatch condition and tuning.

## 5.2 PRINCIPLE OF VECTOR (FIELD-ORIENTATION) CONTROL

In the scalar control method, the voltage or current and the frequency are the basic control variables of the induction motor. In a voltage-fed drive, both the torque and air gap flux are functions of voltage and frequency. This coupling effect is responsible for the sluggish response of the induction motor. If, for example, the torque is increased by increasing the frequency (i.e., the slip), the flux tends to decrease which reduces torque output. But it is compensated by the sluggish flux control loop feeding in additional voltage. This transient dip of flux reduces the torque sensitivity with the slip and therefore, lengthens the response time. This is equally valid for a current-fed drive system.

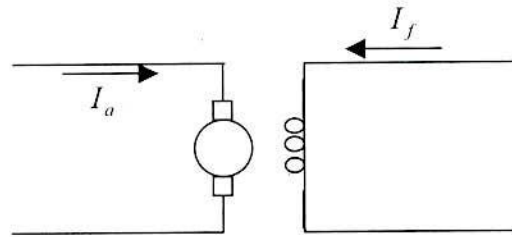
Applying vector or field-orientated control methods one can overcome the foregoing limitation. This control method is applicable to both induction and synchronous machines. In the vector control method, an ac machine is controlled like a separately excited dc machine. This analogy is explained in Fig. 5.1. In a dc machine, neglecting the armature demagnetization effect and field saturation, the torque is given by

$$T_{em} = K_t' I_a I_f \quad (5.1)$$

Where  $I_a$  is the armature or torque component of current and  $I_f$  is the field or flux component of current. In a dc machine, the control variables  $I_a$  and  $I_f$  may be considered as orthogonal or decoupled "vectors". In normal operation, the field current is set to maintain the rated field flux and changing the armature current changes developed torque. Since the current  $I_f$  or the corresponding field flux is decoupled from the armature current  $I_a$ , the torque sensitivity remains maximum in both transient and steady-state operations. This mode of control may be extended to an induction motor also if the machine operation is considered in a synchronously rotating reference frame, where, the sinusoidal variables appear as dc quantities. In Fig. 5.1 the induction motor with inverter and control is shown with two control inputs,  $i_{ds}^*$  and  $i_{qs}^*$ . The currents  $i_{ds}^*$  and  $i_{qs}^*$  are the direct-axis and quadrature-axis component of the stator current respectively, where, both are in a synchronously rotating reference frame. In vector control,  $i_{ds}^*$  is analogous to the field current  $I_f$  and  $i_{qs}^*$  is analogous to the armature

current  $I_a$  of a dc machine. Therefore, the torque can be expressed as

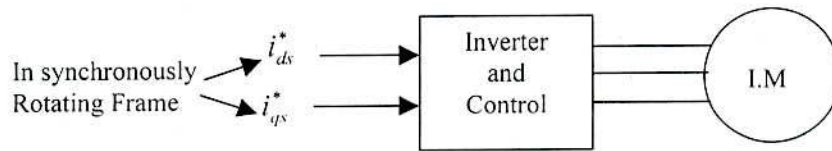
$$T_{em} = K_t |\lambda_r| i_{qs} = K'_t i_{qs} i_{ds} \quad (5.2)$$



$$T_{em} = K_t |\lambda_r| i_{qs} = K'_t i_a i_f$$

Torque producing
Field producing  
i
i

(a)



$$T_{em} = K_t |\lambda_r| i_{qs} = K'_t i_{qs} i_{ds}$$

Torque component
Field component

(b)

Fig.5.1 Analogy of the Induction Motor and the dc Machine in Vector

The basic concept of how  $i_{ds}$  and  $i_{qs}$  can be established as control vectors in the vector control method is explained in Fig.5.2 with the help of of phasor diagrams in a synchronously rotating  $d-q$  reference frame. For simplicity, the rotor leakage inductance is neglected. The phasor diagram is drawn with the air gap voltage  $V_g$  aligned with the  $q$  axis. The stator current  $I_s$  lags the voltage  $V_g$  by  $(90 - \theta^0)$  i.e.,  $i_{qs} = I_s \sin \theta$  is in phase with  $V_g$  and  $i_{ds} = I_s \cos \theta$  is in quadrature with  $V_g$ . The current  $i_{qs}$  is the active or torque component of the stator current and the corresponding active power across the air gap is  $V_g i_{qs}$ . The current  $i_{ds}$  is the reactive or field component of the stator current and is responsible for establishing the rotor flux  $\lambda_r$ . The corresponding reactive power across the air gap is  $V_g i_{ds}$ . From the

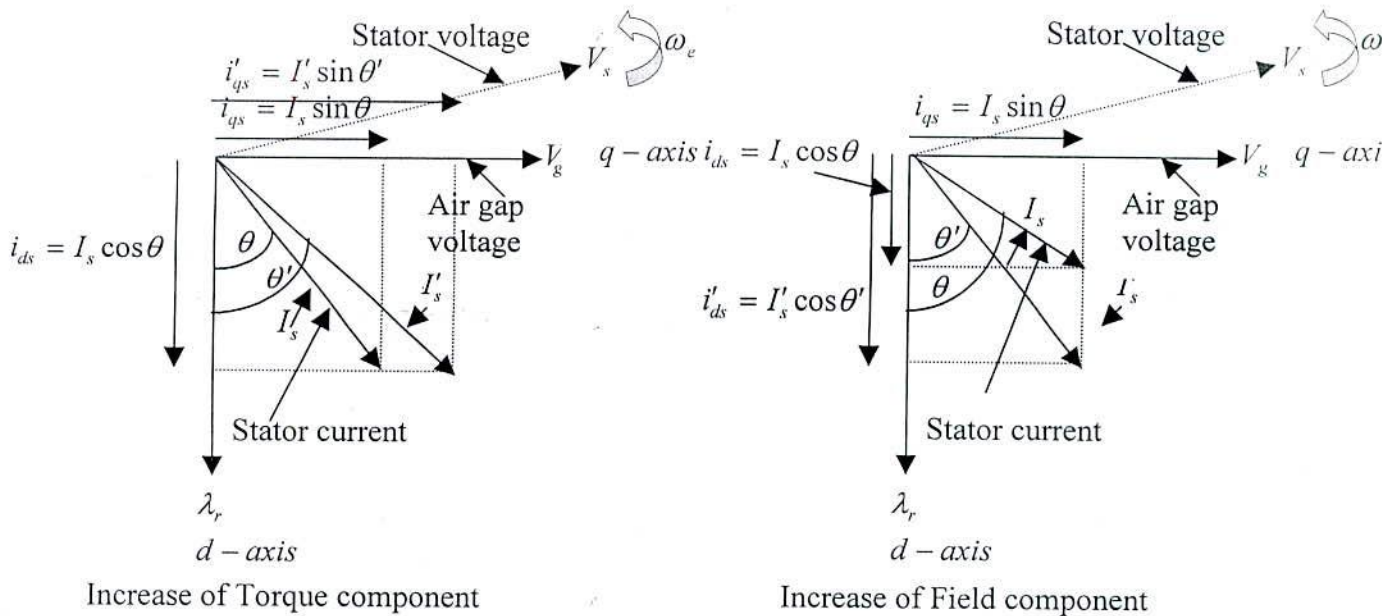


Fig.5.2 Phasor diagrams in the direct vector control (in terms of peak values)

phasor diagram, the developed torque across the air gap is given by  $T_{em} = K_t |\lambda_r| i_{qs} = K_t' i_{qs} i_{ds}$ , where,  $i_{qs}$  and  $i_{ds}$  are shown in Fig.5.2. The torque equation is



therefore identical to that of a dc machine. The variables  $i_{qs}$  and  $i_{ds}$  are mutually decoupled and can be independently varied without affecting the orthogonal component. For normal operation, as in a dc machine, the current  $i_{ds}$  remains constant and the torque is varied by varying the  $i_{qs}$  component. Correspondingly, the polar position of  $I_s$  shifts to  $I'_s$  as shown in Fig. 5.2.

The fundamental of vector control implementation with the machine model can be explained with the help of Fig. 5.3. It is assumed to generate the ideal phase current waves  $i_a, i_b$  and  $i_c$  as dictated by the corresponding reference waves generated by the controller. The machine model is shown on the right.

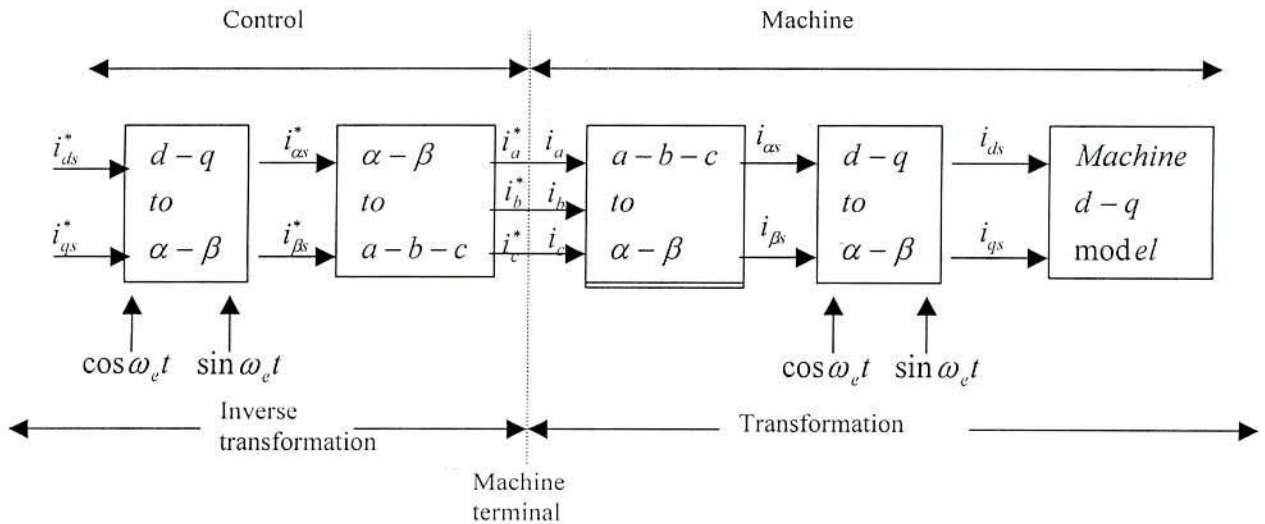


Fig. 5.3 Vector control implementation with the machine model.

The phase currents  $i_a, i_b$  and  $i_c$  are converted to  $i_{\beta s}$  and  $i_{\alpha s}$  components by three-phase/two-phase transformation. These are then converted to a synchronously rotating reference frame by the unit vectors  $\cos \omega_c t$  and  $\sin \omega_c t$  as shown, before being applied to the machine model. The controller makes two stages of inverse transformation so that the control parameters  $i_{ds}^*$  and  $i_{qs}^*$  correspond to machine variables  $i_{ds}$  and  $i_{qs}$ , respectively. The unit vectors assume the alignment of  $i_{ds}$  with the  $\lambda_r$  phasor and  $i_{qs}$  with the  $V_g$  phasor.

There are essentially two general methods of vector control. One, called the direct method, was developed by F. Blaschke[1] and the other is known as the indirect method, was developed by K. Hasse[2].

### 5.3 Direct Method of Vector Control

The direct vector control method depends on the generation of unit vector signals from the air gap fluxes. The air gap fluxes  $\lambda_{dm}$  and  $\lambda_{qm}$  can be measured directly or estimated from the stator voltage and current signals, as explained in Fig.5.4. The currents  $i_{ds}$  and  $i_{qs}$  are to be aligned with the rotating frame  $d$  and  $q$  axes, respectively using the unit vectors. We can write the following relations from Fig.5.4.

$$|\lambda_m| = \sqrt{\lambda_{dm}^2 + \lambda_{qm}^2} = \sqrt{(\lambda_{dm})^2 + (\lambda_{qm})^2} \quad (5.3)$$

$$\lambda_{dm} = |\lambda_m| \cos \omega_e t \quad (5.4)$$

$$\lambda_{qm} = |\lambda_m| \sin \omega_e t \quad (5.5)$$

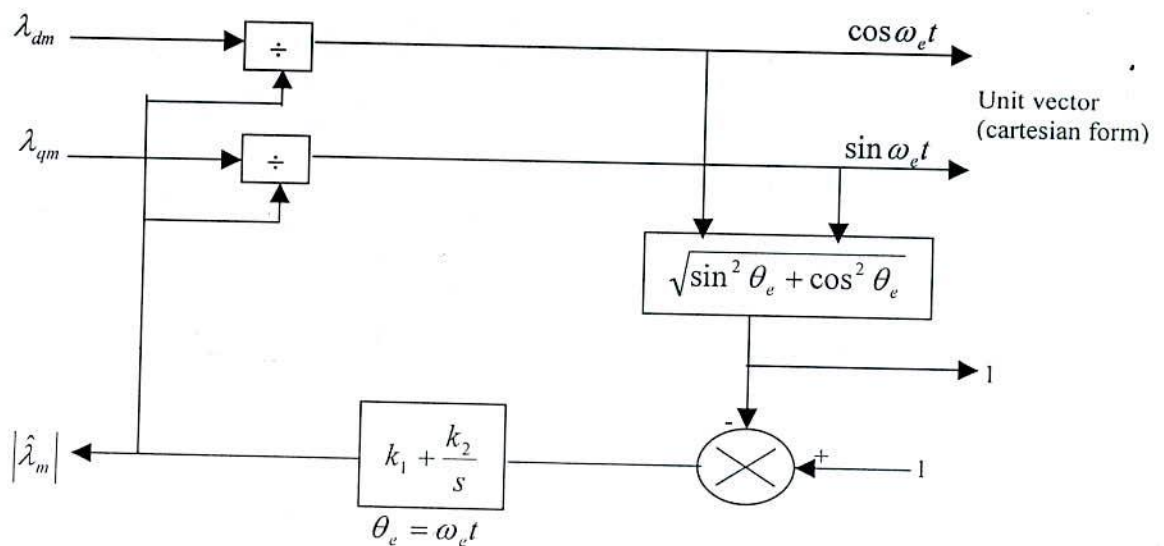


Fig. 5.4 Synthesis of unit vectors

Equations (5.4) and (5.5) indicate that  $\cos \omega_e t$  and  $\sin \omega_e t$  are cophasal to  $\lambda_{dm}$  and  $\lambda_{qm}$  respectively. The synthesis of unit vectors from  $\lambda_{dm}$  and  $\lambda_{qm}$  by the feedback control principle is shown in Fig.5.4.

So far the vector control method neglecting the rotor leakage inductance has been considered. It can be shown that the rotor leakage flux exerts a considerable amount of influence and therefore, cannot be neglected. In fact, the rotor flux should be considered in both the vector and scalar control methods rather than the air gap flux. Blaschke [1] has shown that the vector control on the basis of air gap flux may result in an undesirable stability problem. The air gap flux can be compensated for the rotor leakage as follows:

$$\lambda_{qr} = L_m i_{qs} + L_r i_{qr} \quad (5.6)$$

$$\lambda_{qm} = L_m i_{qs} + L_m i_{qr} \quad (5.7)$$

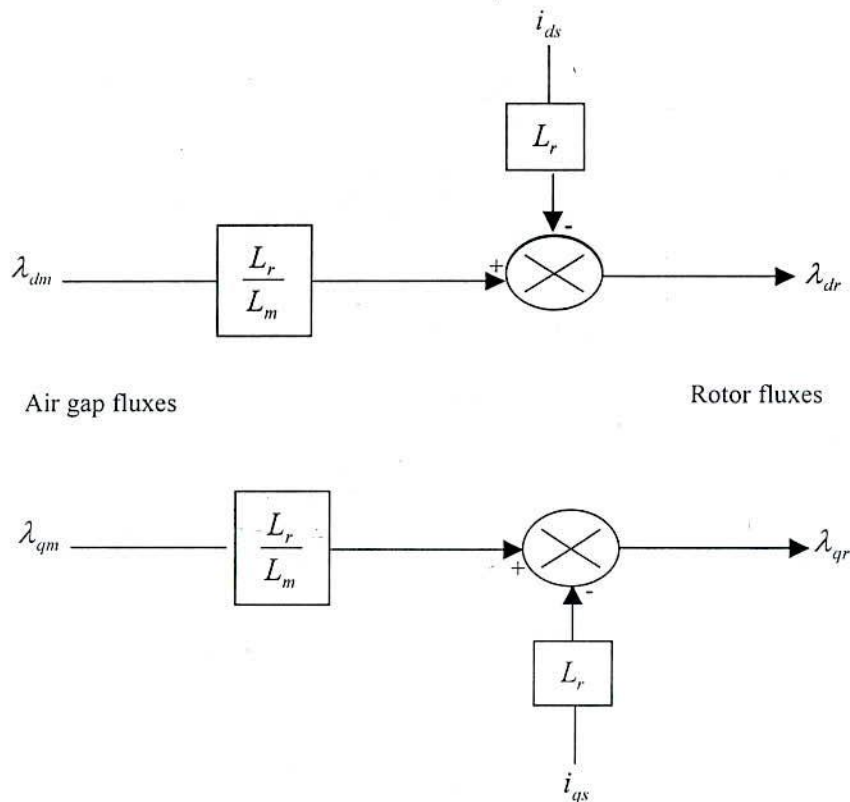


Fig. 5.5 Synthesis of rotor fluxes.

Eliminating  $i_{qr}$  from equation (5.6) yields

$$\lambda_{qr} = \frac{L_r}{L_m} \lambda_{qm} - L_r i_{qs} \quad (5.8)$$

Similarly from the  $d$ -axis equivalent circuit.

$$\lambda_{dr} = \frac{L_r}{L_m} \lambda_{dm} - L_r i_{ds} \quad (5.9)$$

The synthesis of rotor fluxes from equations (5.8 ) and (5.9 ) are shown in Fig.5.5 . The rotor flux  $|\lambda_r|$  and unit vectors for Fig.5.4 can then be given as

$$|\lambda_r| = \sqrt{\lambda_{dr}^2 + \lambda_{qr}^2} = \sqrt{(\lambda_{dr})^2 + (\lambda_{qr})^2} \quad (5.10)$$

$$\cos \omega_e t = \frac{\lambda_{dr}}{|\lambda_r|} \quad (5.11)$$

$$\sin \omega_e t = \frac{\lambda_{qr}}{|\lambda_r|} \quad (5.12)$$

The direct method of vector control described so far can be applied typically above 10% of the base speed because of the difficulty in accurate flux signal synthesis at low speed. In fact, the flux signals obtained by direct integration of phase voltages can be used only in a higher speed range. The resulting coupling effect, although small at higher speed, becomes worse as the speed is reduced. In applications such as servo drives, the drive system must operate at truly zero speed with the best possible transient response. The accurate stator drop compensation near zero speed is very difficult. In the low-speed region, the rotor flux can be synthesized more accurately from speed and stator current signals. The rotor equation of the  $\beta$ -axis stationary frame equivalent circuit can be given as

$$\frac{d\lambda_{\beta r}}{dt} + i_{\beta r} R_r - \omega_r \lambda_{\alpha r} = 0 \quad (5.13)$$

Adding the term  $(\frac{L_m R_r}{L_r}) i_{\beta s}$  on both sides of the equation, we have

$$\frac{d\lambda_{\beta r}}{dt} + \frac{R_r}{L_r} (L_m i_{\beta s} + L_r i_{\beta r}) - \omega_r \lambda_{\alpha r} = \frac{L_m R_r}{L_r} i_{\beta s} \quad (5.14)$$

Substituting equation (5.6 ) and simplification yields

$$\frac{d\lambda_{\beta r}}{dt} = \frac{L_m}{\tau_r} i_{\beta s} + \omega_r \lambda_{\alpha r} - \frac{1}{\tau_r} \lambda_{\beta r} \quad (5.15)$$

Similarly, the equation from the  $\alpha$ -axis equivalent circuit can be derived as,

$$\frac{d\lambda_{\alpha r}}{dt} = \frac{L_m}{\tau_r} i_{\alpha s} + \omega_r \lambda_{\beta r} - \frac{1}{\tau_r} \lambda_{\alpha r} \quad (5.16)$$

where,  $\tau_r = \frac{L_r}{R_r}$  is the rotor circuit time constant. Equations (5.15) and (5.16) give rotor fluxes as functions of stator current and speed.

#### 5.4 VOLTAGE REGULATED INDUCTION MOTOR DRIVE

From (2.6) and (2.7), in practice the rotor flux can not be measured. The only measurable variable is the stator primary current  $i_s$ . It is notable that all variables are handled on the stator co-ordinate system. Fig.5.6. Illustrates the flux observer based field orientation (FOFO) voltage fed controller block diagram. The stator d-axes current  $i_{ds}$  and q-axes current is generated from stator primary current  $i_{\alpha s}$  and  $i_{\beta s}$  as:

$$i_{ds} = i_{\alpha s} \times \cos \omega t + i_{\beta s} \times \sin \omega t \quad (5.17a)$$

$$i_{qs} = -i_{\alpha s} \times \sin \omega t + i_{\beta s} \times \cos \omega t \quad (5.17b)$$

The d-axes reference current  $i_{dsref}$  is generated from rotor reference flux  $\lambda_{ref}$  as

$$i_{dsref} = \frac{\lambda_{ref}}{L_m} \text{ and the q-axes reference current } i_{qsref} \text{ is generated from speed error,}$$

$\omega_{error} = \omega_{rref} - \omega_r$  which is processed through a PI controller. Where,  $\omega_{rref}$  is the reference or set speed. Both the reference currents are compared with the two-axes stator currents. The errors are the input of two PI controller and outputs are the two-axes voltage. From the two-axes voltages the primary voltages are generated as:

$$v_{\alpha s} = v_{ds} \times \cos \omega t - v_{qs} \times \sin \omega t \quad (5.18a)$$

$$v_{\beta s} = i_{ds} \times \sin \omega t + v_{qs} \times \cos \omega t \quad (5.18b)$$

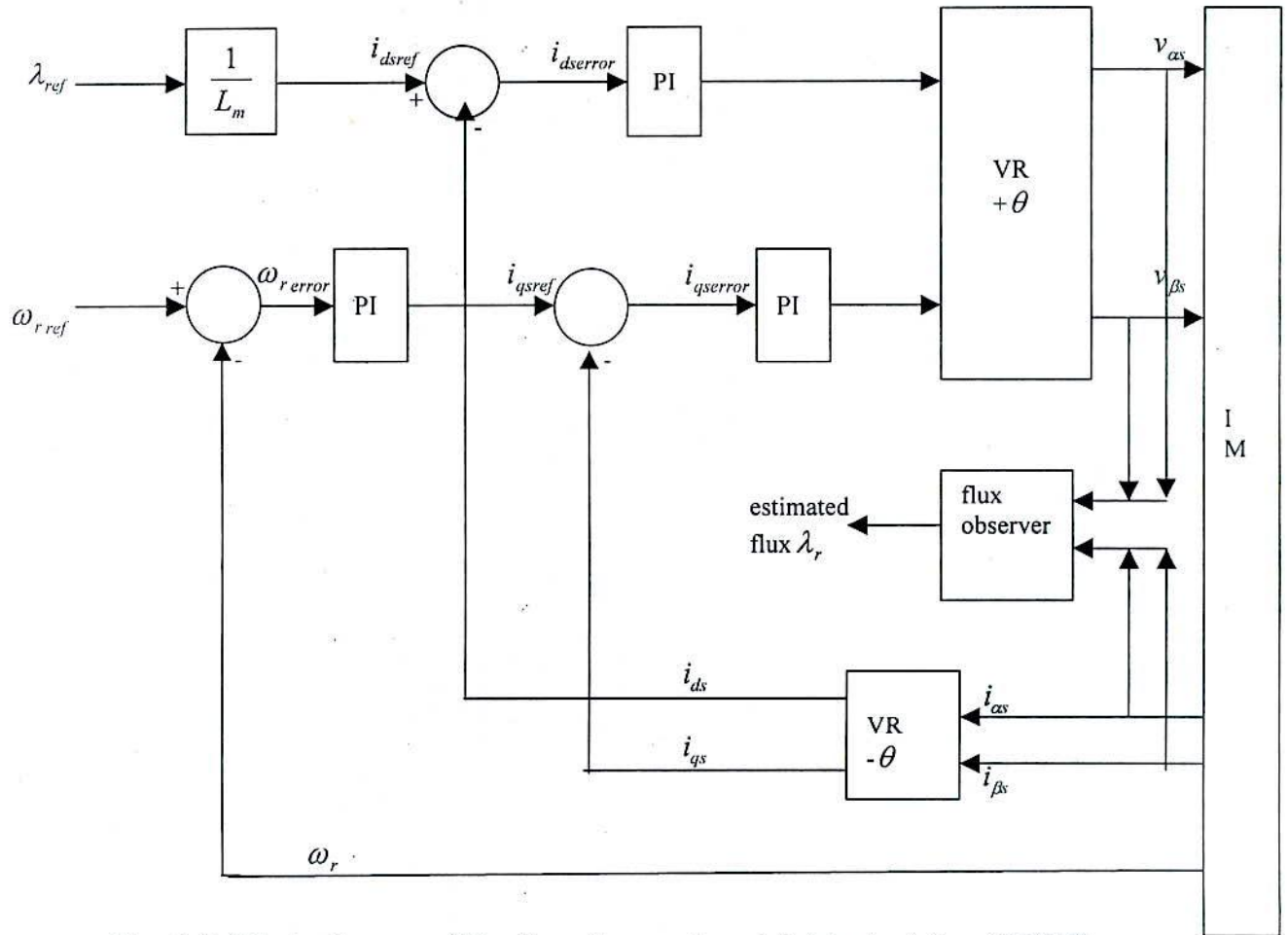


Fig. 5.6 Block diagram of the flux observer based field orientation (FOFO) control with voltage fed inverter.

## 5.5 CURRENT REGULATED INDUCTION MOTOR DRIVE

The basic circuit equations are similar to the voltage fed controller. Fig.5.7. illustrates the flux observer based field orientation (FOFO) current fed controller block diagram. In the current-regulated method, the three-phase sinusoidal reference currents are compared with the instantaneous values of motor currents. The error is input to the controllers and pulse-width modulated (PWM) logic unit. The amplitude of the current reference is obtained from the r.m.s sum of stator d-axis and q-axis current. The controllers and PWM generation block can be either hysteresis controllers or proportional integral (PI) controllers with PWM generation logic.

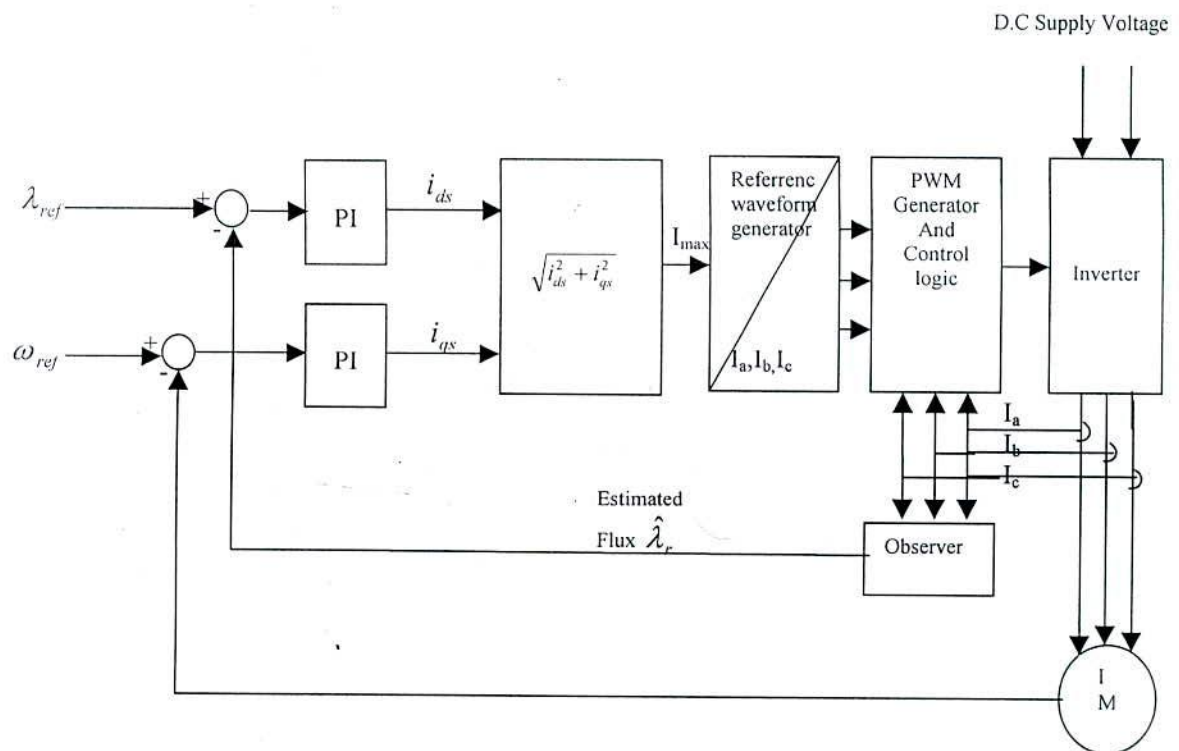


Fig. 5.7 Block diagram of the flux observer based field orientation (FOFO) control with current fed inverter.



### 5.6 Indirect Method of Vector Control

In the direct method of vector control discussed so far, the synthesis of unit vectors is dependent on the machine terminal conditions. In the indirect method of vector control to be discussed here, this dependence does not arise and therefore, the distortion problem does not exist.

Figure 5.8 explains the indirect vector control principle with the help of a phasor diagram. The  $\alpha - \beta$  axes are fixed on the stator while the  $d - q$  axes rotate at synchronous angular velocity  $\omega_e$  as shown. At any instant, the  $q$  electrical axis is at angular position  $\theta_e$  with respect to the  $\beta$  axis. The angle  $\theta_e$  is given by the sum of rotor angular position  $\theta_r$  and slip angular position  $\theta_{sl}$ , where,  $\theta_e = \omega_e t$ ,  $\theta_r = \omega_r t$ , and  $\theta_{sl} = \omega_{sl} t$ . The rotor flux  $\lambda_r$ , consisting of the air gap flux and the rotor leakage flux is aligned to the  $d$  axis as shown in Fig. 5.8. Therefore, for de-coupling control, the stator flux component of current  $i_{ds}$  and the torque component of current  $i_{qs}$  are to be aligned to the  $d$  and  $q$  axes, respectively.

We can write the following equations from rotating frame  $d - q$  equivalent circuit:

$$\frac{d\lambda_{qr}}{dt} + R_r i_{qr} - (\omega_e - \omega_r) \lambda_{dr} = 0 \quad (5.19)$$

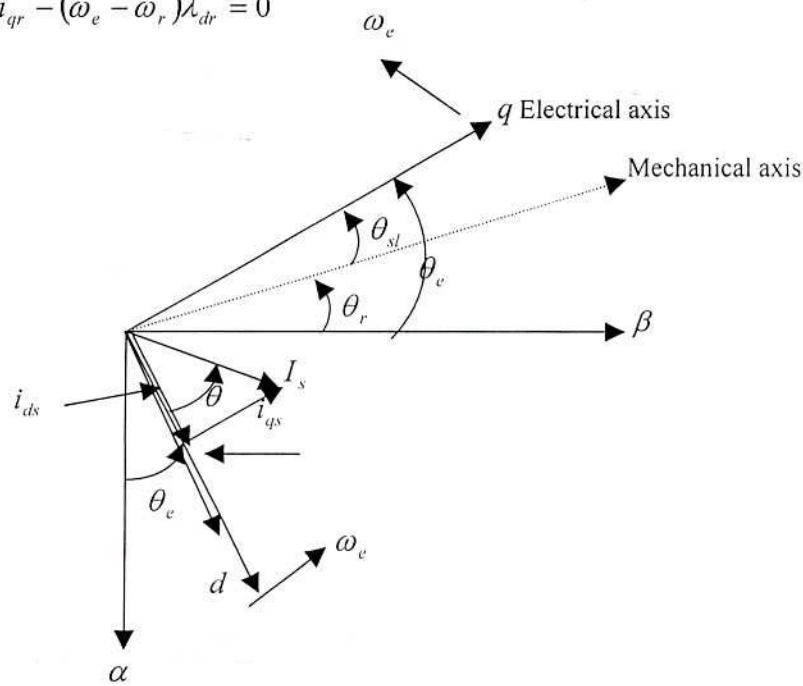


Fig. 5.8 Phasor Diagram for Indirect Vector Control



$$\frac{d\lambda_{dr}}{dt} + R_r i_{dr} - (\omega_e - \omega_r) \lambda_{qr} = 0 \quad (5.20)$$

Again,

$$\lambda_{qr} = L_r i_{qr} + L_m i_{qs} \quad (5.21)$$

$$\lambda_{dr} = L_r i_{dr} + L_m i_{ds} \quad (5.22)$$

From equations (5.21) and (5.22)

$$i_{qr} = \frac{1}{L_r} \lambda_{qr} - \frac{L_m}{L_r} i_{qs} \quad (5.23)$$

$$i_{dr} = \frac{1}{L_r} \lambda_{dr} - \frac{L_m}{L_r} i_{ds} \quad (5.24)$$

The rotor currents from equation (5.19) and (5.20) can be eliminated by substituting equation (5.23) and (5.24) as

$$\frac{d\lambda_{qr}}{dt} + \frac{R_r}{L_r} \lambda_{qr} - \frac{L_m}{L_r} R_r i_{qs} + \omega_{sl} \lambda_{dr} = 0 \quad (5.25)$$

$$\frac{d\lambda_{dr}}{dt} + \frac{R_r}{L_r} \lambda_{dr} - \frac{L_m}{L_r} R_r i_{ds} + \omega_{sl} \lambda_{qr} = 0 \quad (5.26)$$

where,  $\omega_{sl} = \omega_e - \omega_r$

For de-coupling control it is desirable that

$$\lambda_{qr} = \frac{d\lambda_{qr}}{dt} = 0$$

$$\lambda_{dr} = \lambda_r \text{ constant}$$

$$\frac{d\lambda_{dr}}{dt} = 0$$

Substituting the first two conditions, equations ( 5.25) and ( 5.26 ) can be simplified

$$\omega_{sl} = \frac{L_m}{\lambda_r} \left( \frac{R_r}{L_r} \right) i_{qs} \quad (5.27)$$

$$\frac{L_r}{R_r} \frac{d\lambda_r}{dt} + \lambda_r = L_m i_{ds} \quad (5.28)$$

Again, the torque as a function of rotor flux and stator current can be derived as follows:

The stator flux linkage relations can be written as

$$\lambda_{qs} = L_m i_{qr} + L_s i_{qs} \quad (5.29)$$

$$\lambda_{ds} = L_m i_{dr} + L_s i_{ds} \quad (5.30)$$

Substituting equations (5.29) and (5.30) in equations (5.21) and (5.22), we get

$$\lambda_{qs} = \left( L_s - \frac{L_m^2}{L_r} \right) i_{qs} + \frac{L_m}{L_r} \lambda_{qr} \quad (5.31)$$

$$\lambda_{ds} = \left( L_s - \frac{L_m^2}{L_r} \right) i_{ds} + \frac{L_m}{L_r} \lambda_{dr} \quad (5.32)$$

The torque equation as a function of stator currents and stator fluxes is

$$T_{em} = \frac{3}{2} \left( \frac{P_p}{2} \right) (i_{qs} \lambda_{ds} - i_{ds} \lambda_{qs}) \quad (5.33)$$

Equations (5.31) and (5.32) can be substituted in equation (5.33) to eliminate the stator fluxes. Therefore,

$$T_{em} = \frac{3}{2} \left( \frac{P_p}{2} \right) \frac{L_m}{L_r} (i_{qs} \lambda_{dr} - i_{ds} \lambda_{qr}) \quad (5.34)$$

Substituting  $\lambda_{qr} = 0$  and  $\lambda_{dr} = \lambda_r$  the torque expression is

$$T_{em} = \frac{3}{2} \left( \frac{P_p}{2} \right) \frac{L_m}{L_r} i_{qs} \lambda_r \quad (5.35)$$

The equations above together with the mechanical equation

$$\left( \frac{2}{P_p} \right) J \frac{d\omega_r}{dt} = T_{em} - T_L \quad (5.36)$$

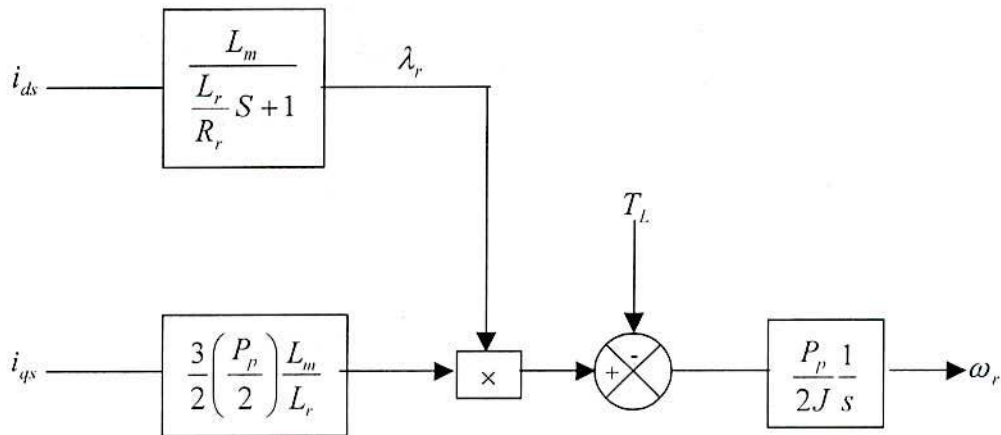


Fig. 5.9 Block diagram of the machine model with decoupling control.

describe the machine model in decoupling control as shown in Fig.5.9. The inverter is assumed to be current controlled and the delay between the command and response currents are neglected. The developed torque  $T_e$  responds instantaneously with current  $i_{qs}$ , but has delayed response due to  $i_{ds}$ . The analogy of the model with a separately excited dc machine is obvious.

### 5.7 CURRENT SOURCE INVERTER FED INDUCTION MOTOR UNDER FIELD ORIENTATION CONTROL

In one approach for framing the relevant mathematical relations to understand and explain the vector control of induction motor, the synchronous reference frame is so aligned that its one axis, say the d-axis, coincides at every instant with a defined flux-vector in the machine. As discussed earlier, the flux-vector may be stator flux, rotor flux and mutual flux. Derivations and the study to follow are for the orientation scheme in which the rotor flux-linkage vector remains in space phase with the d-axis of the synchronous reference frame. For such constrains

$$\lambda_{dr} = L_m i_{ds} + L_r i_{dr} = \lambda_r \quad (5.37a)$$

$$\lambda_{qr} = L_m i_{qs} + L_r i_{qr} = 0 \quad (5.37b)$$

Which by (2.8) and (2.12) becomes

$$L_m i'_R g_{ds} + L_r i_{dr} = \lambda_r \quad (5.38a)$$

$$L_m i'_R g_{qs} + L_r i_{qr} = 0 \quad (5.38b)$$

Elimination of  $i_{dr}$  and  $i_{qr}$  in (5.22) by (5.38) gives

$$v'_R = [(R_s + R'_f) + (L_{\sigma s} + L'_f)p]i'_R + \frac{L_m \omega_e g_{qs}}{L_r} \lambda_r + \frac{L_m g_{ds}}{L_r} p \lambda_r \quad (5.39)$$

where,  $L_{\sigma s} (= L_s - \frac{L_m^2}{L_r})$  is the leakage inductance.

Eqn. 5.39 is similar to the voltage equation of a dc machine except the last term. Even if the field excitation changes, the armature voltage equation of a dc machine does not contain any transformer emf, but (5.39) indicates that the dc voltage applied to the

inverter must contain a component to counteract the transformer emf in the event of the variation of the rotor flux linkage.

Applying the conditions in (5.37) to the rotor circuit emf equations, the third and fourth rows of (2.4) can be written as

$$R_r i_{dr} + p\lambda_r = 0 \quad (5.40a)$$

$$\omega_{sl}\lambda_r + R_r i_{qr} = 0 \quad (5.40b)$$

Eliminating  $i_{dr}$  and  $i_{qr}$  by (5.38),

$$p\lambda_r = \frac{R_r}{L_r} (L_m i'_R g_{ds} - \lambda_r) \quad (5.41a)$$

$$\omega_{sl}\lambda_r = \frac{R_r}{L_r} L_m i'_R g_{qs} \quad (5.41b)$$

Which can be re-written as

$$\lambda_r = \frac{L_m i_{ds}}{(1 + \tau_r p)} \quad (5.42)$$

And

$$\omega_{sl} = \frac{L_m i_{qs}}{\tau_r \lambda_r} \quad (5.43)$$

By the definition of slip-speed, as implied in (2.4), the angular speed of the rotor flux vector, i.e., of the rotating reference frame is given by

$$\omega_c = \omega_r + \frac{L_m i_{qs}}{\tau_r \lambda_r} \quad (5.44)$$

For constant rotor flux operation,

$$\omega_c = \omega_r + \frac{R_r i_{qs}}{L_r i_{ds}} \quad (5.45)$$

It is to be noted that  $\omega_{sl}$  is the slip speed of the rotor with respect to the rotating d-axis (Fig.2.4) i.e., the rotor flux vector. Torque angle changes with the change in the operating condition of the machine, hence during the transitional state stator mmf vector must move at a speed different from that of the rotor flux vector. Slip speed  $\omega'_{sl}$  of the rotor with respect to the stator current vector must be given by

$$\omega'_{sl} = \omega_{sl} + \frac{d\theta}{dt} \quad (5.46)$$

Angular speed of stator mmf vector is then

$$\omega_s = \omega_r + \omega'_{sl} \quad (5.47)$$

$\frac{d\theta}{dt}$  Should be made available in terms of measurable, i.e., transduced, and/or estimated quantities.

For the field oriented condition the torque angle  $\theta$  can be expressed as

$$\cos \theta = \frac{i_{ds}}{i_{qs}} \quad (5.48)$$

And

$$\sin \theta = \frac{i_{qs}}{i_{ds}} \quad (5.49)$$

For constant rotor flux operation, implying constancy of  $i_{ds}$ , differentiation of (5.48) and use of (5.49) gives

$$\frac{d\theta}{dt} = \frac{i_{ds}}{i_{qs}} \frac{1}{i'_R} \frac{di'_R}{dt} \quad (5.50)$$

It may be noted that  $i_{dq} = i'_R$

Use of (2.15) in (5.50) leads to

$$\frac{d\theta}{dt} = \frac{i_{ds}}{i_{qs}} \frac{1}{i'_R} \left( \frac{v'_R - v'_I - R'_f i'_R}{L'_f} \right) \quad (5.51)$$

Expression for  $\frac{d\theta}{dt}$  in (5.51) can conveniently be evaluated by digital processors. These issues are dealt with in a latter section.  $v'_I$ . Depending upon the control circuitry and the strategies adopted, estimated or measured values are used for the remaining quantities.

By combining (2.5) and (5.37) the expression for the electromagnetic torque becomes

$$T_{em} = \frac{3}{2} P_p \frac{L_m}{L_r} \lambda_r i_{qs} \quad (5.52)$$

Alternatively, it is evident from the voltage eqn.(5.39) of the rotor-flux oriented induction machine that the electro-mechanical power  $P_{em}$  is

$$P_{em} = \frac{3}{2} \frac{L_m \omega_e g_{qs} \lambda_r}{L_r} i_R' \quad (5.53)$$

The speed of the reference frame being  $\frac{\omega_e}{P_p}$  mechanical radians per sec, the developed torque is

$$T_{em} = \frac{P_p}{\omega_e} P_{em} = \frac{3}{2} P_p \frac{L_m}{L_r} \lambda_r i_R' g_{qs}$$

$$\text{i.e., } T_{em} = \frac{3}{2} P_p \frac{L_m}{L_r} \lambda_r i_{qs} \quad (5.54)$$

Which is the eqn. 5.52.

Irrespective of the transient or steady state condition the torque function in (5.54) always holds for field oriented condition. Use of (2.14), (2.18) and (5.42) in (5.54) yields the following two widely used expressions for steady state torque.

$$T_{em} = \frac{3}{2} P_p \frac{L_m^2}{L_r} i_{ds} i_{qs} \quad (5.55)$$

$$\text{Or, } T_{em} = \frac{3}{2} P_p \frac{L_m^2}{L_r} i_R'^2 \sin \theta \cos \theta \quad (5.56)$$

## 5.8 FLUX OBSERVER-BASED FIELD ORIENTATION CONTROLLER

Fig.5.10. illustrates the Flux Observer based Field Orientation (FOFO) controller block diagram. The flux Observer plays the important role of generating the reference angle of rotor flux required for the direct coordinate transformation. The flux observer is designed on the stator coordinate system using the different types of observer theory.

The basic circuit equations in the stationary reference frame of induction machine are given by (2.4) and (2.5).

The state and output equations are easily derived from (2.4) and (2.5) are given in (2.6) and (2.7).

Let the given observable plant be

$$\dot{x} = Ax + Bu \quad (5.57.a)$$

$$y = Cx \quad (5.57.b)$$

Where,

$$x = \begin{bmatrix} \lambda_{\alpha r} \\ \lambda_{\beta r} \\ i_{\alpha s} \\ i_{\beta s} \end{bmatrix}, \quad u = \begin{bmatrix} v_{\alpha s} \\ v_{\beta s} \end{bmatrix}, \quad y = \begin{bmatrix} i_{\alpha s} \\ i_{\beta s} \end{bmatrix}$$

$$A = \begin{bmatrix} -\frac{R_r}{L_r} & -\omega_r & \frac{L_m R_r}{L_r} & 0 \\ \omega_r & -\frac{R_r}{L_r} & 0 & \frac{L_m R_r}{L_r} \\ \left(\frac{M}{\sigma L_s L_r}\right) \frac{R_r}{L_r} & \left(\frac{M}{\sigma L_s L_r}\right) \omega_r & -\left\{ \frac{R_s}{\sigma L_s} + \frac{R_r(1-\sigma)}{\sigma L_r} \right\} & 0 \\ \left(\frac{M}{\sigma L_s L_r}\right) (-\omega_r) & \left(\frac{M}{\sigma L_s L_r}\right) \frac{R_r}{L_r} & 0 & -\left\{ \frac{R_s}{\sigma L_s} + \frac{R_r(1-\sigma)}{\sigma L_r} \right\} \end{bmatrix}$$

$$B = \begin{bmatrix} 0 & 0 \\ 0 & 0 \\ \frac{1}{\sigma L_s} & 0 \\ 0 & \frac{1}{\sigma L_s} \end{bmatrix} \quad \& \quad C = \begin{bmatrix} 0 & 0 & 1 & 0 \\ 0 & 0 & 0 & 1 \end{bmatrix}$$

**Full order:**

The system (5.57) is rearranged with this observer as follows:

$$\hat{\dot{x}} = A\hat{x} + BU + G(\hat{i}_s - i_s) \quad (5.58)$$

where,  $G$  is the feedback gain matrix and  $\hat{x}$ ,  $\hat{i}_s$  and  $i_s$  are the estimated full state, estimated stator current and actual stator current respectively.

**Reduced order:**

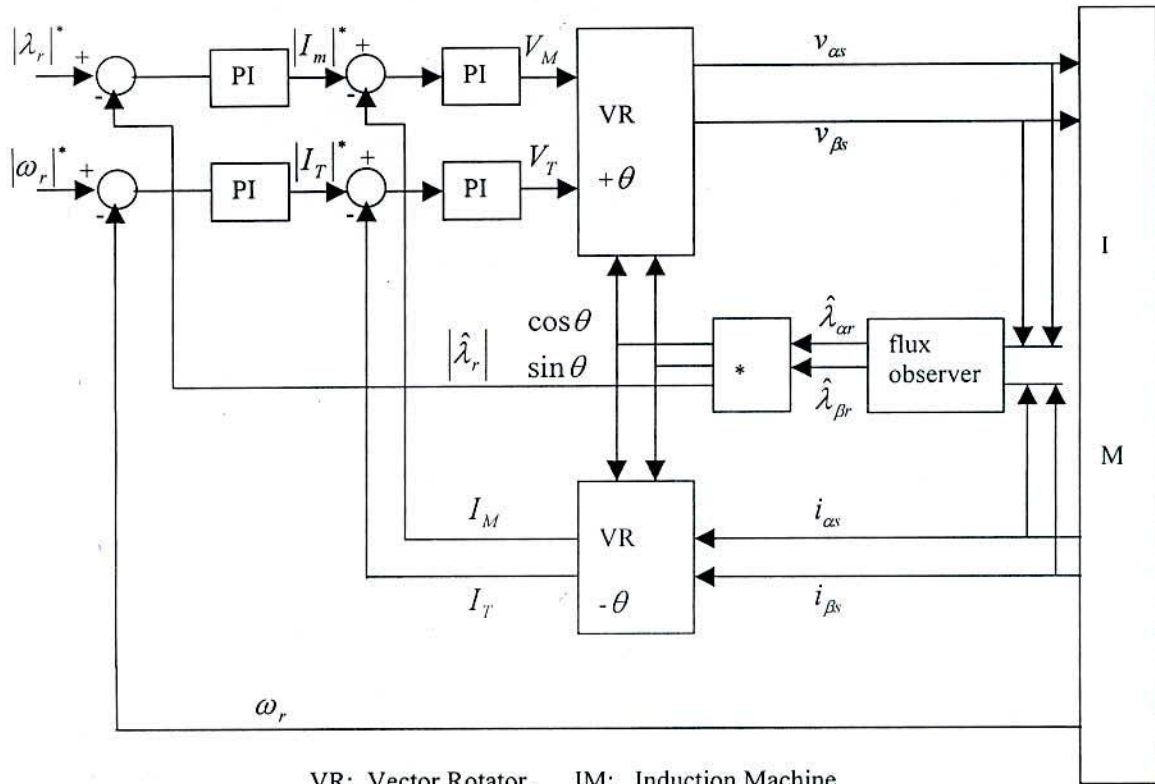
The system (5.57) is rearranged with this observer as follows:

$$\begin{bmatrix} \dot{x}_1 \\ \dot{x}_2 \end{bmatrix} = \begin{bmatrix} A_{11} & A_{12} \\ A_{21} & A_{22} \end{bmatrix} \begin{bmatrix} x_1 \\ x_2 \end{bmatrix} + \begin{bmatrix} B_1 \\ B_2 \end{bmatrix} u \quad (5.59.a)$$

$$y = \begin{bmatrix} 0 & C_q \end{bmatrix} \begin{bmatrix} x_1 \\ x_2 \end{bmatrix} \quad (5.59b)$$

where,  $x_1 = \begin{bmatrix} \lambda_{\alpha r} \\ \lambda_{\beta r} \end{bmatrix}$  &  $x_2 = \begin{bmatrix} i_{\alpha s} \\ i_{\beta s} \end{bmatrix}$





VR: Vector Rotator, IM: Induction Machine

The block indicated by \* in the figure consists of :

$$\cos \theta = \frac{\hat{\lambda}_{\alpha r}}{\hat{\lambda}_r}, \sin \theta = \frac{\hat{\lambda}_{\beta r}}{\hat{\lambda}_r}$$

$$|\hat{\lambda}_r| = \sqrt{\hat{\lambda}_{\alpha r}^2 + \hat{\lambda}_{\beta r}^2}$$

Fig.5.10. Flux Observer based Field Orientation (FOFO) Controller for voltage fed inverter.

$$A_{11} = \begin{bmatrix} -\frac{R_r}{L_r} & -\omega_r \\ \omega_r & -\frac{R_r}{L_r} \end{bmatrix}, A_{12} = \begin{bmatrix} \frac{L_m R_r}{L_r} & 0 \\ 0 & \frac{L_m R_r}{L_r} \end{bmatrix}$$

$$A_{21} = \begin{bmatrix} \left( \frac{M}{\sigma L_s L_r} \right) \frac{R_r}{L_r} & \left( \frac{M}{\sigma L_s L_r} \right) \omega_r \\ \left( \frac{M}{\sigma L_s L_r} \right) (-\omega_r) & \left( \frac{M}{\sigma L_s L_r} \right) \frac{R_r}{L_r} \end{bmatrix}$$

$$A_{22} = \begin{bmatrix} -\left\{ \frac{R_s}{\sigma L_s} + \frac{R_r(1-\sigma)}{\sigma L_r} \right\} & 0 \\ 0 & -\left\{ \frac{R_s}{\sigma L_s} + \frac{R_r(1-\sigma)}{\sigma L_r} \right\} \end{bmatrix}$$

and

$$C_q = \begin{bmatrix} 1 & 0 \\ 0 & 1 \end{bmatrix}$$

The two variables  $x_2 = [i_{\alpha s} \quad i_{\beta s}]^T$  can be directly obtained from (5.59b) as

$$x_2 = [C_q]^{-1} y \quad (5.60)$$

The remaining two state variables require an observer for estimation.

By manipulating the equation in (5.59),  $x_1 = [\lambda_{\alpha r} \quad \lambda_{\beta r}]^T$  may be viewed as the state of a two dimensional subsystem

$$\begin{aligned} \dot{x}_1 &= A_{11}x_1 + A_{12}x_2 + B_1u \\ &= A_{11}x_1 + v \end{aligned} \quad (5.61)$$

$$= A_{21}x_1 \quad (5.62)$$

where,  $v = A_{12}x_2 + B_1u$

$$= A_{12}[C_q]^{-1} y + B_1u \quad (5.63)$$

$v$  can be treated as a known input since  $u$  is known and  $y$  is directly measurable.

The 'output vector'  $z$  may be expressed as

$$\begin{aligned} z &= A_{21}x_1 \\ &= \dot{x}_2 - A_{22}x_2 - B_2u \end{aligned}$$

$$= [C_q]^{-1} \dot{y} - [C_q]^{-1} y - B_2 u \quad (5.64)$$

We can estimate  $x_1$  with an observer

$$\dot{\hat{x}}_1 = (A_{11} + M_1 A_{21}) \hat{x}_1 + v - M_1 z \quad (5.65)$$

Where the  $2 \times 2$  matrix  $M_1$  may be chosen so as to place the poles of (5.65) in any desired configuration. Substituting for  $v$  and  $z$  from (5.63) and (5.64) respectively, we have

$$\dot{\hat{x}}_1 = (A_{11} + M_1 A_{21}) \hat{x}_1 + A_{12} [C_q]^{-1} y + B_1 u - M_1 [C_q]^{-1} \dot{y} + M_1 A_{22} [C_q]^{-1} y + M_1 B_2 u \quad (5.66)$$

Which is  $4 \times 2$  dimensional observer for the system (5.57)

The only apparent difficulty in implementing the observer (5.66) is that differentiation of the output  $y$  is required. This can be avoided by redefining the state of the observer to be

$$\bar{x}(t) = \hat{x}_1(t) + M_1 [C_q]^{-1} y(t) \quad (5.67)$$

Substituting (5.67) in (5.66), we get

$$\dot{\bar{x}} = (A_{11} + M_1 A_{21}) \bar{x} + (B_1 + M_1 B_2) u + [A_{12} + M_1 A_{22} - (A_{11} + M_1 A_{21}) M_1] [C_q]^{-1} y \quad (5.68)$$

#### **Deadbeat observer:**

The system (5.57) is rearranged with this observer as follows:

$$\dot{\hat{x}} = (A + MC) \hat{x} + BU - M \quad (5.69)$$

where,  $M$  is the  $4 \times 1$  gain matrix is suitably chosen that all the observer poles are located at the origin, i.e., all the eigenvalues of  $(A + MC)$  are zero.

## CHAPTER VI

### SIMULATION STUDY OF OBSERVER-BASED FIELD-ORIENTED INDUCTION MOTOR DRIVE

#### 6.1 INTRODUCTION

Field orientation control of induction motors using different types of observers with voltage and current source inverters have been shown in the previous chapter. For voltage and current source drives simulation studies are conducted to study the effectiveness of the observers. The observer systems are tested for steady state and different transient conditions. These studies include existence of field orientation during steady state, transient conditions and restoration of field orientation during parameter deviations.

The induction motor is modeled in its mutually perpendicular stationary axes variables. The state space equations are solved with Runge-Kutta-Gill subroutine in a PC environment. The time step  $\Delta T$  is taken as 0.0005 sec. The observer state equations are also solved using the same routine and time step. The simulation results for different operating conditions are listed in the subsequent sections. Simulation studies of the drive systems are carried out to justify the effectiveness of the observer performance.

#### 6.2 FULL ORDER OBSERVER BASED SYSTEM

##### 6.2.1 VOLTAGE SOURCE INVERTER FED INDUCTION MOTOR DRIVE

The performance evaluation of the control scheme was made by simulation on a digital computer (Intel 586) environment. Parameters of the induction motor and the PI controller gains used for simulation are listed in Appendix I. Sampling time for the speed and the controller was 50ms. Rotor flux command was set at its rated value. Fig. 6.1 through 6.3 that present the behavior of some important control variables following the start up and step change in speed. Fig. 6.1 shows the starting of motor from rest with set speed 150 rad(mech.) per second under starting condition for voltage source inverter shown in Fig. 5.8. The vector control scheme, used here, is the direct field orientation control.

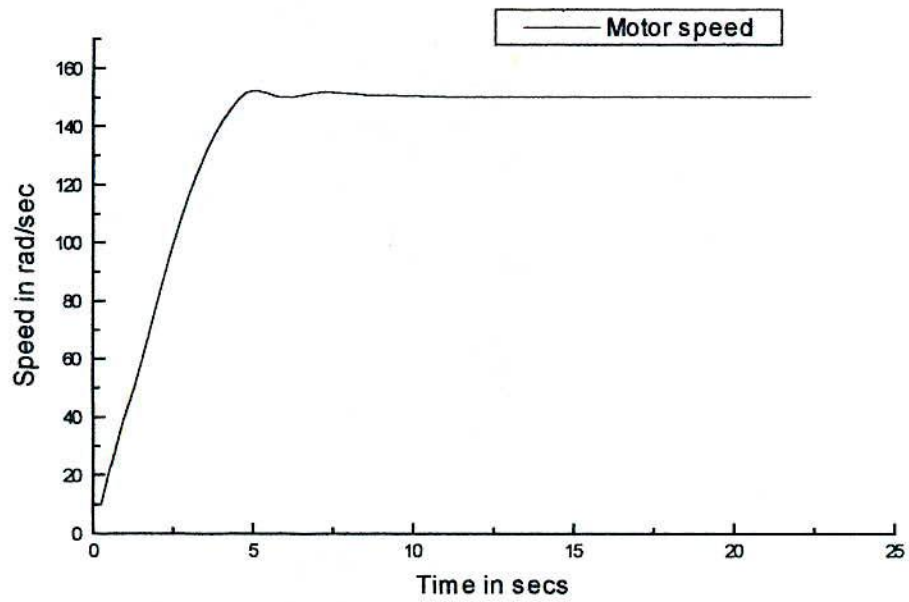


Fig. 6.1 Speed under starting condition for Voltage source inverter.

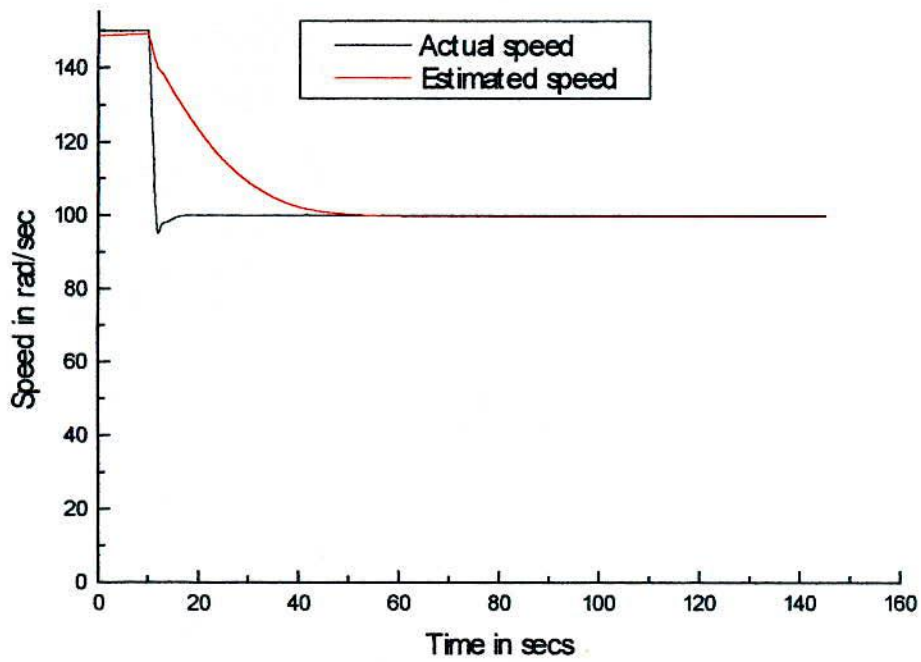
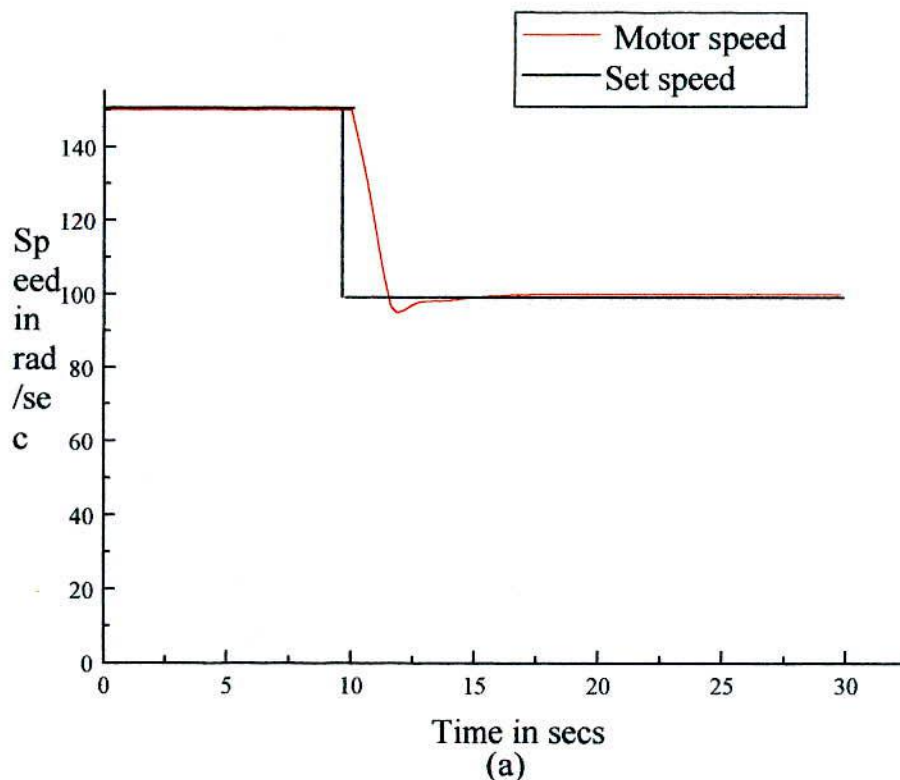


Fig.6.2 Speed adaptation with full order observer.

The PI controller gains are selected for both flux estimation and the speed adaptive scheme is same. Fig. 6.1 shows the motor speed starting up from the rest with set speed 150 rad(mech.) per sec and load torque 1.0 Nm.. At transient period the machine speed overshoot 1.56% by its set speeds 150 rad/sec over a short duration. Fig. 6.2 shows the performance of the same observer in which updating algorithm is used to eliminating speed error. To evaluate its performance after 15 seconds the set speed is changed from 150 rad/sec to 100 rad/sec and observed the estimated speed gradually decreased from its rated speed value and merge as possible to its set speed value. So this observer can also be used as speed prediction purpose. Fig. 6.3(a) presents the behavior for sudden change in the set speed from 150 rad/sec to 100 rad/sec. Simulation results confirm decoupled operation. It is evident from Fig. 6.3(b). Minor deviation of the rotor flux from its set value is noted during the setting period. The observer successfully estimates rotor flux and minor deviation between the actual flux and estimated flux is shown in Fig.6.3 (b).



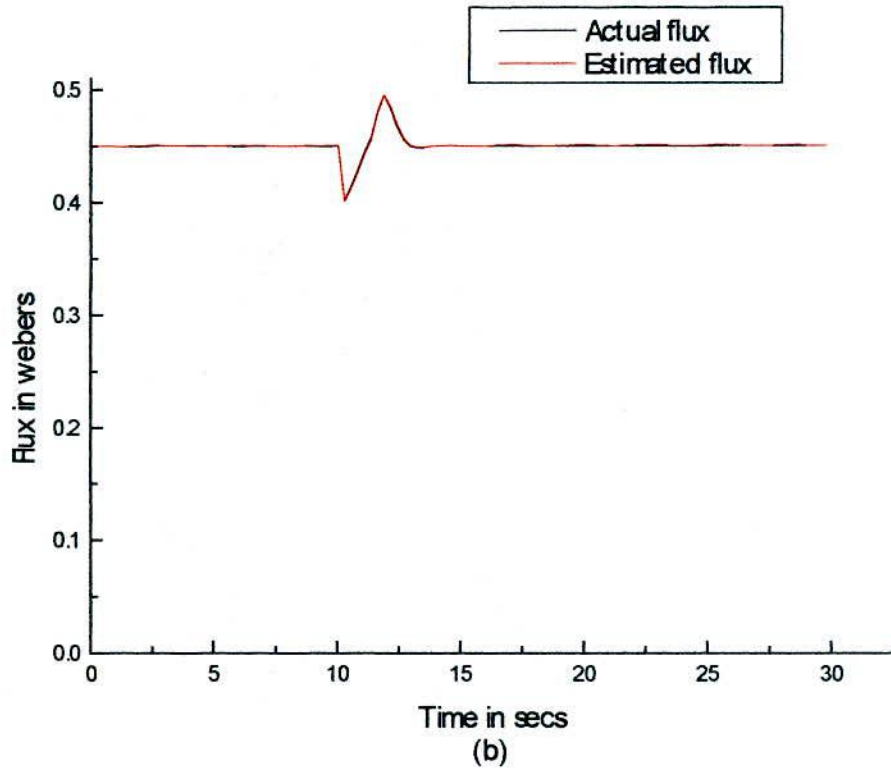


Fig. 6.3(a) Speed and (b) flux when the reference speed decreased in step from 150 rad/sec to 100 rad/sec.

### 6.2.2 CURRENT SOURCE INVERTER FED INDUCTION MOTOR DRIVE

Fig. 6.4 shows the speed and flux for current source inverter fed in Fig. 5.9 in which direct field orientation control technique is used. At transient period the machine speed overshoot 1.50 % from its set speeds 157.0 rad/sec over a short duration which is shown in Fig. 6.4(a). The actual value of flux in Fig. 6.4(b) shows the ripple with nearer distance that occurs due to the fast switching logic of current source inverter. Even that occurred situation, the observer-estimated flux merges the rotor actual flux.

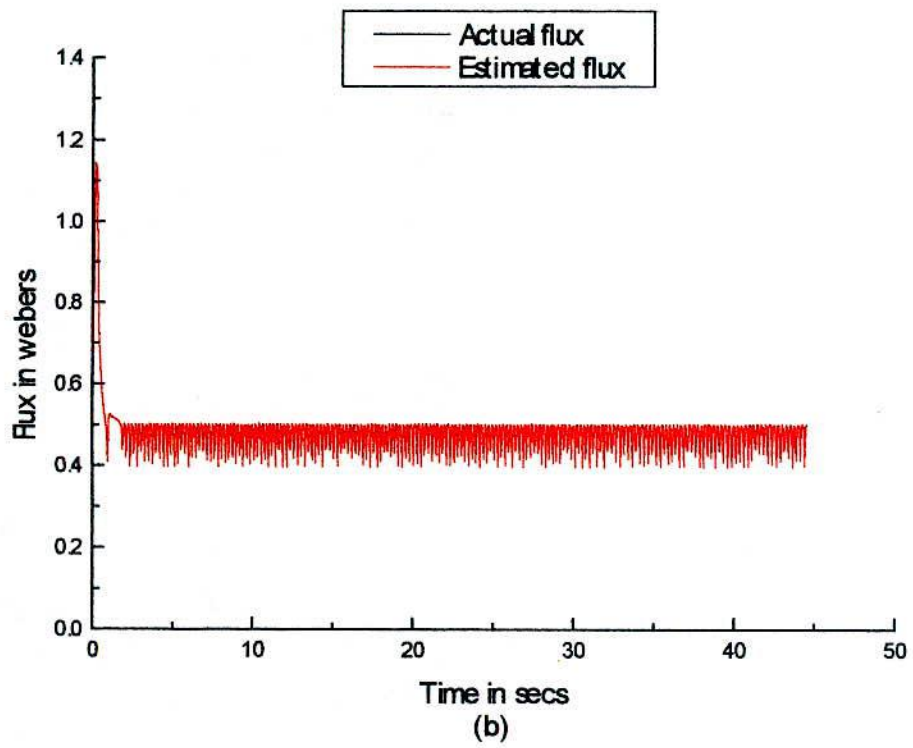
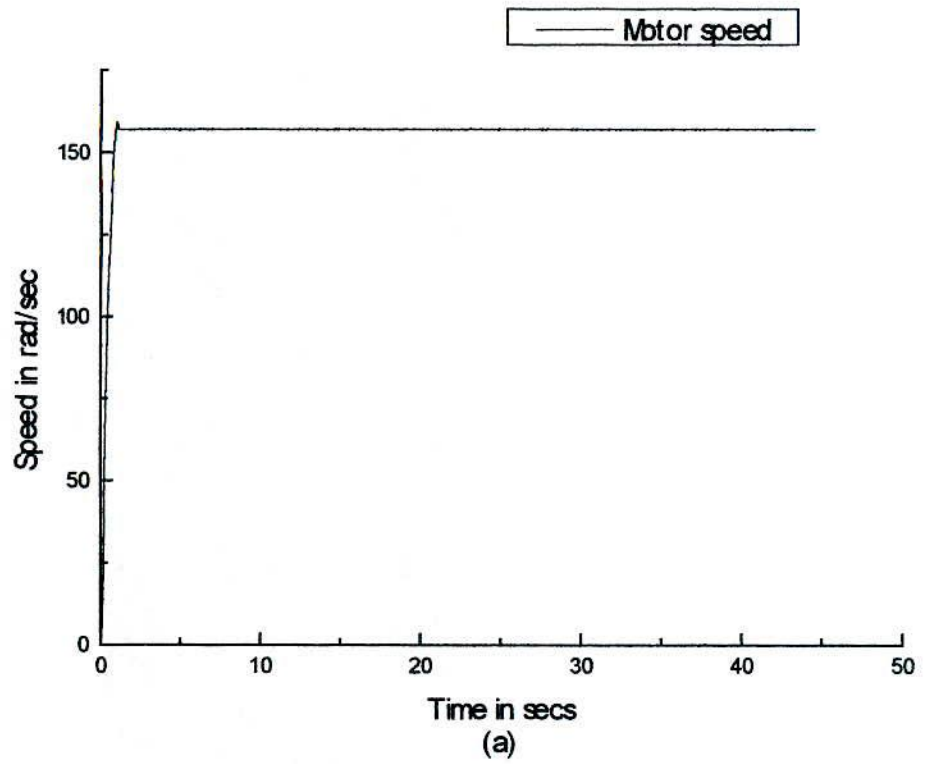
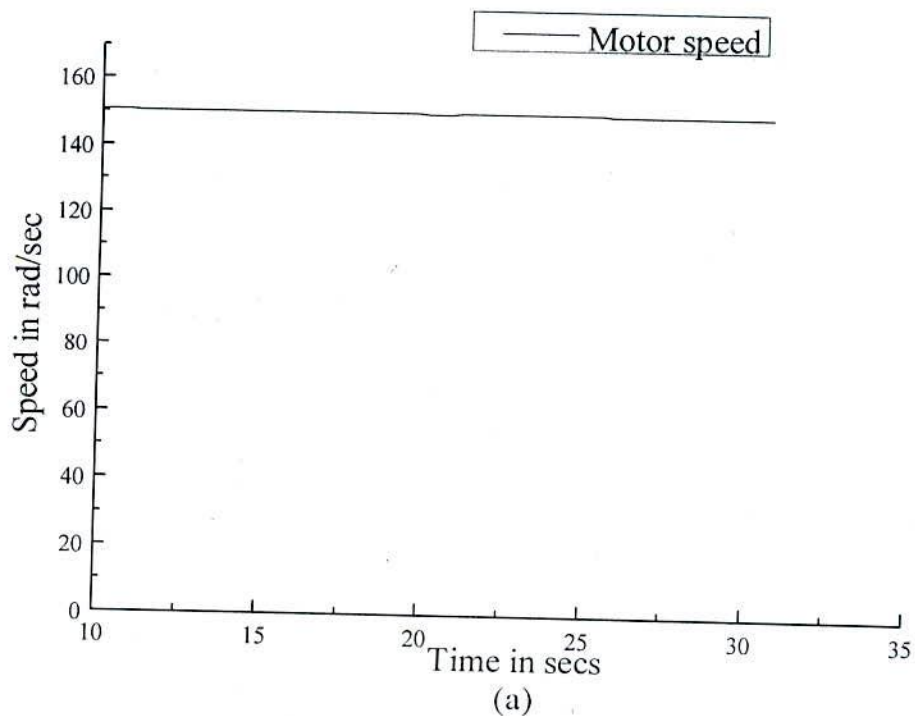


Fig. 6.4 (a) speed and (b) flux for current controlled inverter.



### 6.3 REDUCED ORDER OBSERVER-BASED SYSTEM (GOPINATH TYPE)

Fig. 6.5. Shows the speed and flux responses for voltage source inverter in Fig. 5.10. The technique that is used here is direct field orientation. After 20 seconds the machine resistance is increased by 50 % but the observer resistance is remain fixed. In that time the machine speed is overshoot 0.66% from its set speed 150 rad/sec, which is very negligible amount and the deviation between actual flux and estimated flux is also negligible which is around 1.11%. After transient the motor speed merges the set speed and the observer successfully estimates the machines flux. The observer poles are finally selected as  $\lambda_1 = -0.20$  and  $\lambda_2 = -0.20$ . So its greatest advantages are its robustness and its low sensitivity to the machine parameter variations.



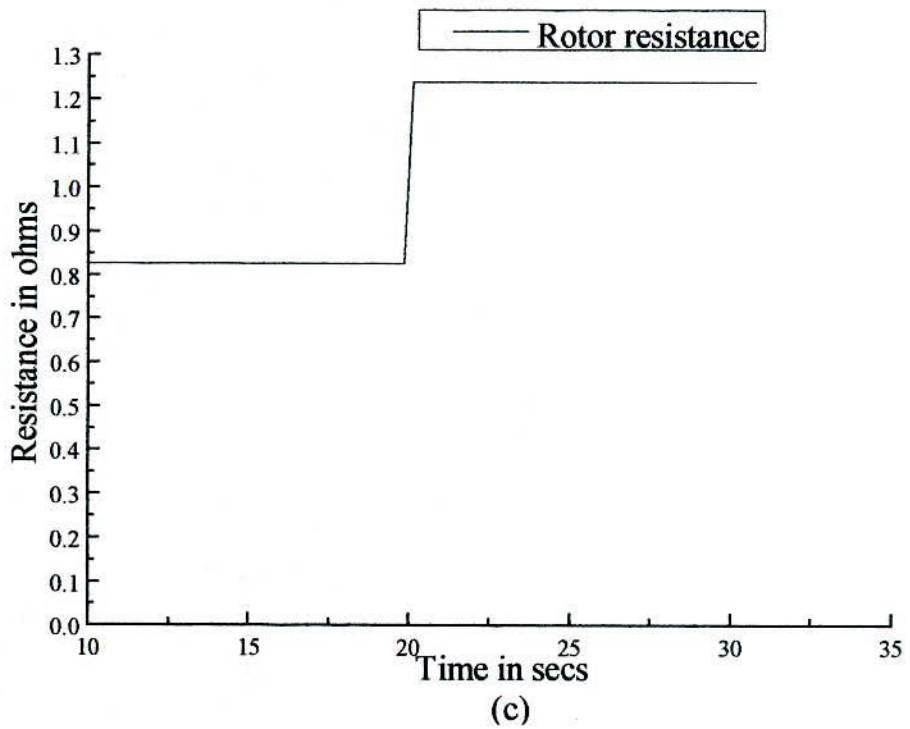
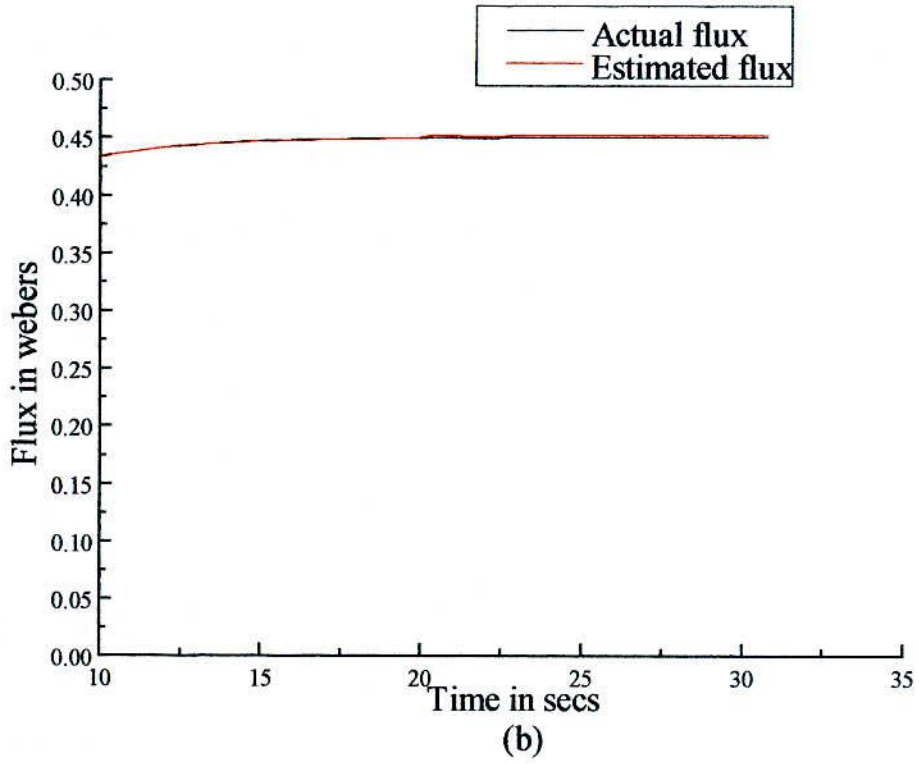


Fig. 6.5 (a) Speed (b) Flux estimation and (c) Rotor resistance for 50% increment in rotor resistance in step for voltage source inverter.

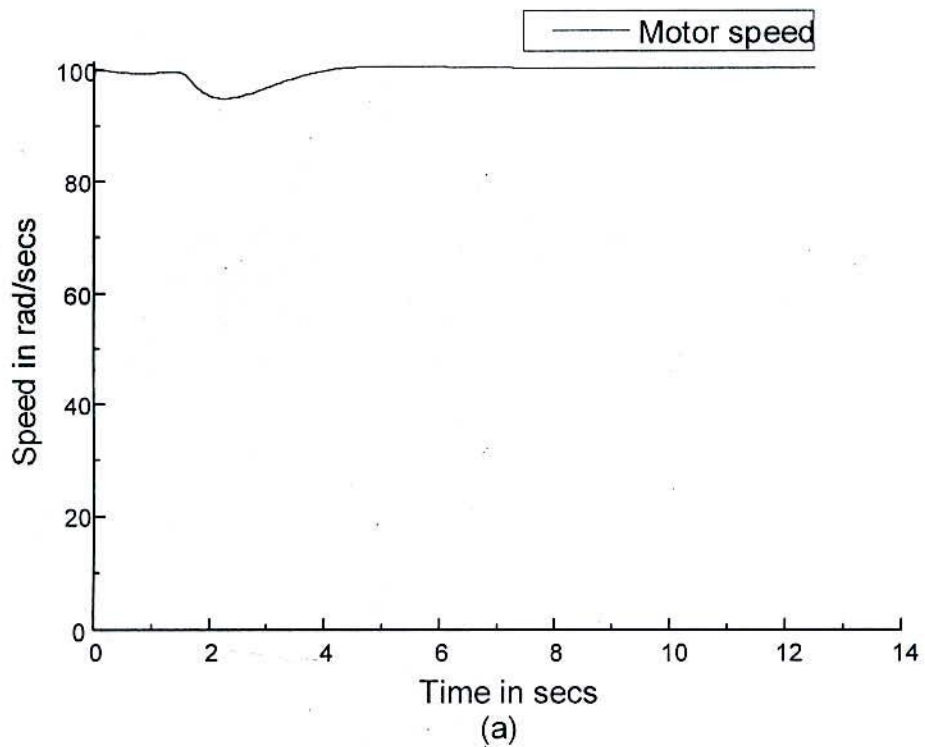
#### 6.4 REDUCED ORDER OBSERVER-BASED SYSTEM (GENERALIZED TYPE)

Fig. 6.6 and Fig.6.8. show the speed and slip speed responses for voltage and current source inverter in Fig. 5.10 and Fig.5.11, where indirect field orientation technique is used. The observer poles are chosen for good flux estimation are  $\lambda_1 = -26.65$  and  $\lambda_2 = -24.65$  for voltage source and  $\lambda_1 = -4.5$  and  $\lambda_2 = -5.0$  and for current source inverter.

To justify the robustness of the observer under parameter mismatch between the controller and the machine, the rotor resistance of the induction motor was increased after time 2 seconds and the value of rotor resistance in the slip calculator was preserved to its nominal value. This creates a notch both speed and slip speed and over fluxing of the induction machine. The deviations of speed, slip speed and the rotor flux from its nominal value are shown in Fig. 6.6 and Fig. 6.8 and Fig.3.8 respectively. The study does not incorporate any change in the rotor resistance for the observer system. An identical value of actual and observed rotor flux indicates robustness of the observer under parameter deviation.

In designing the observer suitable dynamics of the observed flux is the most important factor. This dynamics is governed by the poles of the observer  $\lambda_1$  and  $\lambda_2$ . Usually, deadbeat observers produce dynamics similar to the system. But these observers produce mismatched results for parameter variation. Another important aspect is that the observer poles must not coincide with the poles of the system. This requires a study of system pole variation with the variation of the operating condition. The system matrix (A matrix) has one real pole and two complex conjugate poles. Motor speed is varied from (0 to 160) and slip speed is changed from (0 to 20). For this variations the real poles variation from (-118.548 to -106.716) and the complex conjugate poles vary from  $(-1.193 \pm j 40.925)$  to  $(-7.109 \pm j 7.493)$ . The variation of the poles for variable speed and torque (here  $\omega_{sl}$ ) are

shown in Fig. 6.7. From this curves it is evident that one of the poles is real and is located far left from imaginary axis for variations motor speed and slip. The other two poles are complex conjugates where the imaginary part is dominating. So if the real values are selected for observer poles closer to the imaginary axis there is no probability of coinciding observer poles with the system poles.



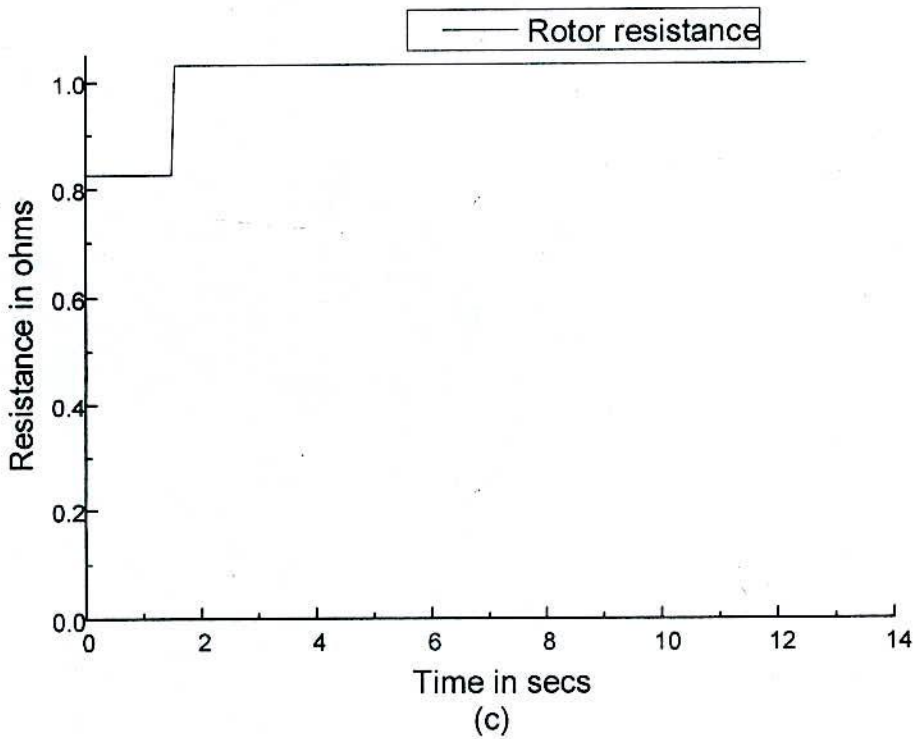
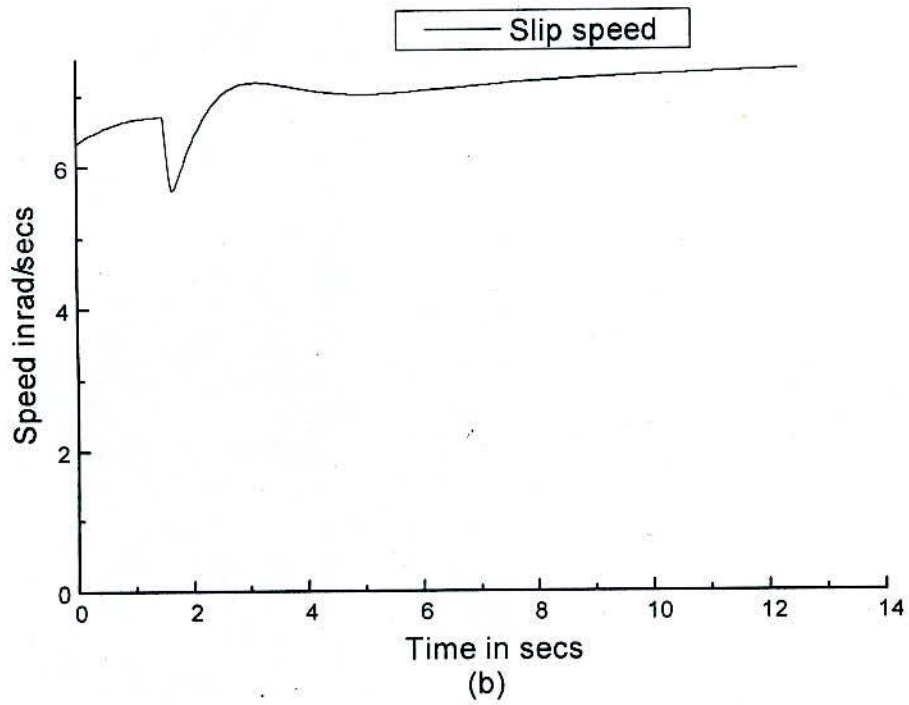
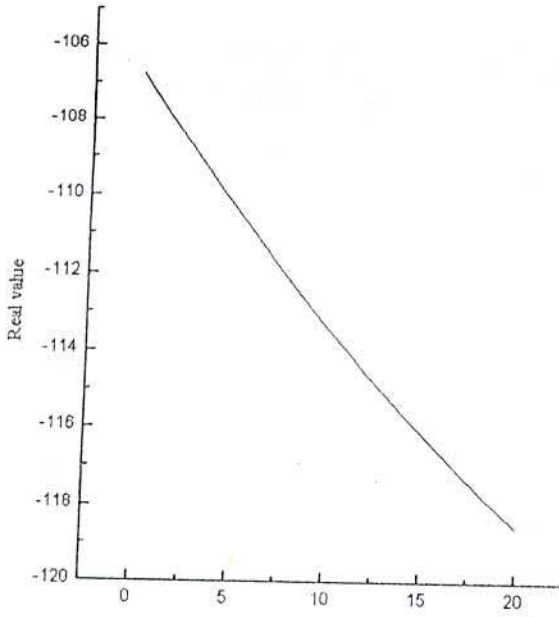
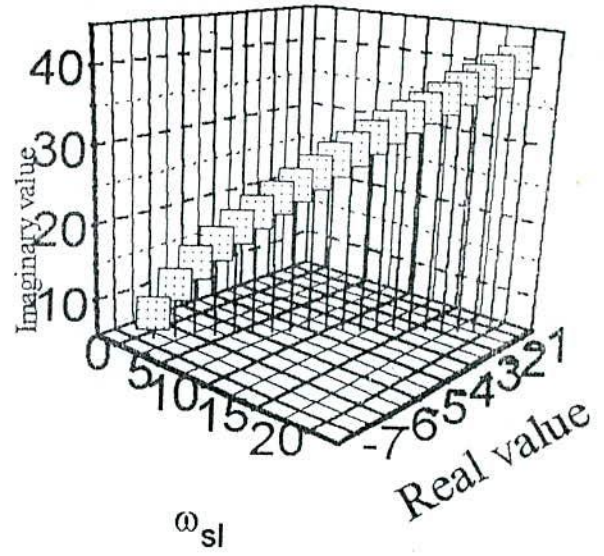


Fig. 6.6 (a) Motor speed (b) slip speed and (c) rotor resistance for 25% increment in rotor resistance for Voltage source inverter.

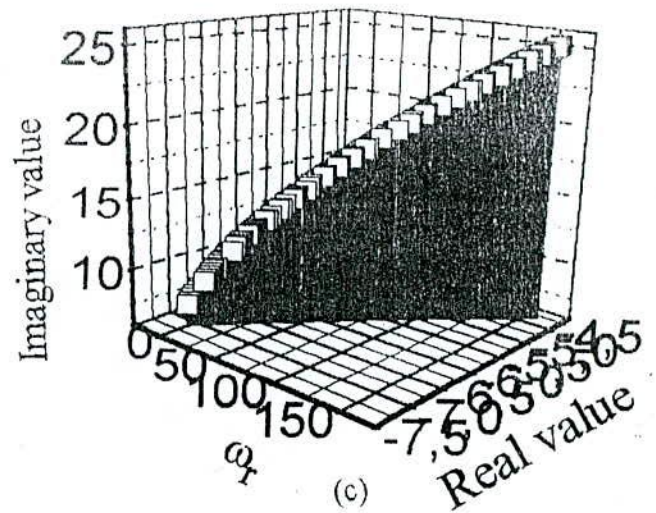


$\omega_{sl}$

(a)



(b)



(c)

Fig. 6.7 Variation of the poles of the system due to variation of slip speed and motor speed.

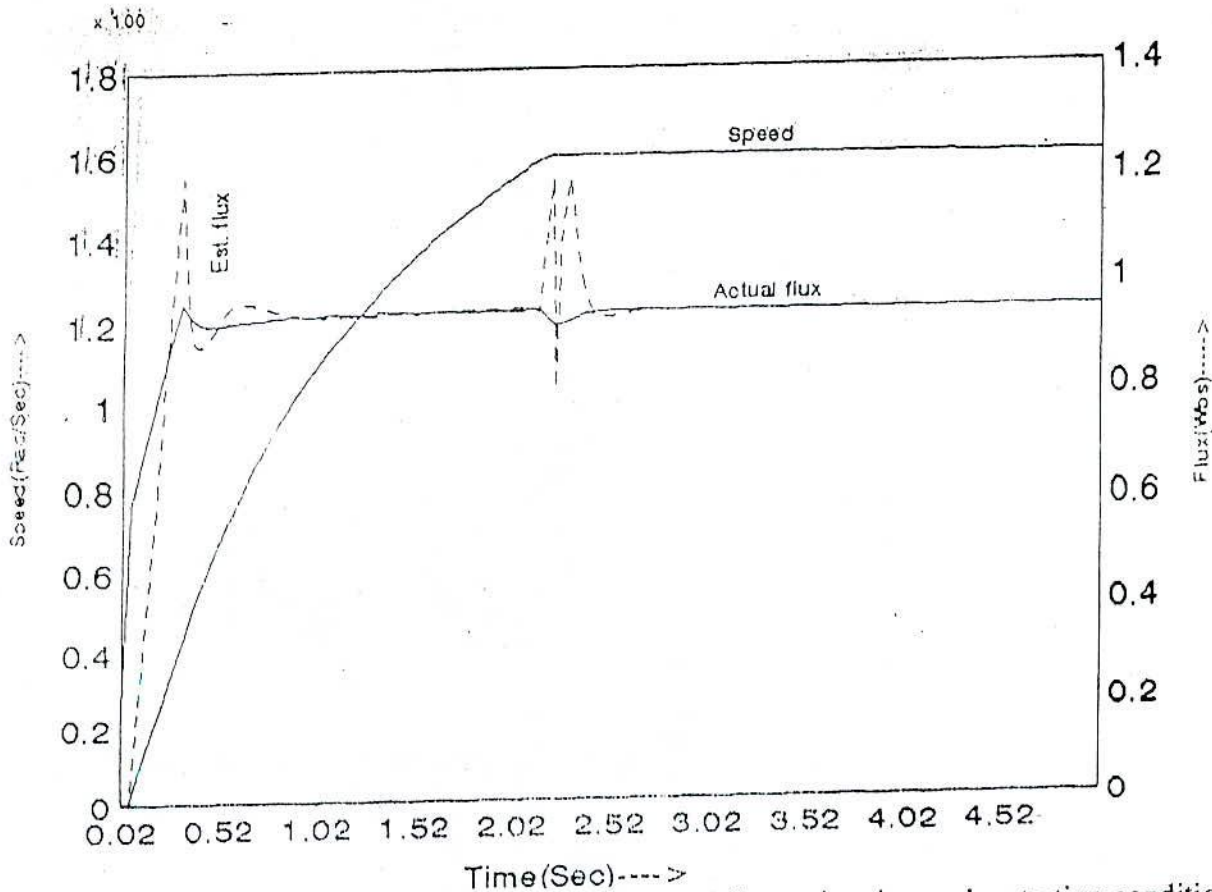


Fig. 6.8 Motor Speed and flux estimation under starting condition for current source inverter.

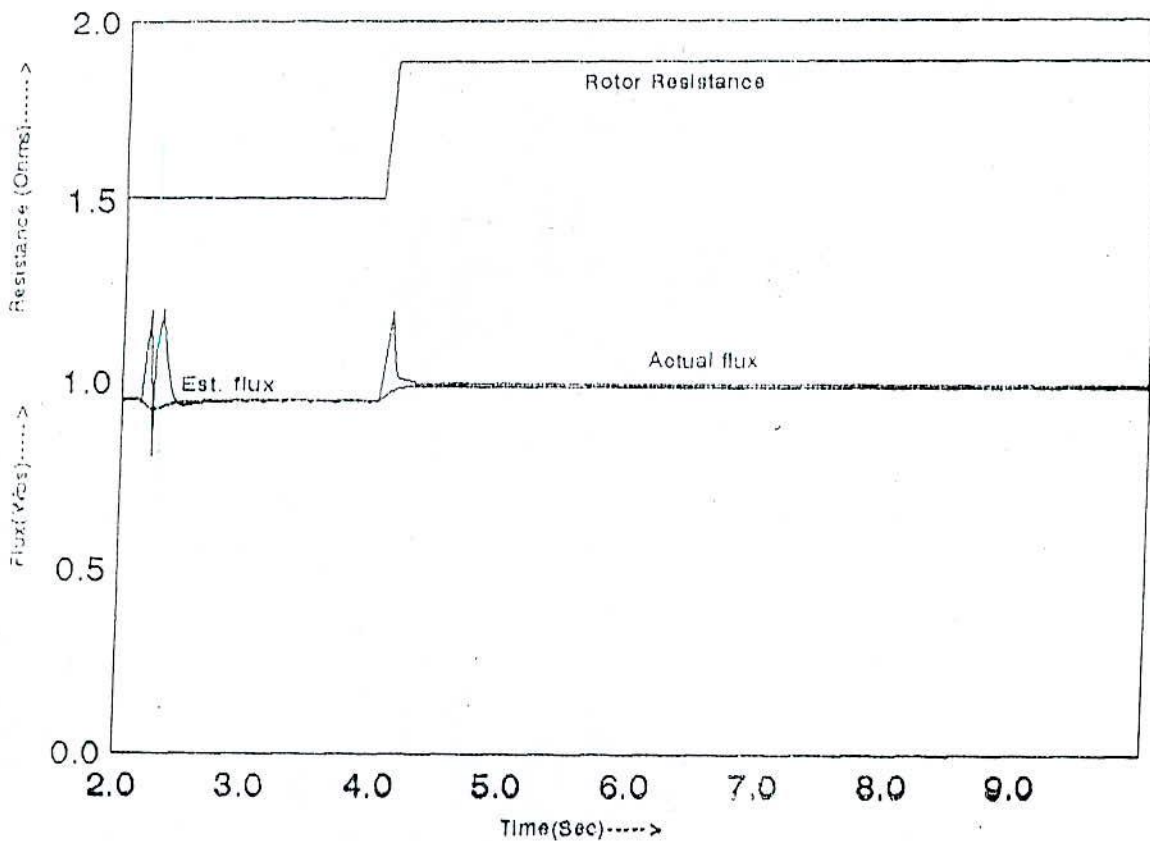


Fig. 6.9 Estimation of Rotor Flux for 25% increment in rotor resistance for current source inverter.

### 6.4.1 ROTOR RESISTANCE ADAPTATION FOR INDIRECT VECTOR CONTROL

Finally, the observer was utilised to adapt the actual rotor resistance of the machine and to use it for slip speed calculation shown in Fig. 6.10. The algorithm uses PI controller to process the error in flux between the observed value and set value. The adaptation process using flux error is presented in Fig. 6.11 and Fig.6.12 for voltage and current source inverter respectably. In this process rotor resistance is increased by 25%. The actual flux and estimated fluxes are initially more than the set value of flux. As the adaptation process is on the adapted rotor resistance in the slip calculator gradually merges to the actual value of rotor resistance and the estimated and actual fluxes are driven to the set value of rotor flux indicating restoration of field orientation condition.

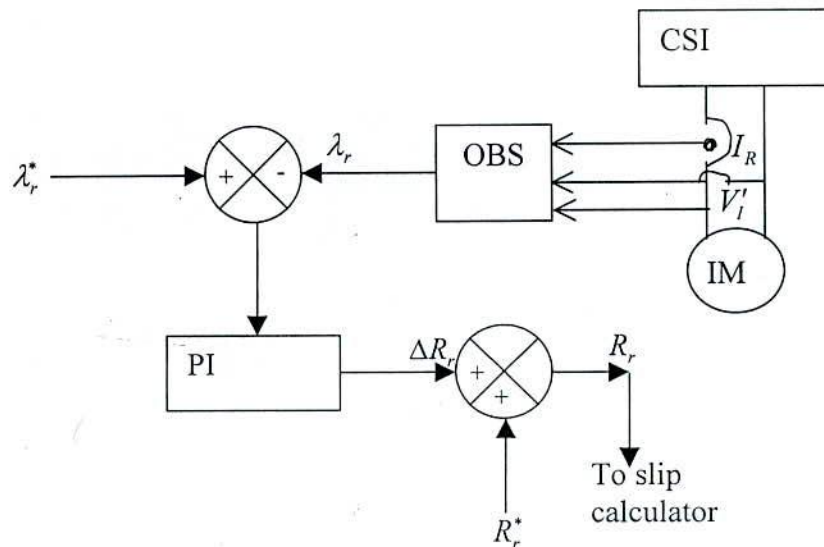
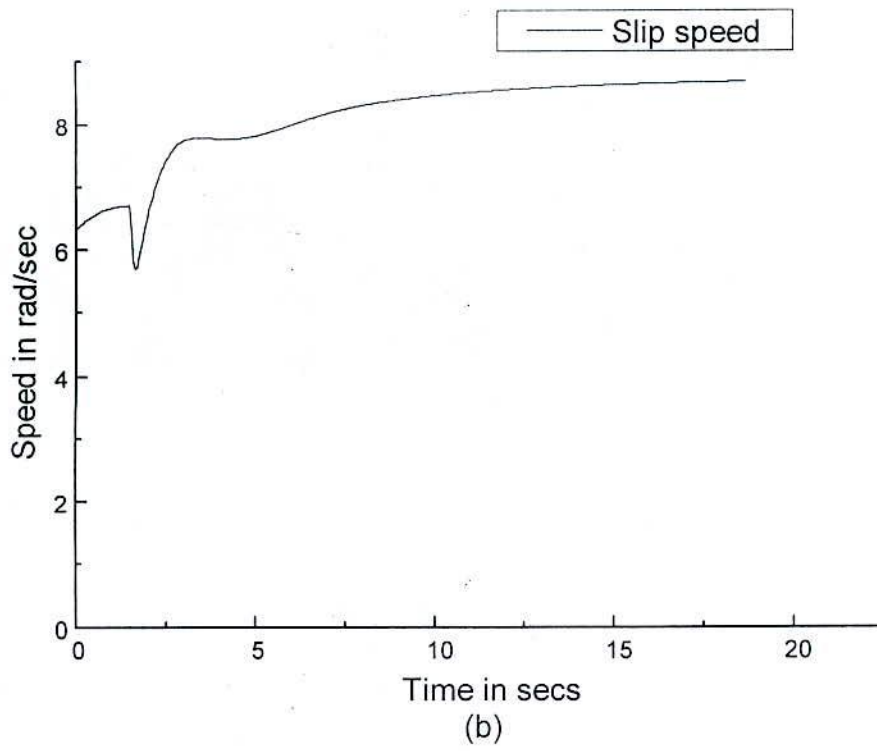
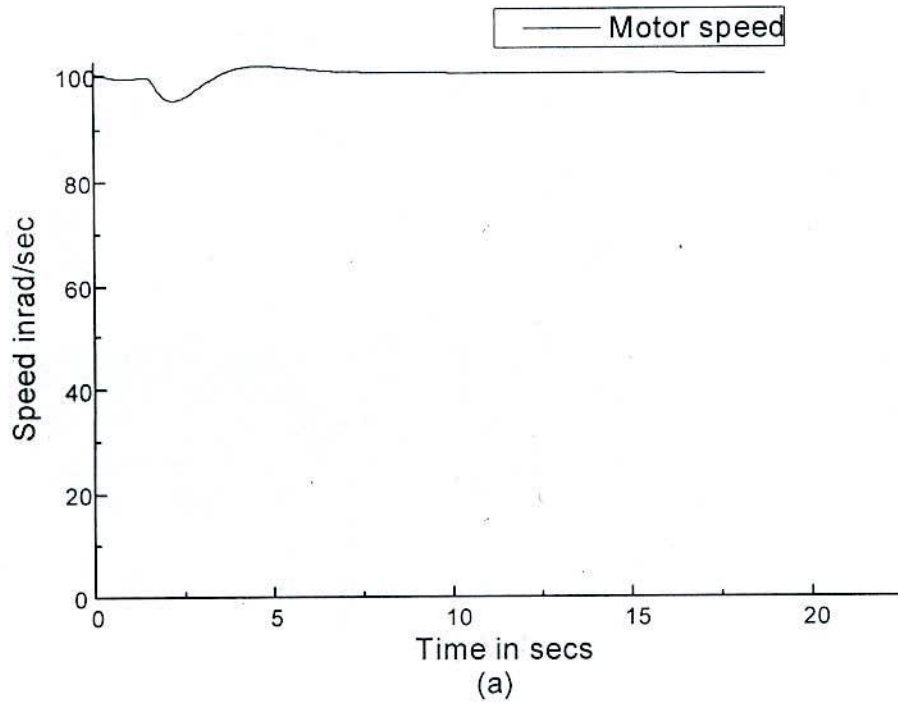


Fig. 6.10 Block diagram of rotor resistance adaptation process.





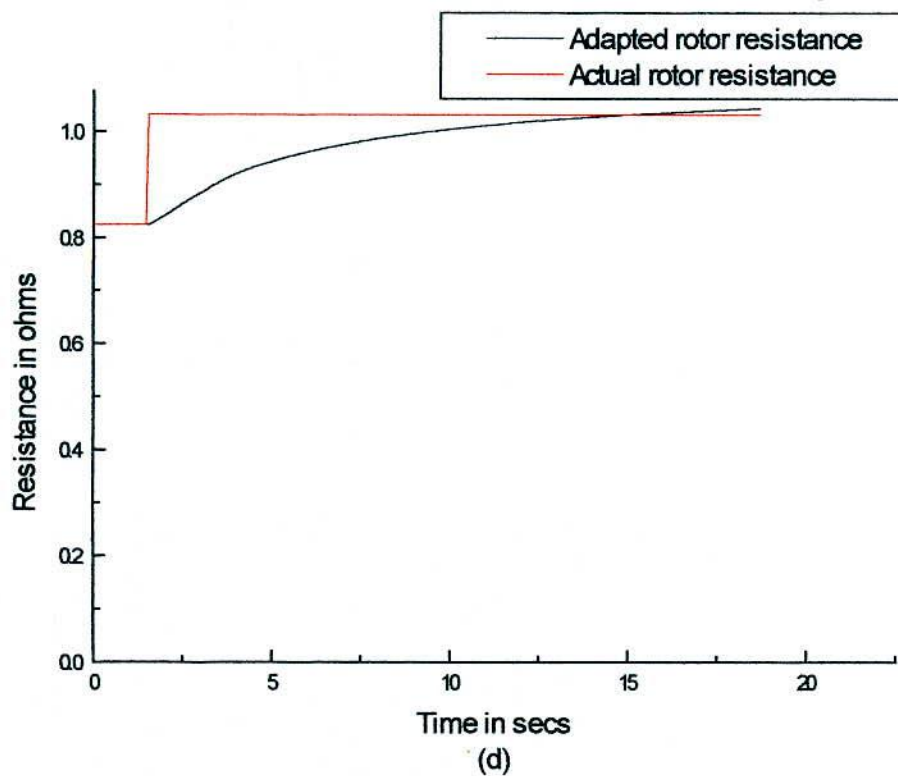
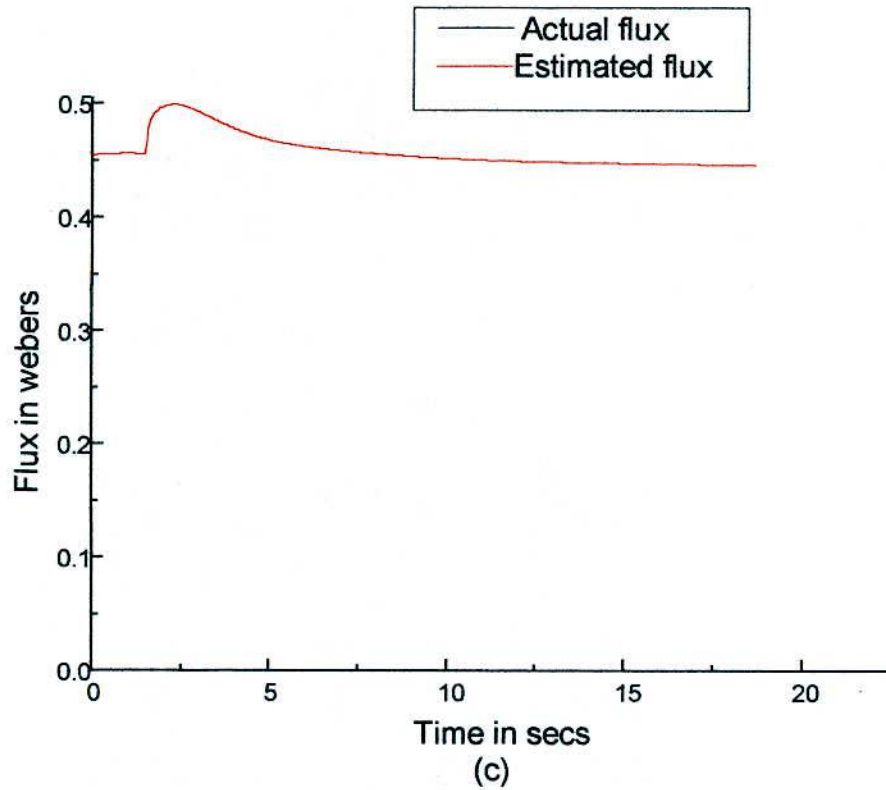


Fig 6.11 (a) Motor Speed (b) Slip speed (c) Actual flux and (d) Adapted rotor resistance using estimated rotor flux for Voltage source inverter.

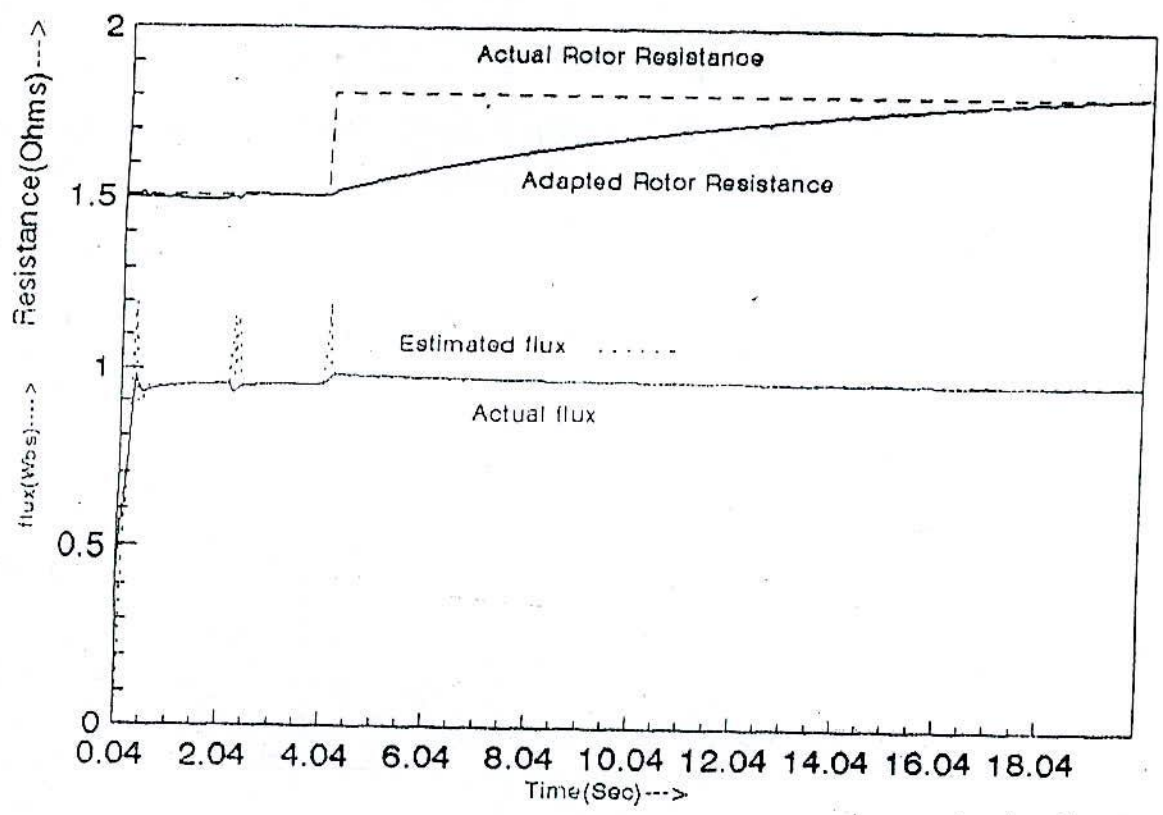


Fig 6.12 Actual rotor flux, estimated rotor flux and Adapted rotor resistance using estimated rotor flux for current source inverter.

### 6.5 DEAD BEAT OBSERVER

The only difference of this observer from the others is its zero poles. Fig. 6.13 shows the motor speed for voltage source inverter in Fig. 5.10 in which direct field orientation technique is used. At transient machines speed is deviated 3.2% by its set value of speed, which is acceptable, and fluxes deviation is 1.55% by its set flux Fig. (3.9). But the observer successfully estimating the rotor flux and there is no difference between the estimated flux and actual flux.

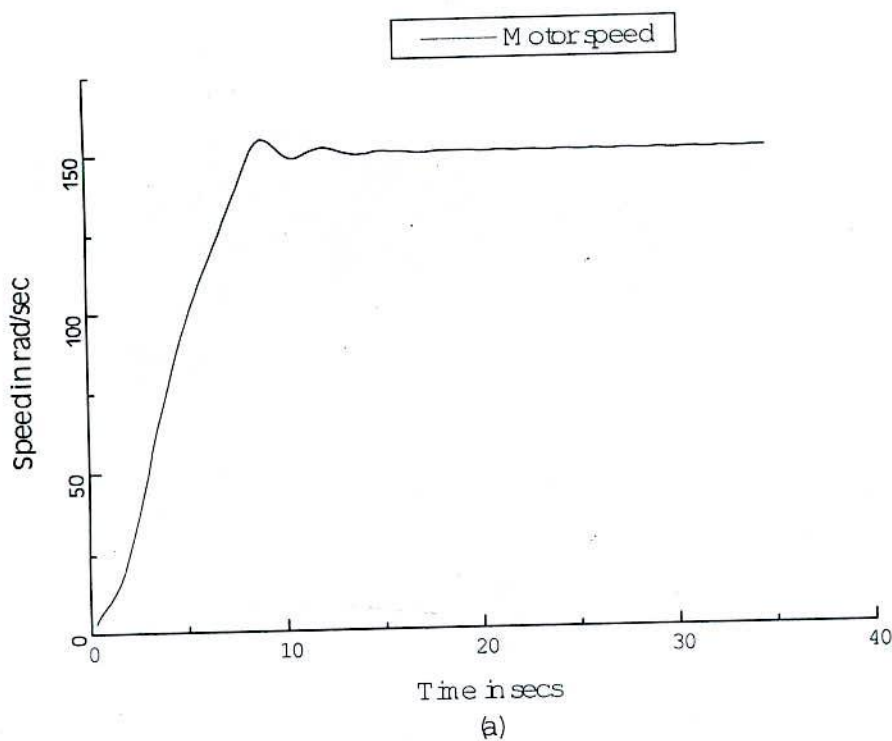


Fig. 6.13 Starting performance for voltage source inverter.

## CHAPTER VII

### FLUX ESTIMATION USING ANN

#### 7.1 INTRODUCTION

The time required to train an ANN with backpropagation training algorithm depends on the size of the training data set and training algorithm. The standard version of the backpropagation algorithm is very slow and requires a large number of iterations. An improve version of this algorithm is the backpropagation with momentum and adaptive learning rate to train to understand the model of the system, which permits a reduction of the number of iterations. The selection of network size is a compromise between output precision, training time, and ANN generalization capabilities. There is no general procedure for determining the right ANN size for a specific problem. With a small number of neurons, the network will take a long time to converge or will not converge to a satisfactory error. On the other hand, if the number of neurons is large or if the training error is very small, the ANN will memorize the training vectors and give a large error for generalization vectors.

#### 7.2 NEURAL-NETWORK ROTOR-FLUX ESTIMATOR

Rotor flux estimation proposes stator two-axis voltages, stator two-axis currents and mechanical speed are taken as input data. While the motor accelerated from standstill to its steady-state speed, 300 samples of each quantity (sampling period of 0.00025 ms for each channel) were recorded and stored in a measurement data file. The principle for training the ANN-flux estimator is shown in Fig. 7.1. Training was achieved with sinusoidal voltages and currents in order to improve the learning process, and it continued until the sum of squared error on the components of flux was below a desired level.

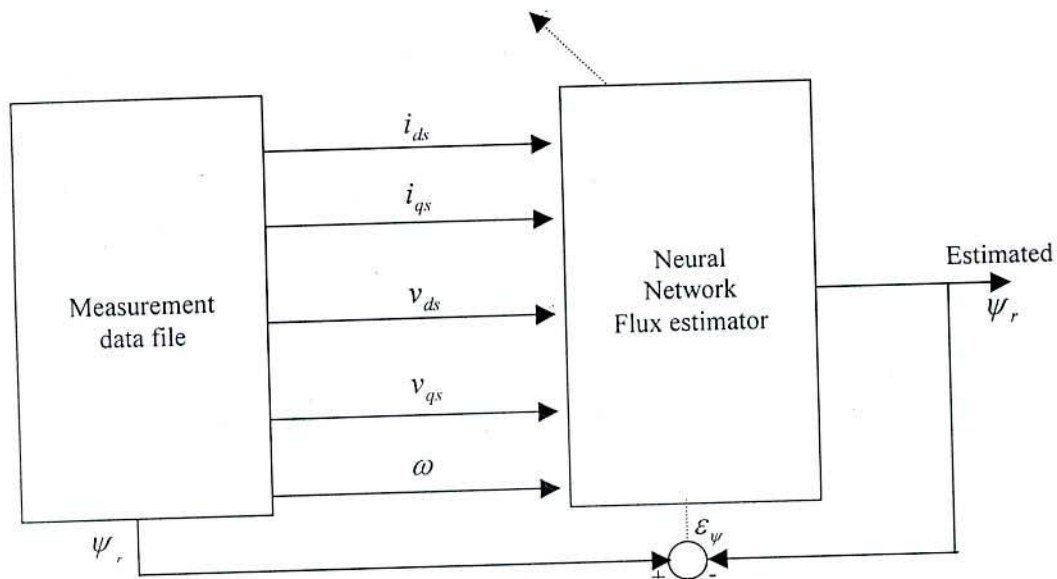


Fig. 7.1 Principle for training the ANN-flux estimator.

### 7.3 SIMULATION RESULTS

A 2-kw induction motor was used as a case of study. The parameters of the machine were determined experimentally and are given as follows:

Pair of poles  $P_p=2$

Resistance of stator =  $1.798 \Omega$

Resistance of rotor =  $0.825 \Omega$

Inductance of stator =  $0.08323 \text{ h}$

Inductance of rotor =  $0.08323 \text{ h}$

Mutual inductance =  $0.07613 \text{ h}$

Moment of inertia  $J_J = 0.095 \text{ Kg.m}^2$

Damping coefficient  $B = 0.0002 \text{ N-m}$

Load torque =  $1.0 \text{ Nm}$

The trained network consists of a three layer neural network with five input nodes connected to eight sigmoid neurons and two output nodes connected to eight sigmoid neurons (5-8-8-2) which is shown in Fig. 7.2. Training was initiated when the error fell below  $0.000571$  with 389 iteration. The results obtained with simulator and theoretical data are almost identical and presented in Fig. 7.3.

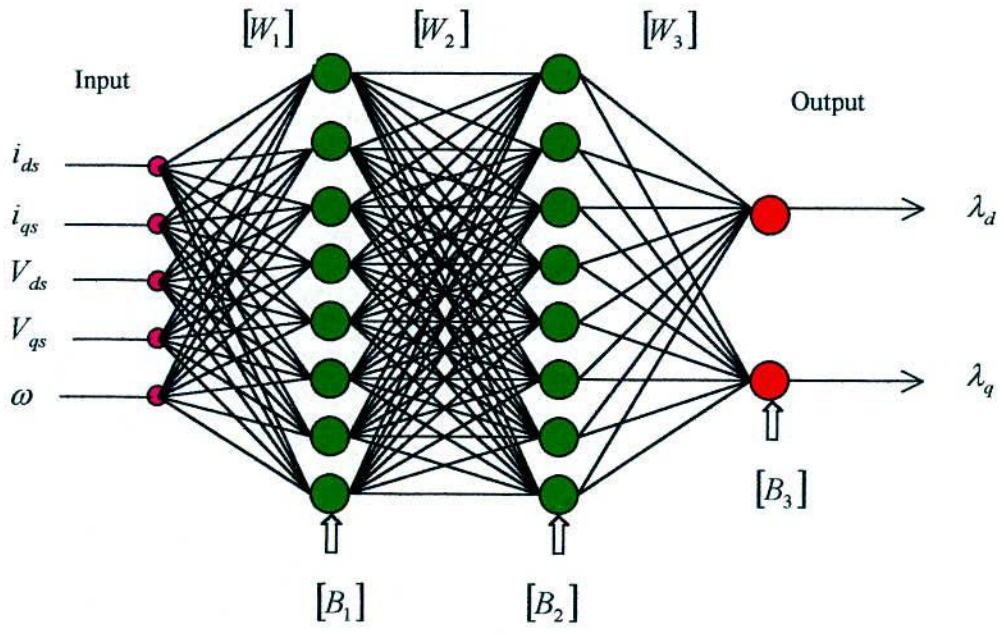
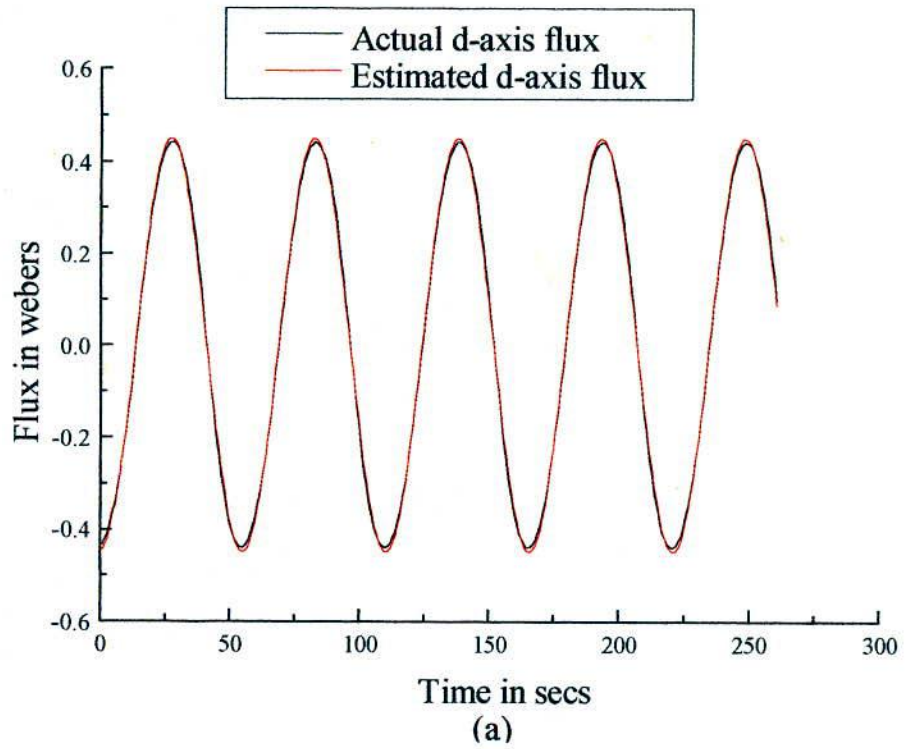


Fig. 7.2 Three-layer ANN Rotor-flux estimator.



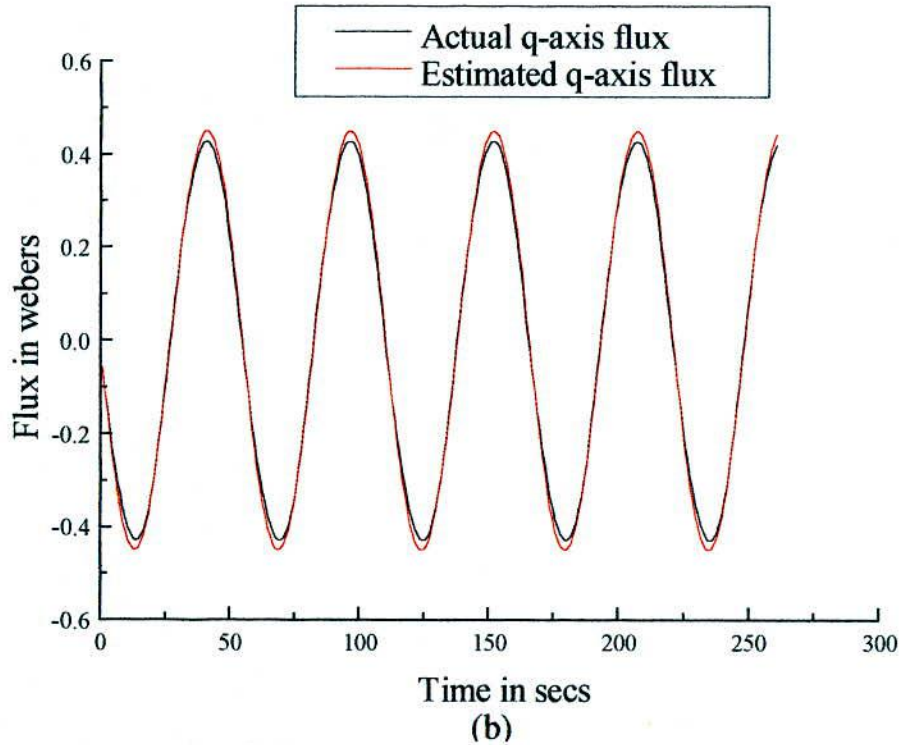


Fig. 7.3 ANN estimated rotor flux (a) d-axis (b) q-axis.

#### 7.4 NEURAL-NETWORK ROTOR-FLUX ESTIMATOR AND DIRECT FIELD ORIENTATION

The block diagram of ANN rotor flux estimator based direct field orientation controller for voltage fed inverter is shown in Fig. 7.4. It is similar to block in Fig. 5.10 but only difference is replacing ANN flux estimator in place of rotor flux observer and one more input that means motor speed is taken in ANN flux estimator. For direct field orientation,  $\cos(\omega_e t)$  and  $\sin(\omega_e t)$  signals are obtained from the estimated rotor-flux signals as given below is

$$\cos(\omega_e t) = \frac{\hat{\lambda}_{dr}}{|\hat{\lambda}_r|} \quad (7.1)$$

$$\sin(\omega_e t) = \frac{\hat{\lambda}_{qr}}{|\hat{\lambda}_r|}$$

where

$$|\hat{\lambda}_r| = \sqrt{(\hat{\lambda}_{dr})^2 + (\hat{\lambda}_{qr})^2}$$



Current command  $|I_M|^*$  can be generated from a flux-control loop, while current command  $|I_T|^*$  can be generated from a speed-control loop.

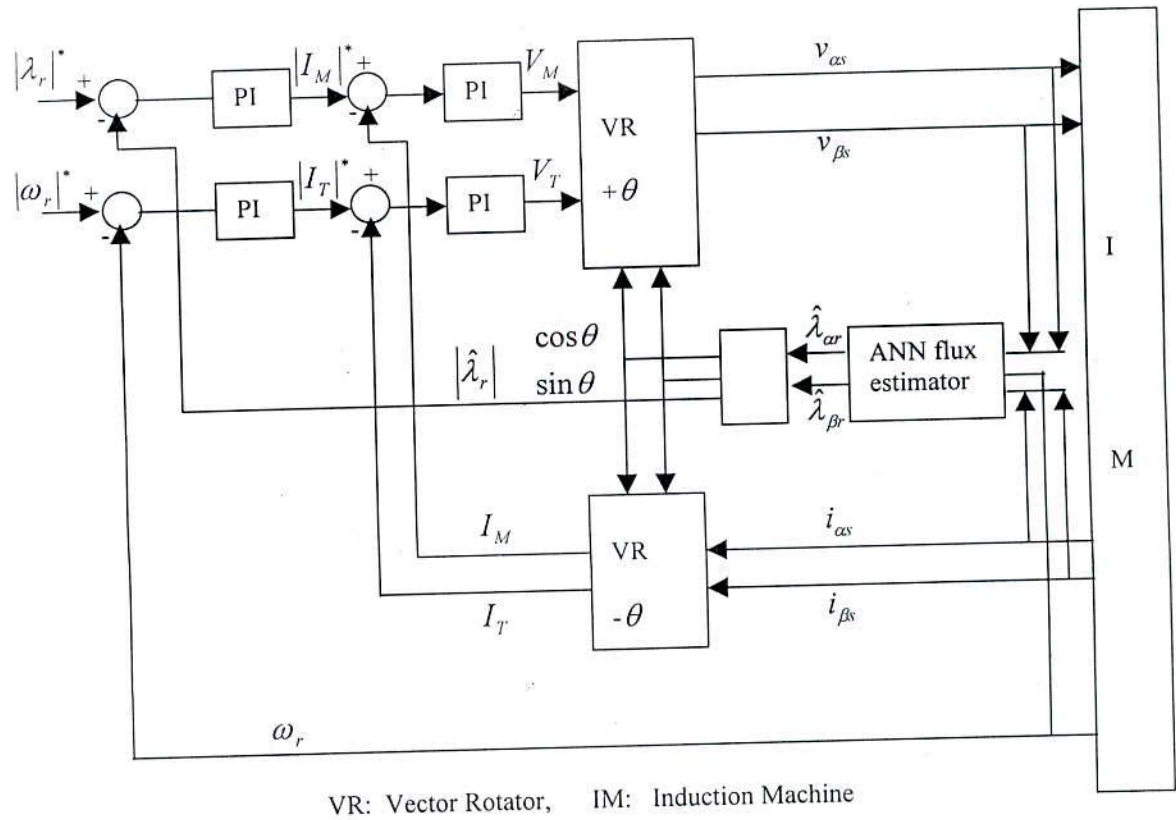


Fig. 7.4. ANN rotor flux estimator based direct field orientation controller for voltage fed inverter.

Simulation results of the direct field orientation are presented in Fig. 7.5. The trained network consists of a three-layer neural network with five input nodes connected to eight sigmoid neurons and two pure linear output nodes connected to eight sigmoid neurons (5-8-8-2). The training was implemented with backpropagation algorithm. In training period due to the lack of larger computer memory, the training is completed by part and part that mean transient, in between of transient and steady state and steady state.

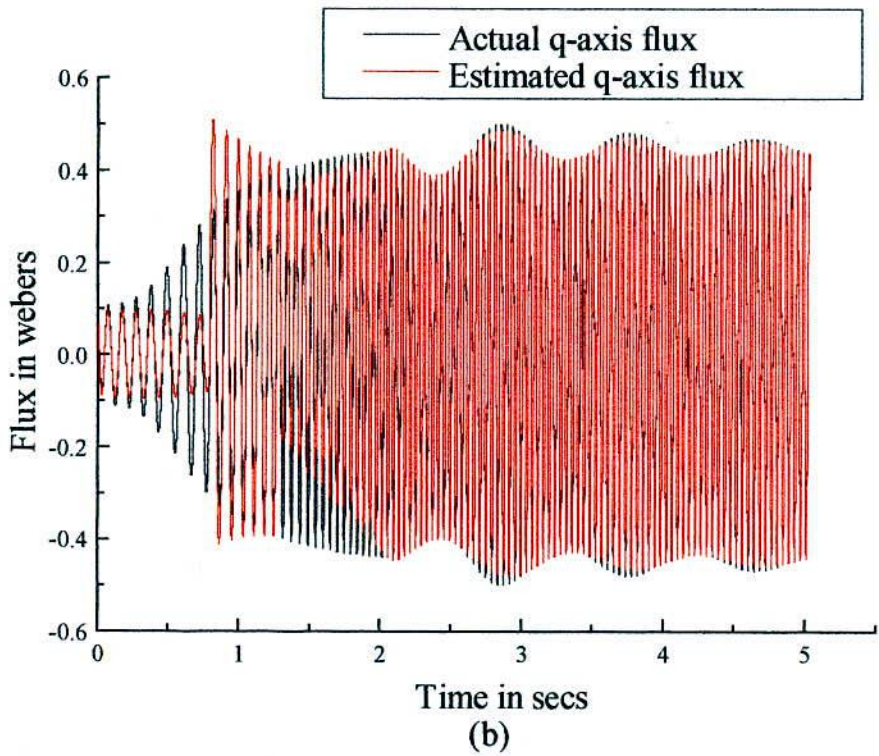
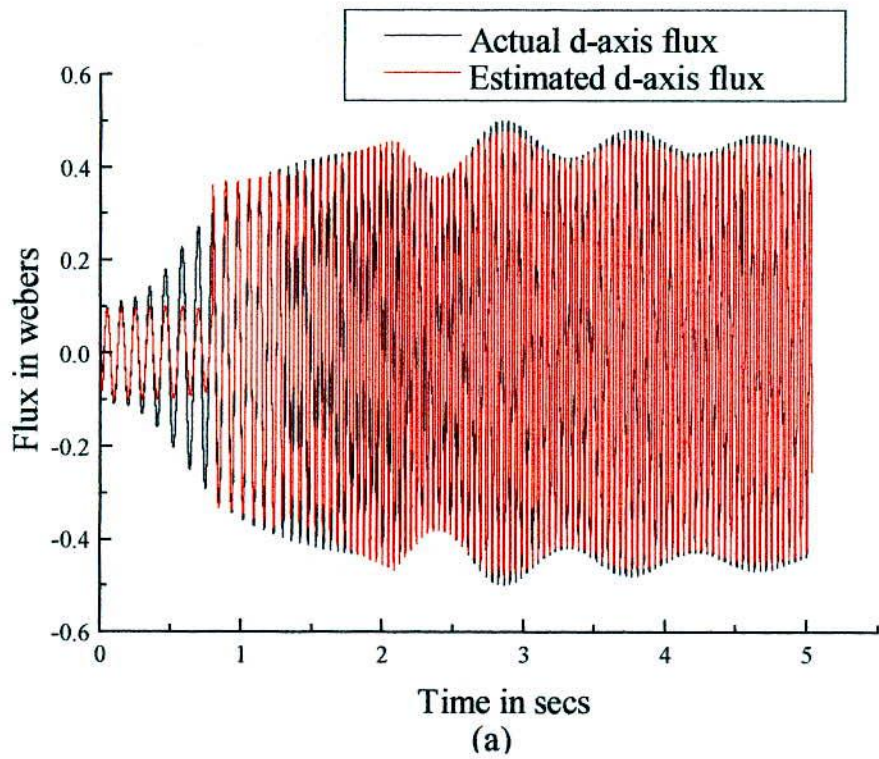


Fig. 7.5 ANN estimated rotor flux (a) d-axis (b) q-axis of direct field orientation based voltage fed inverter.

## CHAPTER VIII

### CONCLUSION

#### 8.1 CONCLUSION

Simulation studies on flux observer based direct and indirect vector control schemes were conducted in this thesis work. Both voltage and current source inverter characteristics were implemented in digital computer environment to study the drive performance. The artificial neural network approaches estimating the flux was simulated to compare the performance with the observer based systems. All the studies were carried out with stationary two-axis model for the induction motor.

In the case of flux estimation using full order observer the number of state variables is high and huge calculations are involved. However, the full order observer may be selected as it provides speed sensorless control of motor. This has been included in this study. The important characteristics of this observer are it is insensitive to parameter deviation and robustness. Direct field orientation control is possible with this observer for both voltage source and current source inverter systems.

In reduced order observers number of state variables handled for computation is lower and are easy to implement practically. Of the three typical reduced order observer studied in the case of Gopinath type the initial transient is not too much when the parameters of induction motor are changed without changing their values of observer equations, the observer works faithfully and it detects the flux under this changed condition. Direct field orientation is possible with this observer that indicates its robustness.

In Generalised observer the transient condition produces a large variation of estimated

flux and the observer is very sensitive to dynamic condition, so direct field orientation is not possible with this observer. This observer is simple and in generalized form and we have used it for parameter adaptation.

In deadbeat observer, the poles are selected at origin. It is also robust and the direct field orientation is possible with this observer. The main advantage of this observer is that it does not require pole selection. Also subsequent stability studies dependent on poles are not required. With this we can avoid the lengthy process of stability and robustness studies of the observer that normally happens when poles are selected.

All the observers discussed in the studies works suitably from very low speed to rated speed, though special emphasis has not been given to the sliding pole based observer design.

Artificial neural network based flux estimation trained by backpropagation algorithm works suitably for particular operating condition only. If the operating condition changes then system gives erroneous result.

## **8.2 SUGGESTIONS FOR FURTHER STUDY**

This motivates to pursue further research in the application of neural networks to new types of controllers in the motor drive industry.

Extension of this work could be the investigation of possible use to update thresholds and weights of the adaptive neuron model algorithm. This can be the optimum algorithm since it combines the gradient descent method with the Newton algorithm.

## APPENDIX I

### TABLES OF INDUCTION MOTOR DATA

Sl. No	Nominal Parameters (referred to stator)	Values in SI units
1.	Stator resistance, $R_s$	1.798
2.	Rotor resistance, $R_r$	0.825
3.	Mutual inductance, $L_m$	0.07613
4.	Stator self inductance, $L_s$	0.08323
5.	Rotor self inductance, $L_r$	0.095
6.	Moment of inertia, $J$	0.0002
7.	Damping coefficient, $B$	

The PI controller constants are:

$$K_{p1} = 1.15, K_{i1} = 63.5, K_{p2} = 1.15, K_{i2} = 63.5$$

## APPENDIX II

### SIMULATION MODEL DISCRETE

The control strategy is formulated for implementation through digital processors. Linear difference equations are used for various controller sections, and are formed from discrete transfer function (Z-transforms) of the controllers. A PI controller in frequency domain is represented as

$$\frac{M(s)}{E(s)} = k_p + \frac{k_i}{s} \quad (\text{B.1})$$

Applying the bilinear transformation  $s = \frac{2}{T} \left( \frac{z-1}{z+1} \right)$  with T as the sampling time and then taking the inverse z-transform gives

$$m(kT) = m(\overline{k-1T}) + \left( k_p + \frac{k_i T}{2} \right) e(kT) - \left( k_p - \frac{k_i T}{2} \right) e(\overline{k-1T}) \quad (\text{B.2})$$

Where  $e(kT)$  and  $m(kT)$  are the respective values at the  $kT$ -th instant.

If the rotor speed is passed through a first order filter (Fig. B.1) one can obtain

$$\omega_{mf}(s) = \frac{k_f}{1 + \tau_f s} \omega_m(s) \quad (\text{B.3})$$

Where  $k_f$  is the gain of the filter and  $\tau_f$

is the time constant of the filter. The difference equation to determine the input to the speed comparator is obtained by applying the above bilinear transformation and taking the inverse z-transform.

$$\omega_{mf}(kT) = \frac{T k_f}{1 + 2\tau_f} [\omega_m(kT) + \omega_m(\overline{k-1T})] - \frac{T - 2\tau_f}{T + 2\tau_f} \omega_{mf}(\overline{k-1T}) \quad (\text{B.4})$$

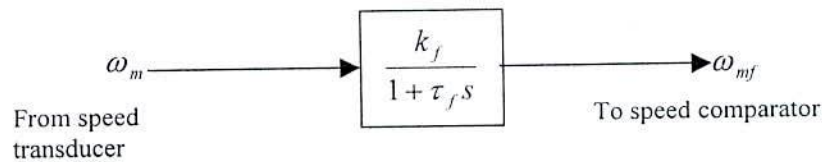


Fig.B.1 First order filter in speed feedback loop.

## REFERENCES

1. F. Blaschke, 'The Principle of Field Orientation as Applied to the New Transvektor Closed Loop Control System for Rotating Field Machines', Siemens Review, 1972, vol. 34, pp. 217-220.
2. K. Hasse, 'Zum dynamischen Verhalten der Asynchronmaschine bei Betrieb mit variabler Staenderfrequenz und Staenderspannung' ("On the Dynamic Behavior of Induction Machines driven by Variable Frequency and Voltage Source"), ETZ-A, Bd 89 H.4, 1968, pp. 77-81.
3. A. Nabae, K. Otsuka, H. Uchino, & R. Kurosawa, "An Approach to flux Control of Induction Motor Operated with Variable Frequency Power Supply", IEEE Trans, Ind. Appl. vol. IA-16, 1980, pp.342-350.
4. R. Gabriel, W. Leonhard and C. J. Nordby, "Field Oriented Control of a Standard AC Motor Using Microprocessors", IEEE Trans., Ind. Appl., vol. IA-16, 1980, pp 186-192.
5. F. Harashima, S. Kondo, K. Ohnishi, M. Kajita and M. Susono, "Multimicroprocessor-based Control System for Quick Response Induction Motor Drive", IEEE Trans., Ind. Appl., vol. IA-21, 1985, pp 602-608.
6. J. Zhang, V. Thiagarajan, T. Grant and T.H. Barton, " New Approach to Field Orientation Control of CSI Induction Motor Drive", IEE proc., vol. 135, pt B, 1988, pp. 1-7.
7. E. Y. Y. Ho and P. C. Sen, "Decoupling Control of Induction Motor Drives", IEEE Trans. Ind. Electron. , vol.35, 1988 pp. 253-262
8. D.S. Ziinger, F. Profumao, T .A. Lipo, D. W. Novatni. " A Direct Field -Oriented Controlar For Induction Motor Drives, using Tapped Stator Winding, IEEE Trans. Power Electronics. vol. 5, 1990, pp. 446-453.
9. H. Matsumoto, H. Takami and R. Takase, "Vector Control Scheme for an Induction Motor Controlled by a Voltage Model Operation with Current Control Loop", Conference rec. IEEE IAS Annual meeting, 1989, pp. 368-374.
10. S. Sathikumar and J. Vithayathil, "Digital Simulation of Field- Oriented Control of Induction Motors", IEEE Trans., Ind. Electron, vol. IE-31, 1984, pp. 141-148.
11. D. Y. Ohm, "Simulation of a Vector-controlled Induction Motor Including Magnetic Saturation of Effects", intelligent Motions, 1989, PC/M, pp. 64-79.

12. C-H. Liu, C-C. Hwu and Y-F. Feng, "Modelling and Implementation of a Microprocessor-based CSI-Fed Induction Motor Drive using Field Oriented Control", IEEE Trans., Ind. Appl., vol. 25, 1989, pp 588-597.
13. S. Bolognani and G. S. Buja, "DC Link Current Control for High-Performance CSIM Drives", IEEE Trans. Ind. Appl., vol. IA-23, 1987, pp. 1043-1047.
14. D. I. Kim, I. J. Ha and M. S. Ko, "Control of Induction Motors Via Feedback Linearization with input-output Decoupling", Int. Journal of Control, vol. 51, pp 863-883.
15. M. Koyama, M. Yano, I. Kamiyama and S. Yano, "Microprocessor-based Vector Control System for Induction Motor Drives with Rotor Time Constant Identification Function," IEEE Trans., Ind. Appl., vol. IA-22, 1986, pp. 453-459.
16. L. J. Garces, "Parameter Adaptation for the Speed Controlled Static AC Drive with Squirrel Cage Induction Motor," IEEE Trans., Ind. Appl., vol. IA-16, 1980, pp. 173-178.
17. D. Y. Ohm, Y. Khersonsky and J. R. Kimzey, "Rotor Time Constant Adaptation Method for Induction Motors Using DC Link Power Measurement," Conf. Rec., IAS-89, pp. 579-587.
18. C. Wang, D. W. Novotny, and T. A. Lipo, "An Automated Rotor Time Constant Measurement System for Indirect Field-Oriented Drives", IEEE Trans., Ind. Appl., vol. IA-24, 1988, pp. 151-159.
19. Bashudeb Chandra Ghosh "Parameter Adaptive Vector Controller for CSI-fed induction Motor drive and Generalized approaches for simulation of CSI-IM System" P.hd. Thesis Department of Electrical Engineering, IIT, Kharagpur, July, 1992.
20. G. Kron, Tensor Analysis of Electrical Networks, John Willey and Sons, New York, 1937.
21. R. Krishnan and F. C. Doran, "A Method of Sensing Line Voltages for Parameter Adaptation of Inverter-fed Induction Motor Drives," IEEE Trans. on Ind. Appl. vol. IA-23, 1987, pp. 617-682.
22. Y. Hori and T. Umeno, "Implementation of Robust Flux Observer Based Field Orientation (FOFO) Controller for Induction Machines", IEEE Conf. Rec., IAS 1989, pp. 523-528.



23. T. Umeno, Y. Hori and H. Suzuki, "Design of the Flux Observer-based Vector Control System of Induction Machines Taking into Consideration Robust Stability", *Journal of Elect. Engg. In Japan*, vol. 110, 1990, pp. 53-65.
24. H. Kubota, K. Matsuse, and T. Fukao, "Indirect Field Oriented Control of CSI-Fed Induction Motor with State Observer", *Conf. Rec., IEEE IAS*, 1987, pp. 138-143.
25. X. Xa, R. De Doncker and D. W. Novotny, "A stator Flux Oriented Induction Machines Drive", *IEEE Power El. Specialist Conf.*, 1988, pp. 870-876.
26. X. Xu, D. W. Novaty, "Implementation of Direct Stator Flux Orientation Control of a Versatile DSP. Based System", *IEEE Trans. on Ind. Appl.* vol. 27 No. 4, 1991, pp. 694-700.
27. Adel Gasteli, Masaki Tonita, T. Takeshita & N. Matsui, "Implement of a Stator Flux Oriented Speed-Sensorless Control of an Induction Motor" *IEEE PCC Yokohama*, 1993, pp. 415-420.
28. H. Tarima and Y. Hori, "Speed Sensorless Field-Orientation Control of the Induction Machine", *IEEE Trans. Ind. Appl.* vol. 29 No. 1, pp. 175-180, 1993.
29. H. Kubata, K. Matsure, T. Nakano, "DSP-based Adaptive Flux Observer of Induction Motor", *IEEE Trans. Ind. Appl.* vol. 29 No. 2, pp. 344-348, 1993.
30. L. Ben-Brahim & R. Kurosawa, "Identification of Induction Motor Speed Using Neural Networks", *IEEE PCC Yokohama* pp. 689-694. 1993.
31. M. G. Simoes & B.K. Bose, "Neural Network Based Estimation of Feedback Signals for a Vector Controlled Induction Motor Drive", *IEEE Trans. Ind. Appl.* vol. 31, No. 3, pp. 620-629, 1993.
32. H. Kubata, K. Matsuse and T, Nakano, "DSP-Based Speed Adaptive Flux Observer of Induction Motor", *IEEE Trans, Ind. Appl.* vol 29, No 2, pp. 344-348 1993.
33. G. Yang, T-Hai Chin, "Adaptive-Speed Identification Scheme for a Vector Controlled Speed Sensorless Inverter-Induction Motor Drive", *IEEE Trans, Ind. Appl.* vol.29, No.4 pp.820-825, 1993.
34. Gopinath B, "On the control of Linear Multiple Input Output System", *The bell System Tech. Journal* vol. 50 No. 3, 1971.
35. N. N. Hancock, *Matrix Analysis of Electrical Machinery*, Pergamon Press Ltd., London, 1984.

36. E. P. Cornell and T. A. Lipo, "Modelling and Design of Control Current Induction Motor Drive System", IEEE Trans., Ind. Appl., 1997, vol. IA-13, PP. 321-330.

